DYNAMICS OF A PLASMA INHOMOGENEITY IN THE UPPER ATMOSPHERE, ITS DIFFUSION, OSCILLATIONS AND TURBULENT MOTIONS

by

RALPH D. HANKEL

A dissertation submitted to the Graduate Faculty in Engineering in partial fulfillment of the requirement for the degree of Doctor of Philosophy, The City University of New York.

1973

This manuscript has been read and accepted for the Graduate Faculty in Engineering in satisfaction of the dissertation requirement for the degree of Doctor of Philosophy.

June 8, 1973
date

Chan Mou Tchen
Chairman of Examining Committee

June 8, 1973
date

Jacques E. Bouvenisse
Executive Officer

Professor Norman Jen
Professor S. B. Menkes
Professor C. M. Tchen

Supervisory Committee

The City University of New York

ACKNOWLEDGMENT

I gratefully acknowledge the assistance provided by the faculty of the Department of Mechanical Engineering and the City College Research Foundation of the City University of New York in support of this research. I also wish to thank Mr. Leonard Strauss of the Rome Air Development Center for providing computer facilities for this study and Gulf United Nuclear Fuels Corporation of Elmsford, N. Y. for their encouragement and cooperation during the years of my graduate studies.

Above all, I am indebted to my research adviser, Professor C. M. Tchen, for his personal interest, valued advice and for the many hours he has generously devoted to guiding me in the present research. It has been a privilege to be associated with a person who exemplifies such high standards of scholarship and professionalism. It is a pleasure for me to express, even in this inadequate manner, my sincere gratitude to Professor Tchen.

ABSTRACT

The study of plasma inhomogeneities, i.e., a system of ions and electrons with a nonuniform distribution of density has increased in importance in view of recent research activities in ionospheric motions and in plasma physics related to thermonuclear fusion. Aurorae, airglow, flares and sporadic bursts in the F layer of the ionosphere are well observed phenomena of natural plasma inhomogeneities. Simulations of these plasma phenomena have recently been achieved by artificially releasing metallic vapor plasmas in the upper atmosphere, or by artificially heating the ionosphere by means of high energy lasers and radars. One of the important applications of this research resides in enhancing or guiding communication systems at large distances. Another area of current interest among the nations pertains to the intense effort directed at achieving controlled nuclear fusion by means of controllable plasmas for the purpose of energy conversion. Theories on the dynamics of plasmas have been devoted mostly to homogeneous plasmas. However, the plasmas associated with these investigations are generally inhomogeneous. Therefore it is the objective of the present thesis to analyze the motions of inhomogeneous plasmas, their interaction with the environment, their properties and certain new phenomena pertinent to plasma inhomogeneities. More specifically one can distinguish the motions of the inhomogeneity to occur on three interconnected scales. The largest scale is that of the gross motion

characterizing the time evolution of a plasma inhomogeneity by diffusion and by drift due to the earth's electric and magnetic fields and atmospheric winds. As this gross evolution is subject to perturbations, oscillations may appear on a somewhat smaller scale, grow and become saturated. These oscillations are called striations, and have been observed in plasma clouds released artificially in the ionosphere. If the instability, which gives rise to these striations, is strong, mode interactions in the oscillations become important. As a consequence, the cascade mechanism of transfer and the generation of modes from large to small scales occur. The fluctuations of the last category will be called plasma turbulence. The fundamental study of the motions of plasma inhomogeneities, in the sequence of the gross evolution of the plasma by diffusion, the oscillations and the development of turbulence, form the main theme of the present research. Particular emphasis is placed on providing theoretical interpretations and predictions for certain anomalous and nonlinear features, such as the splitting of the plasma inhomogeneity in the course of diffusion, the steepening of its front as a consequence of the nonlinear behavior, the appearance of striations and their governing dispersion relation, and finally the spectral structure of turbulence produced in the inhomogeneous plasma under the effects of drifts. Many of the theoretical results obtained here concerning the physical features and phenomena of the plasma inhomogeneities are confirmed by experiments.

CONTENTS

TABLES

FIGURES

Chapter I

General Considerations on the Dynamics of Plasma Inhomogeneities

1. NATURAL AND ARTIFICIAL PLASMA INHOMOGENEITIES

Plasma inhomogeneities, i.e., a system of ions and electrons with a nonuniform density distribution, occur naturally in the form of aurorae and airglow in the skies of northern latitudes. These phenomena are caused by the electron and ion bombardment of the neutral atmosphere, which brings about the ionization of some of its constituents. Auroral bursts occur at altitudes of $\sim$ 100 km. Besides gross motion, such plasma inhomogeneities also exhibit intermediate scale oscillations called striations, and more rapid fluctuations, called micropulsation or turbulence. The striations in aurora have the appearance of rayed arcs, rayed bands or hanging curtains.[1-3] Other examples of natural plasma inhomogeneities are the flares and sporadic bursts in the F layers of the ionosphere. Plasma inhomogeneities are also found in interplanetary space, which contains plasma concentrations of protons and electrons.

For the purpose of simulating these natural plasma phenomena, artificial metallic vapors, ionized by photoionization, have been released in the upper atmosphere from rockets and satellites. Plasma inhomogeneities have also been produced artificially by heating the F_2 layer by means of a high energy radar beam. A possible and interesting application of these experiments may be the enhancement and channeling

of long distance communications. An obvious reason for recent activities in the dynamics of inhomogeneous plasmas lies in guiding the laboratory researches on controlled thermonuclear fusion in achieving their goal of obtaining new methods of energy conversion. Another application of artificial plasmas is the mapping of geophysical parameters, such as the earth's magnetic and electric fields, particularly in the ionosphere, the region surrounding the earth where the largest concentration of charged particles exists. Once the interactions between the plasma and these fields are understood, the strength and orientation of the fields can be deduced from the observed evolution of the plasma inhomogeneities. In addition, the properties of the ionosphere, such as the composition, density and conductivity of the constituent charged particles can be determined.

2. DYNAMICS OF PLASMA INHOMOGENEITY AS ILLUSTRATED BY BARIUM CLOUDS RELEASED IN THE UPPER ATMOSPHERE

The sequence of evolution consisting of gross development, instability, and turbulence, is most comprehensively contained in the experimental program of barium clouds performed by the United States, West Germany and France. Therefore, we shall discuss the experiments, and especially the results pertinent to the dynamics of plasma inhomogeneity in this section, and indicate the approach that is to be taken in the present study to explain these phenomena. The Max-Planck Institute for Extraterrestial Physics, Munich, Germany, the European Space Research Organization (ESRO) and the Center d'Etudes Spatiales in France, are the most prominent

centers for such studies in Europe.[4] In the United States, numerous tests have been conducted recently[5] and are extensively described in the literature.[6-10]

In all of these experiments a mixture of chemicals is sent aloft and ignited at the desired altitude. Materials selected as active components for ion production must have a good potential for obtaining high density and long duration plasma inhomogeneities. Most recent experiments have utilized barium in conjunction with an oxidizing agent such as copper oxide. Upon ignition, a metallic vapor is developed inside the rocket as a result of a chemical reaction such as

$$2\,Ba + CuO \rightarrow BaO + Cu + Ba_{vapor}$$

and ejected into the atmosphere through a nozzle. The vapor expands rapidly for a few seconds until equilibrium with the surrounding atmosphere is reached. The vapor concentration then has a diameter of 1 to 5 km. A high fraction of the released Ba vapor (~ 80%) is in the ionized form, which appears in a time ranging from 5 seconds at 160 km to 30 seconds above 220 km.[10] Additional ions are formed by a slower photoionization process in a characteristic time of about 100 sec, with the energy for the process supplied by the solar radiation. The un-ionized constituent forms a neutral cloud which drifts apart from the ion inhomogeneity (Fig. 1.1a). The shape of the neutral cloud remains spherical. The two types of inhomogeneities can be distinguished by

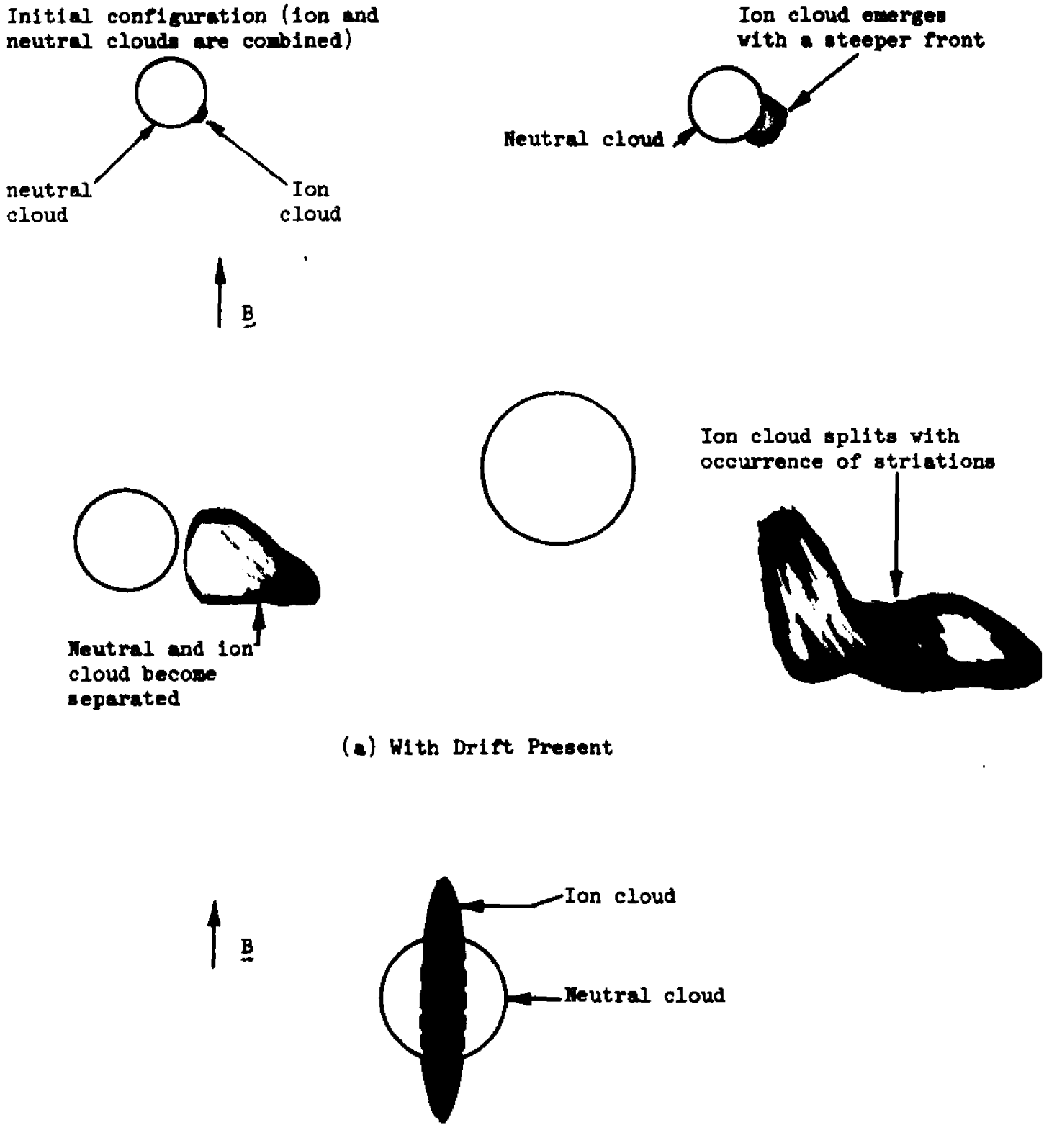

Fig. 1.1. Development of Plasma and Neutral Clouds

their color and optical spectrum. More recently, radar signals have been utilized to obtain additional data on the dynamics of plasma inhomogeneities.

From the release to disappearance, a time span of 20 to 60 minutes, the experiments reveal the evolution of the plasma inhomogeneity in the following sequence:

(i) In the absence of drifts due to a neutral wind, gravity, or an external electric field, the plasma cloud takes on an elliptical shape with the major axis oriented in the direction of the earth's magnetic field(Fig. 1.1b). The case without drift is not of great interest, and will not be discussed further.

(ii) Soon after release, the ion cloud separates from the neutral cloud; each drifts off from the point of origin in specific directions, depending upon the ambient electric and magnetic fields, the neutral winds and the gravity. This drift is accompanied by a process of diffusion. An unusual feature observed in many tests is the formation of a steep density gradient at the front side of the ion cloud which is the side facing the direction of the drift motion. This steepening is caused by the nonlinear behavior of the plasma diffusion. The linear and nonlinear features of the diffusion process are developed in Chapter III after the fundamental equations which govern the general dynamics of a plasma inhomogeneity have been formulated in Chapter II.

(iii) Striations, generally believed to be periodic areas of high density concentrations appear with many of the artificial plasma

inhomogeneities, starting about 10 to 15 minutes after release (Fig. 1.1a). The cloud striations, are aligned nearly always with the lines of force of the earth's magnetic field and their width is estimated to be about 1 km.

These striations are oscillations which occur within the plasma cloud and are therefore a manifestation of the instability of plasma under drift. A theory as to the origin and characteristics of these oscillations is presented in Chapter IV.

(iv) Of special interest is the feature of the separation of the ion cloud into two parts which has been observed in some barium releases in the later stages of evolution such as the one shown in the photographs of Fig. 13 of Reference 11. This anomalous effect arises from the difference in drift velocities between the ions and electrons. This difference gives rise to an electric field that causes the inhomogeneity to move at some mean velocity intermediate between the ion and electron drift velocities and results in a spreading action characterized by two points of peak concentration which move farther and farther apart from each other, a process which eventually leads to a separation of the inhomogeneity. To derive this feature of splitting theoretically, it is necessary to formulate the equations of motion so that the inequality of ion and electron velocity is maintained. The resulting equations and the method of solutions are given in Chapter III. Solutions are presented in the form of density contour plots for a range of plasma conditions.

(v) In strong plasma inhomogeneities, turbulence eventually sets in. The spectrum of the turbulent fluctuations of density and electric field have been observed by means of radar. This type of plasma turbulence can be called "drift turbulence," because its energy is excited by an unstable density gradient, and cascades down the spectrum into smaller and smaller scales. We are interested in predicting analytically the spectral structure of such a drift turbulence. This is done in Chapter V, by means of a theory based on simple dimensional arguments.

(vi) Besides the drift turbulence generated by a plasma inhomogeneity as described above, we may expect that the atmospheric medium presents turbulent motions of its own, called ambient turbulence. When a plasma inhomogeneity evolves in such a turbulent environment, its turbulent diffusion will not follow the development of a laminar diffusion. As a result, observations on the diffusion of an artificial ion cloud, have been reported to possess a larger growth rate in the direction transverse to the magnetic field than predicted by a laminar diffusion theory. Following a laminar theory, the ratio of elongation of a plasma inhomogeneity in the direction parallel and perpendicular to the magnetic field, is given by

$$\ell_{\parallel} / \ell_{\perp} = \left(D_{\parallel} / D_{\perp} \right)^{\frac{1}{2}}$$

$$\simeq \left(\frac{\Omega_i}{\nu_{in}} \frac{\Omega_e}{\nu_{en}} \right)^{\frac{1}{2}}$$

where Ω_i , Ω_e are the ion and electron gyrofrequencies, respectively and ν_{in} , ν_{en} are the collision frequencies of the ions and electrons with the neutrals. For example, according to the data of Fig.(1.2) and Table(1.1) at altitudes between 140 to 200 km, the above formula predicts an elongation of the order of from 500 to 5000, while the observed value is between 5 to 50. Thus a discrepancy of a factor of about 100 exists[12] between experiment and the said theory, see Fig. (1.3). To correct the deficiencies of a laminar theory, a turbulent theory of diffusion is outlined in Chapter V, following the study of the spectral structure of turbulence.

From the sequence of events just described we conclude that we can distinguish three scales of motion in the development of a plasma inhomogeneity.

(i) The largest scale is that of the gross motion of the inhomogeneity and is characterized by the growth of the inhomogeneity by diffusion. A characteristic feature associated with the nonlinear diffusion is the appearance of the steepening of the front side of the inhomogeneity, and as a result of the variable drift, a separation of the cloud into two parts occurs.

(ii) The striations, which appear in most of the artificial ion clouds, belong to smaller scale oscillations.

(iii) Finally the turbulent motions, either generated by the drift instability of the plasma cloud, or as preexisting in the ambient

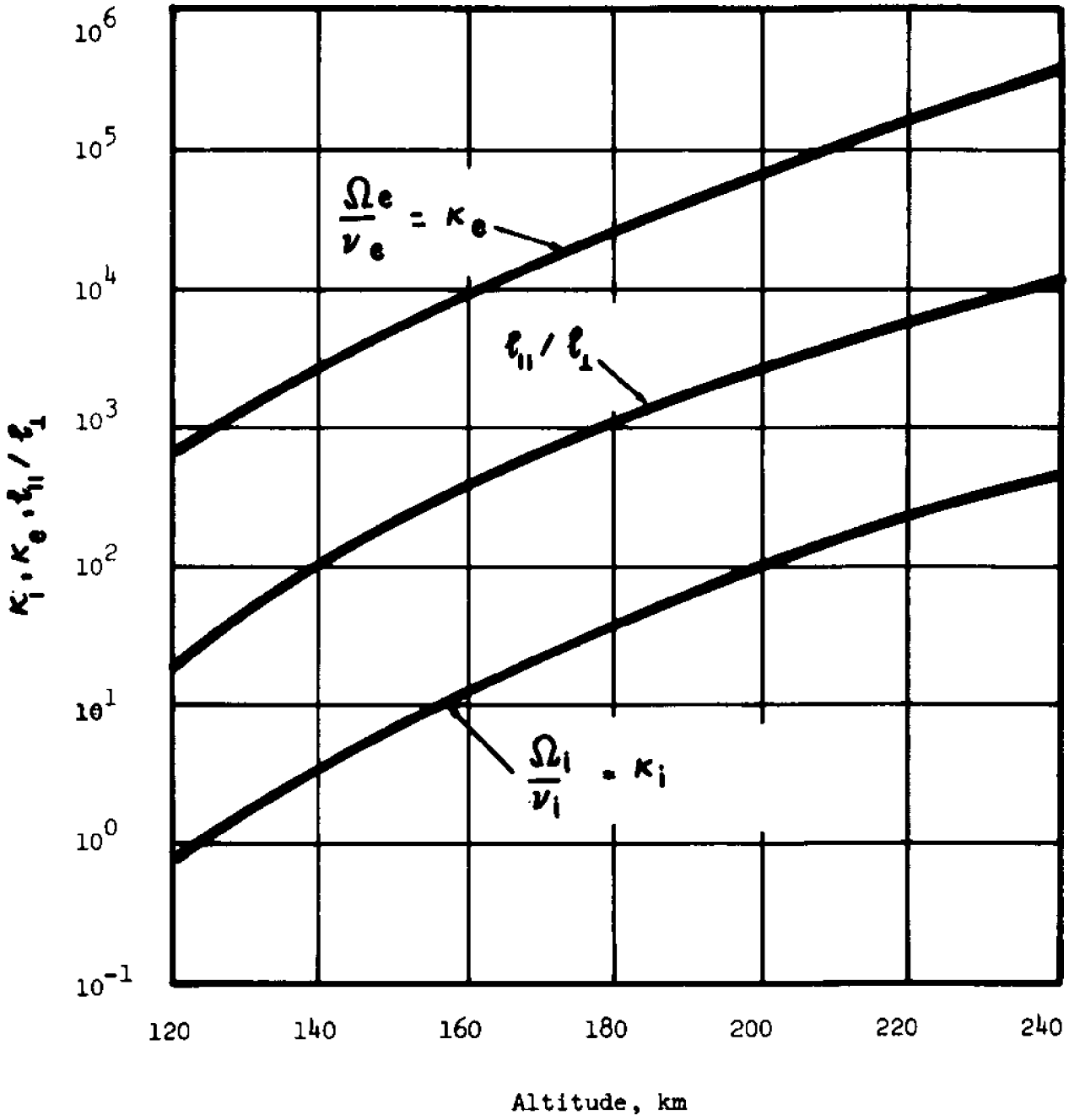

Fig. 1.2. Transport Coefficients and Elongation of Cloud at Various Altitudes.

Table 1.1 Physical Properties of Ion Clouds at 185-200 km Altitude

	Symbol	Approximate Value
Background properties		
Density of neutrals	N_n	10^{10} cm^{-3}
Density of ions	N_i	10^{5} cm^{-3}
Temperature	T	300°K
Wind Velocity	U	100-200 m/sec
Diffusion Coefficient	D_n	0.05-0.08 km^2/sec
Geophysical properties		
Electric field strength, auroral region	E_o	10V/km
Magnetic field strength, auroral region	B	0.5 gauss
Ion properties		
Mass	m_i	2.29×10^{-22} g
Electric charge	e_i	1.6×10^{-19} coulombs
Gyrofrequency	Ω_i	25 sec^{-1}
Collision frequency with neutrals	ν_{in}	1.0 sec^{-1}
Average density (early time)	n_i	10^{7} cm^{-3}

Table 1.1 (continued)

	Symbol	Approximate Value
Electron properties		
Mass	m_e	9.11×10^{-28} g
Electric charge	e_e	-1.6×10^{-19} coulombs
Gyrofrequency	Ω_e	6×10^6 sec^{-1}
Collision frequency with neutrals	ν_{en}	250 sec^{-1}
Average density (early time)	n_e	10^7cm^{-3}
Ambipolar properties		
Diffusion coefficient parallel to magnetic field (early time)	$D_{\parallel}$	0.25 km^2/sec
Diffusion coefficient transverse to magnetic field (early time)	$D_{\perp}$	0.007-0.07 km^2/sec

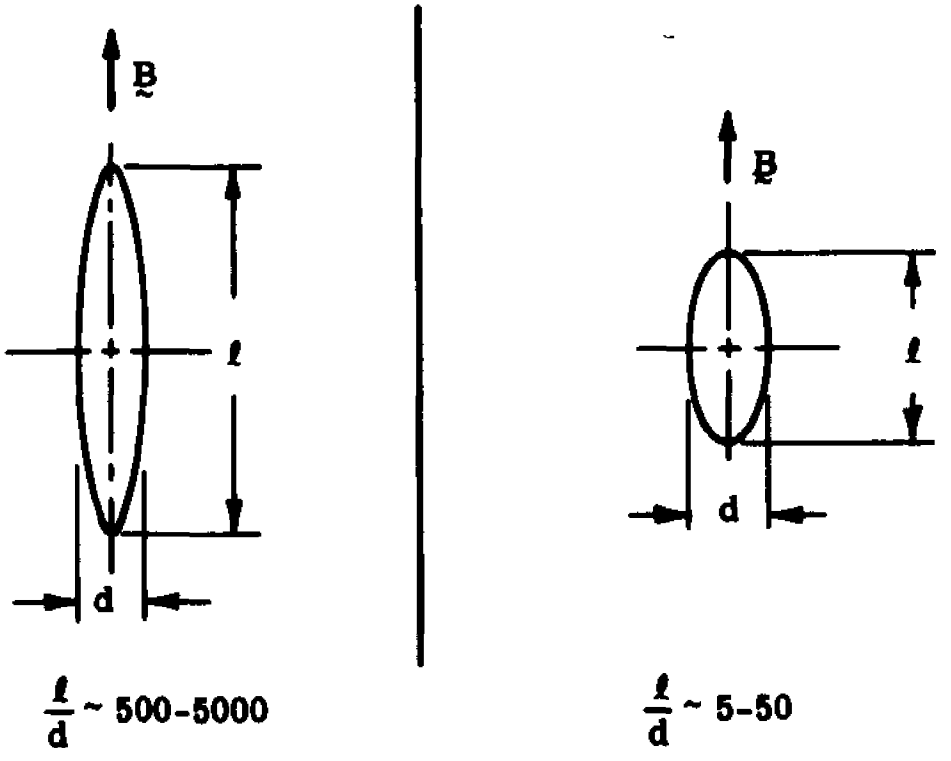

Fig. 1.3. Configuration of Cloud by Diffusion [The elongation calculated by the classical diffusion coefficient shown in (a) is much higher than that found in experiments, see (b).]

atmosphere, have been observed to possess the smallest scales.

The above sequence of events in the development and motions of a plasma inhomogeneity form the main subject of the present research.

3. REVIEW OF EXISTING THEORIES

Before proceeding with the theoretical foundations of the present work, we shall first give a brief review of existing theories relating to the three types of motion mentioned above in Section 2; diffusion, striations and turbulence.

Diffusion theories for plasmas have been advanced among others by Perkins,[13] Holway,[14] Haerendel,[15,16] Gurevich[17,18] and Kaiser[19]. Perkins[13] reported a numerical computation of diffusion which illustrates the nonlinear phenomenon of steepening of the plasma front. His model is two dimensional. The nonlinear model is too difficult to be amenable to analytical solutions. Therefore, the simplified linear model with equal velocities for ions and electrons have been amply reported in the literature.[14-16,19] A more complete model with differential velocities has been reported by Gurevich.[17,18] Our method is similar to that of Gurevich but attempts to include nonlinearity and turbulent effects.

Theories of striations have been proposed by Simon[20,21], Linson[22], Hendel[23] and others.[24,25] These range from simple instability analyses of elementary second order linear diffusion equations to more complicated nonlinear analyses solved by numerical methods. None of these analyses

are based on a more complete diffusion model, i.e., one which leads to a fourth order differential equation, as formulated in the present study.

Theories of plasma turbulence have been advanced by Kadomtsev,[26] and Tchen.[27-31] Kadomtsev's theory applies only to weak turbulence and Tchen's theory on strong turbulence is based upon a repeated-cascade process which requires a rank ensemble average over many scales. The justification on the basis of distribution functions is exceedingly complicated. In order not to obscure the physical features, a dimensional theory is proposed based on physical and phenomenological considerations.

It is hoped that the research reported here will contribute to a better understanding of the diffusion process, particularly as applied to plasma inhomogeneities, and as such will have general application in many areas of physics and engineering.

Chapter II

Dynamical Equations of Plasma Inhomogeneity

1. FUNDAMENTAL EQUATIONS

In order to study the motion of a plasma inhomogeneity in the form of diffusion, oscillation and turbulence, it is necessary to first formulate the fundamental equations which govern the dynamic behavior of the plasma inhomogeneity.

Consider a plasma consisting of ions and electrons, embedded in a medium with a constant magnetic field $\underset{\sim}{B}$, a constant electric field $\underset{\sim}{E}_0$, and a neutral mean velocity $\underset{\sim}{U}$.

The continuity equations, the momentum equations, the energy equations and the Maxwell equations are as follows:

$$\frac{\partial n_a}{\partial t} + \nabla \cdot (n_a \underset{\sim}{v}_a) = 0 \,, \tag{1.1}$$

$$\begin{aligned} m_a n_a \left(\frac{\partial \underset{\sim}{v}_a}{\partial t} + \underset{\sim}{v}_a \cdot \nabla \underset{\sim}{v}_a\right) &= -k \nabla (n_a T_a) + m_a n_a \underset{\sim}{g} \\ &+ n_a e_a \left(\underset{\sim}{E} + \underset{\sim}{v}_a \times \underset{\sim}{B}/c\right) - m_a n_a \nu_{an} (\underset{\sim}{v}_a - \underset{\sim}{U}) \\ &+ m_a n_a \nu_a \nabla^2 \underset{\sim}{v}_a \,, \end{aligned} \tag{1.2}$$

$$\left(\frac{\partial}{\partial t} + \underset{\sim}{v}_a \cdot \nabla\right) T_a = \lambda_a \nabla^2 T_a \,, \tag{1.3}$$

and

$$\nabla \cdot \underset{\sim}{E} = 4\pi \sum_a n_a e_a \,. \tag{1.4}$$

Here the subscript a represents an ion or an electron. Further, t is the time, n_a is the density, m_a the mass, v_a the velocity, T_a the temperature, e_a the electric charge of each species, ν_a and λ_a are the kinematic viscosity and thermal conductivity of the species, ν_{an} is the collision frequency between species a and the neutrals, $\underset{\sim}{E}$ is the perturbed electric field, $\underset{\sim}{g}$ is the acceleration of gravity, c is the speed of light and k is Boltzmann's constant.

The above equations are based on the following assumptions:

(i) The chemical effects are neglected in the continuity equation, because they are important only in the early formation of plasmas by photo-chemical reactions.

(ii) In the momentum equation, the usual pressure term ∇p can be replaced by $k \nabla (T_a n_a)$. The electric field $\underset{\sim}{E}$ is composed of an external electric field $\underset{\sim}{E}_o$ and a self consistent field $\underset{\sim}{E}_s$. The interaction between the charged particles is characterized by a frictional force $\nu_{an} (\underset{\sim}{v}_a - \underset{\sim}{U})$. The interaction between ions and electrons is weak and can be neglected.

(iii) The energy equation is simplified by neglecting compressibility and Rayleigh dissipation.

(iv) In the Maxwell equations, it is assumed that the magnetic field is constant; and that the electric field is longitudinal.

2. TRANSPORT PROPERTIES

The transport properties of a plasma resulting from the coupled motion of ions and electrons can be derived from the fundamental equations formulated above, after some simplifying assumptions are made.

Let

$$\underset{\sim}{v}_a - \underset{\sim}{U} = \underset{\sim}{v}_a^* ; \tag{2.1}$$

Eq. (1.2) then transforms into

$$\begin{aligned} m_a n_a \Big[\frac{\partial \underset{\sim}{v}_a^*}{\partial t} + (\underset{\sim}{v}_a^* + \underset{\sim}{U}) \cdot \nabla \underset{\sim}{v}_a^* + \frac{\partial \underset{\sim}{U}}{\partial t} + \underset{\sim}{U} \cdot \nabla \underset{\sim}{U} + \underset{\sim}{v}_a^* \cdot \nabla \underset{\sim}{U} \Big] \\ = -k (T_a \nabla n_a + n_a \nabla T_a) + m_a n_a \underset{\sim}{g} + n_a e_a (\underset{\sim}{E} + \underset{\sim}{U} \times \underset{\sim}{B}/c) \\ + n_a e_a \underset{\sim}{v}_a^* \times \underset{\sim}{B}/c - m_a n_a \nu_{an} \underset{\sim}{v}_a^* + m_a n_a \nu_a \nabla^2 \underset{\sim}{v}_a^* \\ + m_a n_a \nu_a \nabla^2 \underset{\sim}{U} . \end{aligned} \tag{2.2}$$

In a plasma dominated by collisions, ν_{an} is large and the relaxation time for the approach to equilibrium of the transport properties is short, so that any flux should be proportional to ∇n_a or ∇T_a only, and not to their higher powers or derivatives.

Therefore the terms,

$$\frac{\partial \underset{\sim}{v}_a^*}{\partial t} + (\underset{\sim}{v}_a^* + \underset{\sim}{U}) \cdot \nabla \underset{\sim}{v}_a^*$$

are negligible. This procedure can be called the adiabatic approximation. We can define a turbulent frequency $|\nabla \underset{\sim}{U}|$ due to wind velocity

and express the term $\underset{\sim}{v}_a^* \cdot \nabla \underset{\sim}{U}$ as $\underset{\sim}{v}_a^* \cdot |\nabla \underset{\sim}{U}|$ which can then be combined with the term $\nu_a \underset{\sim}{v}_a^*$ to give

$$\underset{\sim}{v}_a^* \cdot \nabla \underset{\sim}{U} + \nu_a \underset{\sim}{v}_a^* \cong (\nu_a + |\nabla \underset{\sim}{U}|)\underset{\sim}{v}_a^* = \nu_a^* \underset{\sim}{v}_a^* , \tag{2.3}$$

where ν_a^* is an effective frequency defined by

$$\nu_a^* = \nu_{an} + |\nabla \underset{\sim}{U}| . \tag{2.4}$$

Furthermore, since the second derivatives of $\underset{\sim}{v}_a^*$ and $\underset{\sim}{U}$ are small, the last two terms of Eq. (2.2) can be neglected and Eq. (2.2) becomes

$$0 = -k(T_a \nabla n_a + n_a \nabla T_a) + m_a n_a \left(\underset{\sim}{g} - \frac{\partial \underset{\sim}{U}}{\partial t} - \underset{\sim}{U} \cdot \nabla \underset{\sim}{U}\right) + n_a e_a (\underset{\sim}{E} + \underset{\sim}{U} \times \underset{\sim}{B}/c) + n_a e_a \underset{\sim}{v}_a^* \times \underset{\sim}{B}/c - m_a n_a \nu_a^* \underset{\sim}{v}_a^* . \tag{2.5}$$

The solution of this equation is,

$$n_a \underset{\sim}{v}_a^* = \frac{\underset{\approx}{\sigma}_a}{e_a} \cdot (\underset{\sim}{E}_s + \underset{\sim}{E}^* + \underset{\sim}{E}_a) - \underset{\approx}{D}_a \cdot \nabla n_a , \tag{2.6}$$

where the electric fields are

$$\underset{\sim}{E}^* = \underset{\sim}{E}_o + \underset{\sim}{U} \times \underset{\sim}{B}/c \tag{2.7}$$

and

$$\underset{\sim}{E}_a = \frac{m_a}{n_a}\left[\underset{\sim}{g} - \frac{\partial \underset{\sim}{U}}{\partial t} - \underset{\sim}{U} \cdot \nabla \underset{\sim}{U} - \frac{k}{m_a} \nabla T_a\right] .$$

The diffusivity and the conductivity can be written as

$$\underset{\approx}{D}_a = \frac{kT_a}{e^2} \underset{\approx}{\alpha}_a \tag{2.8}$$

and

$$\underset{\approx}{\sigma}_a = n_a \underset{\approx}{\alpha}_a \tag{2.9}$$

with

$$\underset{\approx}{\alpha}_a = \frac{e^2}{m_a \Omega_a} \underset{\approx}{K}_a = \frac{e_a c}{B} \underset{\approx}{K}_a . \tag{2.10}$$

Here

$$\Omega_a = \frac{e_a B}{m_a c} \tag{2.11}$$

is a cyclotron frequency. The tensor $\underset{\approx}{K}_a$ has three nonvanishing components:

$$\begin{aligned} K_{\parallel a} &= \kappa_a \\ K_{\perp a} &= \frac{\kappa_a}{1+\kappa_a^2} \\ K_{Ha} &= \frac{\kappa_a^2}{1+\kappa_a^2} \end{aligned} \tag{2.12}$$

where

$$\kappa_a = \Omega_a / \nu_a^*$$

and is positive for ions and negative for electrons. $K_{\parallel a}$, $K_{\perp a}$ and K_{Ha} are the parallel, transverse and Hall components, respectively. If the magnetic field is in the x_3-direction we find the components of $\underset{\approx}{K}_a$ to be,

$$\begin{aligned} K_{11a} &= K_{22a} = K_{\perp a}, \\ K_{33a} &= K_{\parallel a}, \\ K_{12a} &= K_{21a} = K_{Ha}, \\ K_{23a} &= K_{32a} = K_{13a} = K_{31a} = 0 . \end{aligned} \tag{2.13}$$

The diffusivity $\underset{\approx}{D}$ and the conductivity $\underset{\approx}{\sigma}$ are plasma transport properties, because they relate the density gradient and the electric fields of the plasma to the ion and electron currents. This can be seen in Eq. (2.6) which can be considered a generalized Ohm's law. The effect of turbulence on these transport properties can be significant and is discussed in Chapter V.

3. SYSTEM OF EQUATIONS GOVERNING PLASMA MOTION

For further simplification of the plasma equations the ion and electron velocities are eliminated between the continuity and momentum equations.

By writing the self-consistent field, $\underset{\sim}{E}_s$ in Eq. (2.6) in terms of a potential $-\nabla\phi$, Eq. (2.6) transforms to

$$n_a \underset{\sim}{v}_a = -n_a \underset{\sim}{U} + n_a \frac{\underset{\approx}{\alpha}_a}{e_a} \cdot \left(-\nabla\phi + \underset{\sim}{E}^* + \underset{\sim}{E}_a\right) - \underset{\approx}{D}_a \cdot \nabla n_a . \qquad (3.1)$$

Substitution of Eq. (3.1) into Eq. (1.1) results in

$$\frac{\partial n_a}{\partial t} + \nabla\cdot\left(n_a \underset{\sim}{U}\right) + \nabla\cdot n_a \frac{\underset{\approx}{\alpha}_a}{e_a} \cdot \left(-\nabla\phi + \underset{\sim}{E}^* + \underset{\sim}{E}_a\right) = \nabla\cdot \underset{\approx}{D}_a \cdot \nabla n_a . \qquad (3.2)$$

The Maxwell equation (1.4) transforms to

$$\nabla^2\phi = -4\pi e\left(n_i - n_e\right) . \qquad (3.3)$$

We now have a system of three equations with three unknowns, n_i, n_e and ϕ, which in principle can be solved. Here it is assumed that the species temperature T_a is known, which eliminates the necessity of solving the coupled energy equations.

To simplify the equations further, we introduce two new variables,

$$n = \frac{1}{2}\left(n_i + n_e\right)$$

and (3.4)

$$\rho = \frac{1}{2}\left(n_i - n_e\right) .$$

To abbreviate the writing, we introduce the following notations

$$\underset{\sim}{V}_a = \frac{\alpha_a}{e_a}\cdot(\underset{\sim}{E}^* + \underset{\sim}{E}_a) + \underset{\sim}{U}$$

$$= \underset{\approx}{K}_a \cdot \left(\frac{c}{B}\underset{\sim}{E}_o + \underset{\sim}{U}\times\hat{e}_B + \frac{c}{B}\underset{\sim}{E}_a\right) + \underset{\sim}{U}, \qquad (3.5)$$

$$\underset{\sim}{Q}_a = -\frac{\alpha_a}{e_a}\cdot\nabla\phi + \underset{\sim}{V}_a, \qquad (3.6)$$

$$Q^{\pm} = \frac{1}{2}(Q_i \pm Q_e), \qquad (3.7)$$

$$\underset{\approx}{D}^{\pm} = \frac{1}{2}(\underset{\approx}{D}_i + \underset{\approx}{D}_e), \qquad (3.8)$$

where $\underset{\sim}{V}_a$ is called the drift velocity .

For the case where $\underset{\sim}{E}_a = 0$ and $\underset{\sim}{E}_o$ and $\underset{\sim}{U}$ have only components transverse to the magnetic field, we obtain, by substituting the components of the tensor $\underset{\approx}{K}$ in (3.5), the drift velocity,

$$\underset{\sim}{V}_a = \frac{1}{1+K_a^2}\left(K_a\frac{c}{B}E_{o_1} + K_a^2\frac{c}{B}E_{o_2} + U_1 + K_a U_2\right)\hat{x}_1$$

$$+ \frac{1}{1+K_a^2}\left(K_a\frac{c}{B}E_{o_2} + K_a^2\frac{c}{B}E_{o_1} + U_2 - K_a U_1\right)\hat{x}_1, \qquad (3.9)$$

where $\hat{x}_1$ and $\hat{x}_2$ are unit vectors in the x_1 and x_2 - direction, respectively. To simplify further, let

$$\underset{\sim}{u}^* \equiv -\frac{c}{B}\nabla\phi$$

and

$$\underset{\sim}{U}_a^* \equiv \frac{c}{B}(\underset{\sim}{E}^* + \underset{\sim}{E}_a) . \qquad (3.10)$$

Then

$$\underset{\sim}{Q}_a = \underset{\approx}{K}_a \cdot (\underset{\sim}{u}^* + \underset{\sim}{U}_a^*) + \underset{\sim}{U}$$

and with

$$\kappa_e \gg \kappa_i \gg 1$$

$$\underset{\sim}{Q}_i = \frac{1}{\kappa_i}(\underset{\sim}{u}^* + \underset{\sim}{U}_i^*) + (\underset{\sim}{u}^* + \underset{\sim}{U}_i^*) \times \hat{e}_B + \underset{\sim}{U} \,, \tag{3.11}$$

$$\underset{\sim}{Q}_e = (\underset{\sim}{u}^* + \underset{\sim}{U}_e^*) \times \hat{e}_B + \kappa_e (\underset{\sim}{u}^* + \underset{\sim}{U}_e^*) \cdot \hat{e}_B \hat{e}_B + \underset{\sim}{U} \,, \tag{3.12}$$

where $\hat{e}_B$ is a unit vector in the x_3- direction.

Equation (3.2) for ions and electrons can be written as,

$$\frac{\partial n}{\partial t} + \nabla \cdot n\underset{\sim}{Q}^+ + \nabla \cdot \rho \underset{\sim}{Q}^- = \nabla \cdot \underset{\approx}{D}^+ \cdot \nabla n + \nabla \cdot \underset{\approx}{D}^- \cdot \nabla \rho \,, \tag{3.13}$$

$$\frac{\partial \rho}{\partial t} + \nabla \cdot \rho \underset{\sim}{Q}^+ + \nabla \cdot n\underset{\sim}{Q}^- = \nabla \cdot \underset{\approx}{D}^+ \cdot \nabla \rho + \nabla \cdot \underset{\approx}{D}^- \cdot \nabla n \,. \tag{3.14}$$

These two equations together with the Poisson equation, (3.3) which can be written as

$$\nabla^2 \phi = -4\pi e \rho \tag{3.15}$$

constitute the general equations of motion for a plasma.

a. High Frequency Plasma

For a high frequency plasma, ρ varies much more rapidly than n, so that n can be regarded as quasi-stationary and eliminated. The system of equations, (3.13) and (3.14) then reduces to

$$\frac{\partial \rho}{\partial t} + \nabla \cdot \rho \underset{\sim}{Q}^+ = \nabla \cdot \underset{\approx}{D}^+ \cdot \nabla \rho \,, \tag{3.16}$$

$$\nabla \cdot \rho \underset{\sim}{Q}^- = \nabla \cdot \underset{\approx}{D}^- \cdot \nabla \rho \,. \tag{3.17}$$

Subtracting these two equations yields

$$\frac{\partial \rho}{\partial t} + \nabla \cdot \rho \underset{\sim}{Q}_e = \nabla \cdot \underset{\approx}{D}_e \cdot \nabla \rho \,. \tag{3.18}$$

Equation (3.17) and (3.18) together with Eq. (3.15) determines ρ in the terms of the external fields, wind, gravity and temperature effects represented by $\underset{\sim}{U}_i^*$ and $\underset{\sim}{U}_e^*$.

b. *Low Frequency Plasma*

For a low frequency plasma, quasi-neutrality between ions and electrons is reached so that

$$\rho \ll n .$$

As a consequence, Eq. (2.35) becomes,

$$\nabla^2 \phi = 0 \tag{3.19}$$

and terms containing ρ in equations (3.13) and (3.14) can be eliminated. These equations become,

$$\frac{\partial n}{\partial t} + \nabla \cdot n \underset{\sim}{Q}^+ = \nabla \cdot \underset{\approx}{D}^+ \cdot \nabla n , \tag{3.20}$$

$$\nabla \cdot n \underset{\sim}{Q}^- = \nabla \cdot \underset{\approx}{D}_e \cdot \nabla n . \tag{3.21}$$

Subtracting these two equations yields,

$$\frac{\partial n}{\partial t} + \nabla \cdot n \underset{\sim}{Q}_e = \nabla \cdot \underset{\approx}{D}_e \cdot \nabla n . \tag{3.22}$$

Equation (3.21) and (3.22) represent the system of equations which determine the density n and the self consistent field $\underset{\sim}{u}^*$ for a low frequency plasma. These equations can be written in terms of $\underset{\sim}{U}^*$ and $\underset{\sim}{U}$ by substituting for $\underset{\sim}{Q}_i$ and $\underset{\sim}{Q}_e$ from Eq. (3.11) and (3.12) as follows:

$$\frac{\partial n}{\partial t} + \nabla \cdot n \underset{\sim}{U} + \nabla \cdot n \left[(\underset{\sim}{u}^* + \underset{\sim}{U}_e^*) \times \hat{e}_B + \kappa_e (\underset{\sim}{u}^* + \underset{\sim}{U}_e^*) \cdot \hat{e}_B \hat{e}_B \right]$$

$$= \nabla \cdot \underset{\approx}{D}_e \cdot \nabla n \tag{3.23}$$

$$\nabla \cdot n\left[\frac{1}{2\kappa_i}\left(\underset{\sim}{u}^* + \underset{\sim}{U}^*\right) - \frac{\kappa_e}{2}\left(\underset{\sim}{u}^* + \underset{\sim}{U}^*\right)\cdot \hat{e}_B \hat{e}_B\right]$$

$$= \nabla \cdot \underset{\approx}{D} \cdot \nabla n . \tag{3.24}$$

c. Two dimensional Motion

In a plane perpendicular to the magnetic field, the system of equations, Eq. (3.17) and (3.18) and Eq. (3.21) and (3.22) reduce to:

(i) for high frequency plasma with $D_{\perp i} \gg D_{\perp e}$,

$$\frac{\partial \rho}{\partial t} + \nabla \cdot \rho\left[\underset{\sim}{U} + \left(\underset{\sim}{u}^* + \underset{\sim}{U}_e^*\right) \times \hat{e}_B\right] = D_{\perp e} \nabla^2 \rho \tag{3.25}$$

and

$$\nabla \cdot \rho\left[\frac{1}{\kappa_i}\left(\underset{\sim}{u}^* + \underset{\sim}{U}_i^*\right)\right] = D_{\perp i} \nabla^2 \rho , \tag{3.26}$$

(ii) for a low frequency plasma,

$$\frac{\partial n}{\partial t} + \nabla \cdot n\left[\underset{\sim}{U} + \left(\underset{\sim}{u}^* + \underset{\sim}{U}_e^*\right) \times \hat{e}_B\right] = D_{\perp e} \nabla^2 n \tag{3.27}$$

and

$$\nabla \cdot n\left[\frac{1}{\kappa_i}\left(\underset{\sim}{u}^* + \underset{\sim}{U}_i^*\right)\right] = D_{\perp i} \nabla^2 n , \tag{3.28}$$

or, rewritten in an alternate form,

$$\frac{\partial n}{\partial t} + \nabla \cdot n\left[\left(\underset{\sim}{u}^* + \underset{\sim}{U}_e^*\right) \times \hat{e}_B\right] = D_{\perp e} \nabla^2 n \tag{3.29}$$

and

$$\nabla \cdot n\left[\left(\underset{\sim}{u}^* + \underset{\sim}{U}_i^*\right) + \underset{\sim}{U} \times \hat{e}_B\right] = D_{\perp i} \nabla^2 n , \tag{3.30}$$

4. CONCLUSIONS

(i) The fundamental equations governing the motion of a plasma inhomogeneity in a magnetic field under the action of an external field and an atmospheric wind are the continuity, momentum, energy and Maxwell equations for ions and electrons. The coupled system has been reduced to a system of two equations with two unknowns, the density and the self-consistent field.

(ii) The transport coefficients governing the ion and electron motions are the diffusivity and conductivity tensors $\underset{\sim}{\mathfrak{D}}$ and $\underset{\sim}{\sigma}$, which are functions of $\mathcal{K}$, the ratio of the gyrofrequency to the collision frequency with the neutrals. The conductivity tensor is proportional to the density n, and leads to the nonlinear behavior of the plasma inhomogeneity.

Chapter III

Diffusion of a Plasma Inhomogeneity in the Upper Atmosphere

1. THEORETICAL MODELS OF DIFFUSION

In Chapter II, a system of equations II,(3.2) and II,(3.3) governing the motion of a plasma inhomogeneity has been derived. These equations express the evolution of plasma density in the presence of density dependent forces, and therefore they are nonlinear.

In view of this fact, the diffusion possesses the following characteristic features:

(i) Splitting of an inhomogeneity into two parts.

(ii) Steepening of the front (leading edge) of a moving inhomogeneity.

(iii) Development of striations, as the result of instability.

(iv) Onset of turbulence.

The first two features, i.e., the splitting of the plasma inhomogeneity and the steepening of the front are large scale effects and will be discussed in the present chapter, while the striations and the structure of turbulence are smaller scale effects and will be investigated in Chapters IV and V.

The system of two equations developed in Chapter II refers to ions and electrons and governs the motions of a plasma inhomogeneity. It

can be transformed into a single equation of diffusion, describing the evolution of the density of the quasi-neutral plasma in time and space. The diffusion equation then takes the form of a fourth order nonlinear partial differential equation, which, in a certain sense, is simpler to solve than the coupled systems, because the self-consistent electric field has been eliminated. For this purpose, we assume the quasi-neutral condition

$$n_i = n_e = n$$

and rewrite Eq. II,(3.2) separately for ions and electrons as follows:

$$\frac{\partial n}{\partial t} - \nabla \cdot n \frac{\underset{\approx}{\alpha}_i}{e} \cdot \nabla \phi + \nabla \cdot n \underset{\sim}{V}_i = \nabla \cdot \underset{\approx}{D}_i \cdot \nabla n , \tag{1.1}$$

$$\frac{\partial n}{\partial t} + \nabla \cdot n \frac{\underset{\approx}{\alpha}_e}{e} \cdot \nabla \phi + \nabla \cdot n \underset{\sim}{V}_e = \nabla \cdot \underset{\approx}{D}_e \cdot \nabla n , \tag{1.2}$$

where n is the density, ϕ is the potential of the self-consistent electric field, $\underset{\approx}{\alpha}_i$, $\underset{\approx}{\alpha}_e$, $\underset{\approx}{D}_i$, $\underset{\approx}{D}_e$ are transport properties, and $\underset{\sim}{V}_i$, $\underset{\sim}{V}_e$ are drift velocities, defined in Chapter II. We note that the variable ϕ is associated with the operators

$$\nabla \cdot n \underset{\approx}{\alpha}_i \cdot \nabla \tag{1.3a}$$

and

$$\nabla \cdot n \underset{\approx}{\alpha}_e \cdot \nabla \tag{1.3b}$$

in Eqs. (1.1) and (1.2) respectively. For the purpose of eliminating ϕ we obtain a uniform operator

$$\left(\nabla \cdot n \underset{\approx}{\alpha}_i \cdot \nabla \right) \left(\nabla \cdot n \underset{\approx}{\alpha}_e \cdot \nabla \right)$$

associated with ϕ , if we multiply Eqs. (1.1) and (1.2) by the operators (1.3a) and (1.3b) respectively. A subsequent addition will give

$$\left[(\nabla \cdot n\underset{\approx}{\alpha}_i \cdot \nabla) + (\nabla \cdot n\underset{\approx}{\alpha}_e \cdot \nabla) \right] \frac{\partial n}{\partial t}$$

$$+ \left[(\nabla \cdot n\underset{\approx}{\alpha}_i \cdot \nabla)(\nabla \cdot n\underset{\approx}{\alpha}_e \cdot \nabla) - (\nabla \cdot n\underset{\approx}{\alpha}_e \cdot \nabla)(\nabla \cdot n\underset{\approx}{\alpha}_i \cdot \nabla) \right] \cdot \nabla\phi$$

$$= (\nabla \cdot n\underset{\approx}{\alpha}_i \cdot \nabla) \left[\nabla \cdot (-n\underset{\sim}{V}_e + \underset{\approx}{D}_e \cdot \nabla n) \right]$$

$$+ (\nabla \cdot n\underset{\approx}{\alpha}_e \cdot \nabla) \left[\nabla \cdot (n\underset{\sim}{V}_i + \underset{\approx}{D}_i \cdot \nabla n) \right] . \qquad (1.4)$$

With the use of the commutability relation

$$(\nabla \cdot n\underset{\approx}{\alpha}_i \cdot \nabla)(\nabla \cdot n\underset{\approx}{\alpha}_e \cdot \nabla) = (\nabla \cdot n\underset{\approx}{\alpha}_e \cdot \nabla)(\nabla \cdot n\underset{\approx}{\alpha}_i \cdot \nabla) \qquad (1.5)$$

the term containing ϕ in (1.4) vanishes and there remains,

$$\left[(\nabla \cdot n\underset{\approx}{\alpha}_i \cdot \nabla) + (\nabla \cdot n\underset{\approx}{\alpha}_e \cdot \nabla) \right] \frac{\partial n}{\partial t}$$

$$= (\nabla \cdot n\underset{\approx}{\alpha}_i \cdot \nabla) \left[\nabla \cdot (-n\underset{\sim}{V}_e + \underset{\approx}{D}_e \cdot \nabla n) \right]$$

$$+ (\nabla \cdot n\underset{\approx}{\alpha}_e \cdot \nabla) \left[\nabla \cdot (-n\underset{\sim}{V}_i + \underset{\approx}{D}_i \cdot \nabla n) \right] . \qquad (1.6)$$

This is a diffusion equation describing the evolution of the density $n(\underset{\sim}{x}, t)$ with transport coefficients $\underset{\approx}{\alpha}_a$ and $\underset{\approx}{D}_a$ and with a drift $\underset{\sim}{V}_a$ defined by II,(2.10), II,(2.8) and II,(3.5), respectively, where $a = i, e$ denotes ions or electrons. Equation (1.6) describes the nonlinear diffusion of a plasma inhomogeneity. In order to distinguish between

the linear and nonlinear effects, we write the operator $\nabla \cdot n \underset{\approx}{\alpha}_a \cdot \nabla$ of Eq. (1.6) in two parts,

$$\nabla \cdot n \underset{\approx}{\alpha}_a \cdot \nabla = n \left[\nabla \cdot \underset{\approx}{\alpha}_a \cdot \nabla + \frac{\nabla n}{n} \left(\underset{\approx}{\alpha}_a \cdot \nabla \right) \right] , \tag{1.7}$$

which upon dividing by n , becomes

$$\left\{ \left[\nabla \cdot \underset{\approx}{\alpha}_i \cdot \nabla + \frac{\nabla n}{n} \left(\underset{\approx}{\alpha}_i \cdot \nabla \right) \right] + \left[\nabla \cdot \underset{\approx}{\alpha}_e \cdot \nabla + \frac{\nabla n}{n} \left(\underset{\approx}{\alpha}_e \cdot \nabla \right) \right] \right\} \frac{\partial n}{\partial t}$$

$$= \left[\nabla \cdot \underset{\approx}{\alpha}_i \cdot \nabla + \frac{\nabla n}{n} \left(\underset{\approx}{\alpha}_i \cdot \nabla \right) \right] \left(- \nabla \cdot n \underset{\sim}{V}_e + \nabla \cdot \underset{\approx}{D}_e \cdot \nabla n \right) \right]$$

$$+ \left(i \leftrightarrow e \right) , \tag{1.8}$$

where $(i \leftrightarrow e)$ represents similar terms obtained by interchanging the subscripts i and e. In order to further simplify the writing, we introduce a new differential operator,

$$A_a \equiv \nabla \cdot \underset{\approx}{\alpha}_a \cdot \nabla + \frac{\nabla n}{n} \left(\underset{\approx}{\alpha}_a \cdot \nabla \right) , \tag{1.9}$$

which reduces Eq. (1.8) to the form

$$\left(A_i + A_e \right) \frac{\partial n}{\partial t} = A_i \left(- \nabla \cdot n \underset{\sim}{V}_e + \nabla \cdot \underset{\approx}{D}_e \cdot \nabla n \right) + A_e \left(- \nabla \cdot n \underset{\sim}{V}_i + \nabla \cdot \underset{\approx}{D}_i \cdot \nabla n \right) . \tag{1.10}$$

We note that the linear and nonlinear terms are now separated and associated with

$$A_a^{\circ} = \nabla \cdot \underset{\approx}{\alpha}_a \cdot \nabla$$

and

$$A_a' = \frac{\nabla n}{n} \left(\underset{\approx}{\alpha}_a \cdot \nabla \right)$$

respectively, with

$$A_a = A_a^{\circ} + A_a' . \tag{1.11}$$

More specifically we have

$$A_a^{\circ} = \alpha_{\perp a}\left(\frac{\partial^2}{\partial x_1^2} + \frac{\partial^2}{\partial x_2^2}\right) + \alpha_{\parallel a}\frac{\partial^2}{\partial x_3^2} \tag{1.12}$$

$$A_a' = \frac{\alpha_{\perp a}}{n}\left(\frac{\partial n}{\partial x_1}\frac{\partial}{\partial x_1} + \frac{\partial n}{\partial x_2}\frac{\partial}{\partial x_2}\right) + \frac{\alpha_{\parallel a}}{n}\frac{\partial n}{\partial x_3}\frac{\partial}{\partial x_3} + \frac{\alpha_{Ha}}{n}\left(\frac{\partial n}{\partial x_1}\frac{\partial}{\partial x_2} - \frac{\partial n}{\partial x_2}\frac{\partial}{\partial x_1}\right), \tag{1.13}$$

where $\alpha_{\perp a}$, $\alpha_{\parallel a}$, α_{Ha} are the transverse, longitudinal and Hall transport coefficients, defined by II,(2.10) and II,(2.12).

Similarly, we write

$$n = n_0 + n' , \tag{1.14}$$

where n_0 is the density governed by a linear equation of diffusion, and n' represents the nonlinear effect. Upon substitution of (1.12) and (1.13) into Eq. (1.14), we obtain

$$\begin{aligned} A_i^{\circ}\frac{\partial n}{\partial t} - A_i^{\circ}\left(-\underset{\sim}{V}_e\cdot\nabla n + \nabla\cdot\underset{\approx}{D}_e\cdot\nabla n\right) + (i \leftrightarrow e) \\ = A_i'\frac{\partial n}{\partial t} + A_i'\left(-\underset{\sim}{V}_e\cdot\nabla n + \nabla\cdot\underset{\approx}{D}_e\cdot\nabla n\right) + (i \leftrightarrow e) \\ \equiv H(\underset{\sim}{x}, t) . \end{aligned} \tag{1.15}$$

This is a fourth order nonlinear partial differential equation, governing the density $n(\underset{\sim}{x}, t)$. For the diffusion of a plasma inhomogeneity connected with the release of an artificial plasma cloud in the ionosphere of a constant density background, we can assume that the concentration is weak. The zeroth order solution can be approximated by linearizing Eq. (1.15) to the form

$$A_i\frac{\partial n_0}{\partial t} - A_i\left(-\underset{\sim}{V}_e\cdot\nabla n_0 + \nabla\cdot\underset{\approx}{D}_e\cdot\nabla n_0\right) + (i \leftrightarrow e) = 0 , \tag{1.16}$$

obtained by neglecting terms associated with A_i' and A_e'. The zeroth order solution n_o of Eq. (1.16) can then be substituted into the non-linear terms, in Eq. (1.15), as represented by $H(\underset{\sim}{x},t)$ to give

$$A_i^o \frac{\partial n}{\partial t} - A_i^o\left(-\underset{\sim}{V}_e \cdot \nabla n + \nabla \cdot \underset{\simeq}{D}_e \cdot \nabla n\right) + (i \leftrightarrow e) = H_o(\underset{\sim}{x},t), \qquad (1.17)$$

where,

$$H_o(\underset{\sim}{x},t) = H(n = n_o)$$
$$\equiv A_i'(n_o)\frac{\partial n_o}{\partial t} + A_i'(n_o)\left(-\underset{\sim}{V}_e \cdot \nabla n_o + \nabla \cdot \underset{\simeq}{D}_e \cdot \nabla n_o\right) + (i \leftrightarrow e) \qquad (1.18)$$

is calculated from $H(\underset{\sim}{x},t)$ of Eq. (1.15) by taking $n \cong n_o$. The term $H_o(\underset{\sim}{x},t)$ in Eq. (1.17) therefore becomes a source term which is a known function of t and $\underset{\sim}{x}$, as determined by (1.18). The left hand side of Eq. (1.17) contains only linear terms, as A_a^o is a linear operator defined by Eq. (1.12), and $\underset{\sim}{V}_a$ and $\underset{\simeq}{D}_a$ are independent of n, while the right hand side becomes a known function of $\underset{\sim}{x}$ and t, as mentioned above. The solution of this equation will be investigated in the next section.

2. GENERAL FORMULATION OF THE RELATIONS GOVERNING THE DIFFUSION OF A PLASMA INHOMOGENEITY

We write the diffusion equation (1.17) explicitly upon substituting for the differential operators from Eq. (1.12), and obtain

$$\left[\alpha_{\perp i}\left(\frac{\partial^2}{\partial x_1^2} + \frac{\partial^2}{\partial x_2^2}\right) + \alpha_{\parallel i}\frac{\partial^2}{\partial x_3^2}\right]\frac{\partial n}{\partial t}$$
$$-\left[\alpha_{\perp i}\left(\frac{\partial^2}{\partial x_1^2} + \frac{\partial^2}{\partial x_2^2}\right) + \alpha_{\parallel i}\frac{\partial^2}{\partial x_3^2}\right]\left[-\underset{\sim}{V}_e \cdot \nabla n + \nabla \cdot \underset{\simeq}{D}_e \cdot \nabla n\right]$$
$$+(i \leftrightarrow e) = H_o(\underset{\sim}{x},t). \qquad (2.1)$$

For the purpose of finding the solution, we make a Fourier transform of Eq. (2.1) with respect to the space. We obtain

$$A_a^{\circ}(k) = -\alpha_{\perp a}\left(k_1^2 + k_2^2\right) - \alpha_{\parallel a} k_3^2, \tag{2.2}$$

which leads to

$$\begin{aligned}&\left[\alpha_{\perp i}\left(k_1^2 + k_2^2\right) + \alpha_{\parallel i} k_3^2\right] \frac{\partial n(\underset{\sim}{k}_1, t)}{\partial t} \\ &+ \left[\alpha_{\perp i}\left(k_1^2 + k_2^2\right) + \alpha_{\parallel i} k_3^2\right]\left\{ i \underset{\sim}{k} \cdot \underset{\sim}{V}_e + \left[D_{\perp e}\left(k_1^2 + k_2^2\right) + D_{\parallel e} k_3^2\right]\right\} n(\underset{\sim}{k}_1, t) \\ &+ (i \leftrightarrow e) = H_o(\underset{\sim}{k}_1, t),\end{aligned} \tag{2.3}$$

where $n(\underset{\sim}{k}_1, t)$ and $H_o(\underset{\sim}{k}_1 t)$ are the Fourier transforms of $n(\underset{\sim}{x}_1, t)$ and $H_o(\underset{\sim}{x}_1, t)$ respectively. Consider spherical coordinates, with wave number vector

$$\underset{\sim}{k} = \underset{\sim}{k}(k, \mu, \phi)$$

and unit vector

$$\mu = \frac{\underset{\sim}{k} \cdot \hat{e}_B}{|k|}$$

where ϕ is the angle between $\underset{\sim}{k}$ and the $\underset{\sim}{x}$ direction. With

$$\begin{aligned} k_1^2 + k_2^2 &= k^2(1 - \mu^2) \\ k_3^2 &= k^2 \mu^2 \end{aligned} \tag{2.4}$$

and upon dividing by

$$\left(\alpha_{\perp i} + \alpha_{\perp e}\right)\left(k_1^2 + k_2^2\right) + \left(\alpha_{\parallel i} + \alpha_{\parallel e}\right) k_3^2$$

Eq. (2.3) can be reduced to the simpler form

$$\frac{\partial n(\underset{\sim}{k}_1, t)}{\partial t} + \left(i \underset{\sim}{k} \cdot \underset{\sim}{V}_{ie} + k^2 D_{ie}\right) n(\underset{\sim}{k}_1, t) = H_{ie}(\underset{\sim}{k}_1, t), \tag{2.5}$$

where

$$\underset{\sim}{V}_{ie}(\mu) = \frac{\left[\alpha_{\perp i}(1-\mu^2)+\alpha_{\parallel i}\mu^2\right]\underset{\sim}{V}_e + \left[\alpha_{\perp e}(1-\mu^2)+\alpha_{\parallel e}\mu^2\right]\underset{\sim}{V}_i}{(\alpha_{\perp i}+\alpha_{\perp e})(1-\mu^2)+(\alpha_{\parallel i}+\alpha_{\parallel e})\mu^2}\,, \tag{2.6}$$

$$D_{ie}(\mu) = \frac{\left[\alpha_{\perp i}(1-\mu^2)+\alpha_{\parallel i}\mu^2\right]\left[D_{\perp e}(1-\mu^2)+D_{\parallel e}\mu^2\right]+\left[\alpha_{\perp e}(1-\mu^2)+\alpha_{\parallel e}\mu^2\right]\left[D_{\perp i}(1-\mu^2)+D_{\parallel i}\mu^2\right]}{(\alpha_{\perp i}+\alpha_{\perp e})(1-\mu^2)+(\alpha_{\parallel i}+\alpha_{\parallel e})\mu^2}\,, \tag{2.7}$$

$$H_{ie}(\underset{\sim}{k},t) = \frac{H_o(\underset{\sim}{k},t)}{(\alpha_{\perp i}+\alpha_{\perp e})(1-\mu^2)+(\alpha_{\parallel i}+\alpha_{\parallel e})\mu^2}\,. \tag{2.8}$$

In Eqs. (2.6) and (2.7) the ambipolar drift $\underset{\sim}{V}_{ie}(\mu)$ and ambipolar diffusion coefficient $D_{ie}(\mu)$ have been derived to be functions of μ. The solution of Eq. (2.5) in k-space can be written as,

$$n(\underset{\sim}{k},t) = n_o(\underset{\sim}{k},t) + \int_0^t dt'\, H_{ie}(\underset{\sim}{k},t')\, G(\underset{\sim}{k},t-t')\,, \tag{2.9}$$

where G represents

$$G(\underset{\sim}{k},t-t') \equiv e^{-(i\underset{\sim}{k}\cdot\underset{\sim}{V}_{ie}+k^2D_{ie})(t-t')} \tag{2.10}$$

and n_o is found to be

$$n_o(\underset{\sim}{k},t) = n(\underset{\sim}{k},0)\, e^{-(i\underset{\sim}{k}\cdot\underset{\sim}{V}_{ie}+k^2D_{ie})t} \tag{2.11}$$

and is the solution in $\underset{\sim}{k}$-space of the linear diffusion equation (1.16). Its inversion takes the form

$$n_o(\underset{\sim}{x},t) = \frac{1}{(2\pi)^3}\int_{-\infty}^{\infty} d\underset{\sim}{k}\; n(\underset{\sim}{k},0)\, e^{-i\underset{\sim}{k}\cdot(\underset{\sim}{x}-\underset{\sim}{V}_{ie}t)-k^2D_{ie}t}\,. \tag{2.12}$$

We invert Eq. (2.9) to obtain,

$$n(\underset{\sim}{x},t) = n_o(\underset{\sim}{x},t) + \int_0^t dt' \int_{-\infty}^{\infty} d\underset{\sim}{x}' \, H_{ie}(\underset{\sim}{x}',t') \, G(\underset{\sim}{x}-\underset{\sim}{x}', t-t') \,, \quad (2.13)$$

where $H_{ie}(\underset{\sim}{k},t)$ and $G(\underset{\sim}{x}-\underset{\sim}{x}', t-t')$ are the inverted Fourier transforms of $H_{ie}(\underset{\sim}{k},t')$ and $G(\underset{\sim}{k}, t-t')$, respectively. It may be remarked that, in two dimensions, i.e., in the transverse plane

$$\mu = 0$$

and equations (2.6) and (2.7) reduce to the simpler expressions

$$\underset{\sim}{V}_{ie}(\mu=0) = \frac{\alpha_{\perp i}\,\underset{\sim}{V}_e + \alpha_{\perp e}\,\underset{\sim}{V}_i}{\alpha_{\perp i} + \alpha_{\perp e}} \equiv \underset{\sim}{V}_{\perp} \,, \quad (2.14)$$

$$D_{ie}(\mu=0) = \frac{\alpha_{\perp i} D_{\perp e} + \alpha_{\perp e} D_{\perp i}}{\alpha_{\perp i} + \alpha_{\perp e}} \equiv D_{\perp} \quad (2.15)$$

known as ambipolar drift and ambipolar diffusion in the classical literature. Similarly, in the direction parallel to the magnetic field, (2.6) and (2.7) reduce to

$$\underset{\sim}{V}_{ie}(\mu=1) = \frac{\alpha_{\parallel i}\,\underset{\sim}{V}_e + \alpha_{\parallel e}\,\underset{\sim}{V}_i}{\alpha_{\parallel i} + \alpha_{\parallel e}} \equiv \underset{\sim}{V}_{\parallel} \,, \quad (2.16)$$

$$D_{ie}(\mu=1) = \frac{\alpha_{\parallel i} D_{e\parallel} + \alpha_{\parallel e} D_{i\parallel}}{\alpha_{\parallel i} + \alpha_{\parallel e}} \equiv D_{\parallel} \,. \quad (2.17)$$

The ratio $D_\perp / D_\parallel$ is obtained from (2.15) and (2.17) by substitution of the $\underset{\approx}{\alpha}$ and $\underset{\approx}{D}$ components from II,(2.8) and II,(2.10) leading to

$$\frac{D_\perp}{D_\parallel} = \frac{1}{1 + |\kappa_i \kappa_e|} \,. \quad (2.18)$$

3. LINEARIZED DIFFUSION EQUATION FOR A PLASMA INHOMOGENEITY

The linear solution n_o , as given by (2.12) is one component of the general solution (2.13) which describes the nonlinear features of the diffusion process. In the present section, we analyze the physical features connected with the linear solution, such as the splitting of the plasma inhomogeneity. For the sake of simplicity, we assume that the inhomogeneity is a point source at time $t=0$ in which case $n(\underset{\sim}{x},0)$ is represented as a δ-function, corresponding to

$$n(\underset{\sim}{k},0) = (2\pi)^{-3} N_o ,$$

which reduces Eq. (2.12) to

$$n_o(\underset{\sim}{x},t) = \frac{N_o}{(2\pi)^3} \int_{-\infty}^{\infty} d\underset{\sim}{k}\, e^{i\underset{\sim}{k}\cdot(\underset{\sim}{x} - \underset{\sim}{V}_{ie}t) - k^2 D_{ie} t}$$

$$= \frac{N_o}{(2\pi)^3} \int_{-\infty}^{\infty} d\underset{\sim}{k}\, e^{-k^2 D_{ie} t} \cos \underset{\sim}{k}\cdot(\underset{\sim}{x} - \underset{\sim}{V}_{ie}t) \qquad (3.1)$$

if we note that n_o is real.

We calculate the triple integration with respect to $d\underset{\sim}{k}$ in spherical polar coordinat-- [illegible]

$$= k \sin\vartheta \cos\phi$$

$$k_1 = k \sin\vartheta \cos\phi$$

$$k_2 = k \sin\vartheta \sin\phi$$

$$k_3 = k \cos\vartheta$$

and

$$n_1 = n \sin\theta \cos\varphi$$

$$n_2 = n \sin\theta \sin\varphi \qquad (3.2)$$

$$n_3 = n\cos\theta$$

with

$$n = \underset{\sim}{x} - \underset{\sim}{V}_{ie}t$$

giving

$$\begin{aligned}\underset{\sim}{k}\cdot\underset{\sim}{n} &= k_1 n_1 + k_2 n_2 + k_3 n_3 \\ &= kn\,(\sin\theta\sin\vartheta\cos\varphi\cos\phi \\ &\quad + \sin\theta\sin\vartheta\sin\varphi\sin\phi + \cos\theta\cos\varphi \\ &= kn\left[\sin\theta\sin\vartheta\,(\cos\varphi\cos\phi + \sin\varphi\sin\phi)\right. \\ &\quad \left. + \cos\theta\cos\vartheta\right] \\ &= kn\left[\sin\theta\sin\vartheta\cos(\phi-\varphi) + \cos\theta\cos\vartheta\right]. \qquad (3.3)\end{aligned}$$

$\cos(\phi-\varphi)$ can be written as $\cos\phi$ without loss of generality, if we choose $\varphi = 0$ so that (3.3) simplifies to

$$\begin{aligned}\underset{\sim}{k}\cdot\underset{\sim}{n} &= kn\left[\sin\theta\sin\vartheta\cos\phi + \cos\theta\cos\vartheta\right] \\ &\equiv kn\Gamma\end{aligned}$$

with

$$\Gamma \equiv \sqrt{(1-\mu^2)(1-\gamma^2)}\cos\phi + \mu\gamma \qquad (3.4)$$

and

$$d\underline{k} = dk\, k^2 d\vartheta \sin\vartheta\, d\phi$$
$$= dk\, k^2 d\mu\, d\phi, \qquad (3.5)$$

where

$$\mu = \cos\vartheta \quad ; \quad \gamma = \cos\theta.$$

Upon substituting (3.4) and (3.5) into (3.1), we obtain

$$n_o(\underset{\sim}{x},t) = \frac{N_o}{(2\pi)^3}\int_{-1}^{1} d\mu \int_0^{2\pi} d\phi \int_0^{\infty} dk\, k^2 e^{-k^2 D_{ie} t} \cos(k r T). \qquad (3.6)$$

The integral with respect to k is

$$\int_0^{\infty} dk\, k^2 e^{-k^2 D_{ie} t} \cos(k r T) = \frac{\sqrt{\pi}}{4 D_{ie} t}\left[1 - \frac{(rT)^2}{2 D_{ie} t}\right] e^{-\frac{(rT)^2}{4 D_{ie} t}}$$

$$= \frac{\sqrt{\pi}}{4 D_{ie} t}\left[1 - g\right] e^{-\frac{g}{2}}, \qquad (3.7)$$

where

$$g = \frac{(rT)^2}{2 D_{ie} t}. \qquad (3.8)$$

Substituting (3.7) in Eq. (3.6) gives

$$n_o(\underset{\sim}{x},t) = \frac{N_o}{32\pi^{3/2} t^{3/2}} \int_{-1}^{1} d\mu\, D_{ie}^{-3/2} \int_0^{2\pi} d\phi\, (1-g) e^{-\frac{g}{2}}. \qquad (3.9)$$

As the function to be integrated is symmetrical about $\mu = 0$ and $\phi = \pi$ we can change the limits of integration to give

$$n_o(\underset{\sim}{x},t) = \frac{N_o}{8\pi^{3/2} t^{3/2}} \int_0^{1} d\mu\, D_{ie}^{-3/2} \int_0^{\pi} d\phi\, (1-g) e^{-\frac{g}{2}}. \qquad (3.10)$$

The double integral of Eq. (3.10) has been evaluated numerically. Results are given in Section 5.

4. ANOMALOUS DIFFUSION FROM A SEPARATION OF THE PLASMA INHOMOGENEITY

a. General Behavior

The most striking and interesting feature revealed from the linear solution (3.10) and the nonlinear solution (2.13) is the anomalous splitting, which is discussed below:

It is apparent that n_o will be a maximum when $g = 0$. This occurs at points where $\underset{\sim}{n} = 0$. The points of maximum density therefore occur at

$$\underset{\sim}{x} = \underset{\sim}{V}_{ie}(\mu)\, t \tag{4.1}$$

Since the integration of (3.10) includes all values of μ, there is a line of maximal densities with extrema located at $\underset{\sim}{V}_{ie}(\mu=0)t$ and $\underset{\sim}{V}_{ie}(\mu=1)t$ respectively, separated by a saddle point of low density. Such a line of extrema does not arise when $\underset{\sim}{V}_{ie}$ is a constant as in classical diffusion, but only when $\underset{\sim}{V}_{ie}$ is a variable, specifically a function of μ, as derived in the present theory. Therefore, the diffusion with a locus of maxima will be called anomalous diffusion. The fundamental maximum is the maximum located at $\underset{\sim}{V}_{ie}(\mu=0)t$. The velocity $\underset{\sim}{V}_{ie}(\mu=0)t$ has been defined by (2.14). The other maximum, located at $\underset{\sim}{V}_{ie}(\mu=1)t$ is called the secondary maximum, with velocity given by (2.16). Equation (3.10) with $\underset{\sim}{V}_{ie}$ and $\underset{\sim}{D}_{ie}$ defined by (2.6) and (2.7), describes the evolution of density, $n_o(\underset{\sim}{x},t)$ in the presence of drift by neutral wind and external electric field. To be specific, two special cases will be discussed:

(i) Case A - Plasma inhomogeneity in a neutral wind transverse to the magnetic field, with

$$\underset{\sim}{E}_o = 0 . \tag{4.2}$$

(ii) Case B - Plasma inhomogeneity in an ambient electric field which is perpendicular to the magnetic field, with

$$\underset{\sim}{U} = 0 . \tag{4.3}$$

b. Plasma in a Neutral Wind

Under the conditions (4.2) of Case A, we reduce II,(3.9) to

$$\underset{\sim}{V}_a = \frac{1}{1+\kappa_a^2}\,\underset{\sim}{U} + \frac{\kappa_a}{1+\kappa_a^2}\,\underset{\sim}{U}\times\hat{e}_B \tag{4.4}$$

and a further substitution of (4.4) into (2.6) reduces (2.6) to

$$\underset{\sim}{V}_{ie}(\mu) = \frac{1}{A(\mu)}\left[(1+\kappa_e^2\mu^2)\underset{\sim}{U} + \kappa_i\kappa_e^2\mu^2\,\underset{\sim}{U}\times\hat{e}_B\right], \tag{4.5}$$

where

$$A(\mu) = 1 + |\kappa_i\kappa_e| + \kappa_e^2(1+\kappa_i^2)\mu^2 .$$

In writing (4.5) we have made use of the approximation $|\kappa_e| \gg \kappa_i$, valid for most plasma. The velocities of the two maxima are obtained from (4.5) with

$$\underset{\sim}{V}_{ie}(\mu=0) = \frac{1}{1+|\kappa_i\kappa_e|}\,\underset{\sim}{U} \equiv \underset{\sim}{V}_\perp \tag{4.6}$$

and

$$\underset{\sim}{V}_{ie}(\mu=1) = \frac{1}{A(\mu=1)}\left[(1+\kappa_e^2)\underset{\sim}{U} + \kappa_i\kappa_e^2\,\underset{\sim}{U}\times\hat{e}_B\right] \equiv \underset{\sim}{V}_{11}, \tag{4.7}$$

where

$$A(\mu=1) = 1 + |\kappa_e\kappa_i| + \kappa_e^2(1+\kappa_i^2) .$$

On the other hand, the ambipolar diffusion coefficient as defined by (2.7) reduces to

$$D_{ie}(\mu) = k(T_e + T_i)\left[\frac{m_i \nu_i (1+\kappa_i^2)}{1+\kappa_i^2\mu^2} + \frac{m_e \nu_e (1+\kappa_e^2)}{1+\kappa_e^2\mu^2}\right]^{-1}. \tag{4.8}$$

For numerical solutions it is desirable to express D_{ie} in terms of $D_{\|i}$ with

$$T_e = T_i = T, \tag{4.9}$$

simplifying (4.8) to

$$D_{ie}(\mu) = \frac{2 D_{\|i}}{1+(\kappa_i \kappa_e)^2}\left[\frac{1+\kappa_i^2}{1+\kappa_i^2\mu^2} + \frac{1+\kappa_e^2}{1+\kappa_e^2\mu^2}\right]^{-1}, \tag{4.10}$$

where

$$D_{\|i} = \frac{kT}{m_i \nu_i^4},$$

on account of II,(2.8).

An examination of Eq. (4.6) and (4.7) show that the fundamental maximum moves in the same direction as the neutral wind $\underset{\sim}{U}$ i.e., in the x_1- direction while the secondary maximum moves along the direction making an angle α with the x_1- axis, and given by,

$$\tan\alpha = \frac{\kappa_i \kappa_e^2}{1+\kappa_e^2} \simeq \kappa_i \tag{4.11}$$

as shown in Fig. (3.1).

Two distances d_1 and d_2 are characteristic of locations of the maxima, where d_1 is the distance of the fundamental maximum from the origin, and

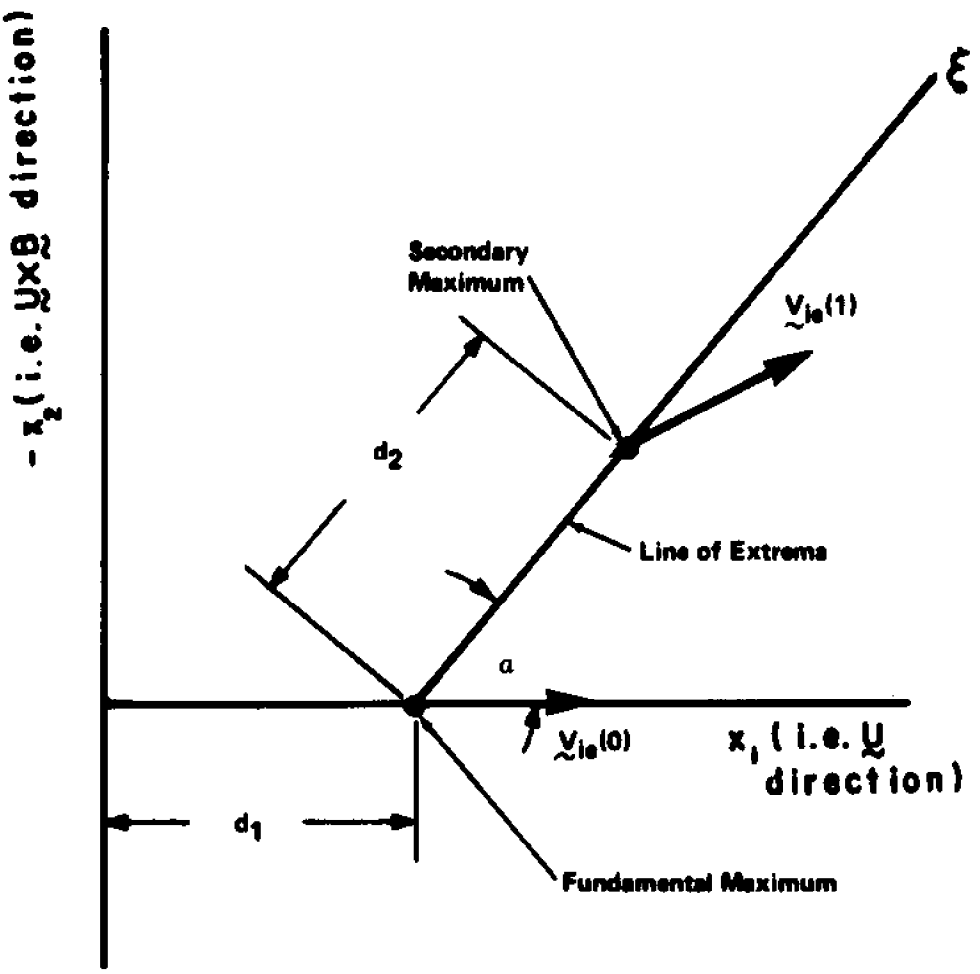

Fig. 3.1. Fundamental and Secondary Maxima.

d_2 is the distance between the two maxima. We have

$$d_1 = \frac{Ut}{1 + |\kappa_i \kappa_e|} , \tag{4.12}$$

$$d_2 = \frac{Ut\,|\kappa_i \kappa_e|\,(|\kappa_e| - \kappa_i)}{(1 + |\kappa_i \kappa_e|)\sqrt{(1+\kappa_i^2)(1+\kappa_e^2)}} . \tag{4.13}$$

For $\kappa_e \gg \kappa_i$ and $\kappa_i \kappa_e \gg 1$, these expressions reduce to,

$$d_1 = \frac{Ut}{\kappa_i \kappa_e} , \tag{4.14}$$

$$d_2 = \frac{Ut}{\sqrt{1+\kappa_i^2}} . \tag{4.15}$$

From (4.14) and (4.15) it can be concluded that

(i) The secondary maximum moves faster than the fundamental maximum;

(ii) The distance between the maxima increases with time leading to the splitting of the inhomogeneity;

(iii) The splitting will be more pronounced, the smaller the value of κ_i .

c. Plasma in an Electric Drift

Under the conditions (4.3) of Case (B), II,(3.9) reduces to

$$\underset{\sim}{V}_a = \frac{\kappa_a}{1+\kappa_a^2} \frac{c}{B} \left[\underset{\sim}{E}_0 + \kappa_a \underset{\sim}{E}_0 \times \hat{e}_B \right] . \tag{4.16}$$

We introduce a drift speed

$$\underset{\sim}{W}_0 = - \frac{c}{B} \underset{\sim}{E}_0 \times \hat{e}_B \tag{4.17}$$

to simplify (4.16) to

$$\underset{\sim}{V}_a = \frac{\kappa_a}{1+\kappa_a^2}\left[-\kappa_a \underset{\sim}{W}_o + \underset{\sim}{W}_o \times \hat{e}_B\right] \tag{4.18}$$

and reduce (2.6) to

$$\underset{\sim}{V}_{ie}(\mu) = -\underset{\sim}{W}_o + \frac{1}{A(\mu)}\left[(1+\kappa_e\mu^2)\underset{\sim}{W}_o + \kappa_i\kappa_e\mu^2 \underset{\sim}{W}_o \times \hat{e}_B\right]. \tag{4.19}$$

Eq. (4.19) reduces to the velocities of the two maxima:

$$\underset{\sim}{V}_{ie}(\mu=0) = -\underset{\sim}{W}_o + \frac{\underset{\sim}{W}_o}{1+|\kappa_i\kappa_e|} \equiv \underset{\sim}{V}_\perp , \tag{4.20}$$

$$\underset{\sim}{V}_{ie}(\mu=1) = -\underset{\sim}{W}_o + \frac{1}{A(\mu=1)}\left[(1+\kappa_e^2)\underset{\sim}{W}_o + \kappa_i\kappa_e^2 \underset{\sim}{W}_o \times \hat{e}_B\right] \equiv \underset{\sim}{V}_\parallel . \tag{4.21}$$

A comparison between Eq. (4.5) and (4.19) shows that the ambipolar drifts for the two cases of the diffusions in a neutral wind and in an external electrical field are similar, except for a shift of a speed $-\underset{\sim}{W}_o$ in the case of the diffusion in an electric field. This occurs because the $\underset{\sim}{E}\times\underset{\sim}{B}$ field transports the plasma with a constant speed $-\underset{\sim}{W}_o$. Because of the similarity, we shall not present computational data or graphs for the diffusion by an electric drift, but restrict ourselves to the diffusion by a neutral wind.

5. NUMERICAL SOLUTION OF THE LINEARIZED EQUATIONS OF DIFFUSION

We now elaborate on the numerical computation of the expression for the diffusion in Eq. (3.10). In order to express the variables in terms of dimensionless parameters, we introduce a reference length,

$$\ell = \frac{2D_{\parallel i}}{U} , \tag{5.1}$$

a reference time

$$\tau = \frac{D_{\parallel i}}{U^2} , \tag{5.2}$$

a reference density

$$n_1 = \frac{N_0}{8\pi^{3/2} t^{3/2}} \int_0^1 d\mu \, D_{ie}^{-3/2} , \tag{5.3}$$

which represents the density at $x=0$ for a diffusion without drift, i.e., with $V_{ie}=0$. We obtain the following dimensionless variables,

$$\begin{aligned} \tilde{t} &= t/\tau , \\ \tilde{x} &= x/\ell , \\ \tilde{n}_0 &= n_0/n_1 . \end{aligned} \tag{5.4}$$

It is to be remembered that, by eliminating U between (5.1) and (5.2), we obtain

$$D_{\parallel i} = \ell^2/4\tau ,$$

a relationship well known in diffusion. That is the reason the reference length has been defined with a coefficient of 2 in (5.1).

The coordinates are chosen so that $\underset{\sim}{U}$ is in the x_1 direction, $-(\underset{\sim}{U}\times\underset{\sim}{B})$ in the x_2 direction and the magnetic field $\underset{\sim}{B}$ in the x_3 direction with unit vectors $\hat{x}_1, \hat{x}_2, \hat{x}_3$ respectively. Then Eq. (3.10) can be rewritten in the following dimensionless form,

$$\tilde{n}_0(\tilde{x},t) = \frac{1}{\pi}\left[\int_0^1 d\mu (\tilde{D}_{ie})^{-\frac{3}{2}}\right]^{-1} \int_0^1 d\mu (\tilde{D}_{ie})^{-\frac{3}{2}} \int_0^\pi d\phi (1-g) e^{-\frac{g}{2}} , \tag{5.5}$$

where

$$\tilde{D}_{ie}(\mu) \equiv \frac{D_{ie}(\mu)}{D_{\parallel i}} = \frac{2}{1+(\kappa_i\kappa_e)^2}\left[\frac{1+\kappa_i^2}{1+\kappa_i^2\mu^2} + \frac{1+\kappa_e^2}{1+\kappa_e^2\mu^2}\right]^{-1} , \tag{5.6}$$

$$g = \frac{|2\tilde{x} - \tilde{\underset{\sim}{V}}_{ie} t|^2 \Gamma^2}{2 \tilde{D}_{ie} t} , \tag{5.7}$$

$$\tilde{\underset{\sim}{V}}_{ie}(\mu) \equiv \frac{\underset{\sim}{V}_{ie}}{U} = \frac{\left[\frac{\kappa_i}{1+\kappa_i^2}(1-\mu^2)+\kappa_i\mu^2\right]\tilde{\underset{\sim}{V}}_e + \left[\frac{|\kappa_e|}{1+\kappa_e^2}(1-\mu^2)+|\kappa_e|\mu^2\right]\tilde{\underset{\sim}{V}}_i}{\left[\frac{\kappa_i}{1+\kappa_i^2}+\frac{|\kappa_e|}{1+\kappa_e^2}\right](1-\mu^2)+(\kappa_i+|\kappa_e|)\mu^2}, \tag{5.8}$$

$$\begin{aligned} \tilde{\underset{\sim}{V}}_i &\equiv \frac{\underset{\sim}{V}_i}{U} = \frac{1}{1+\kappa_i^2}(\tilde{x}_1 - \kappa_i \tilde{x}_2), \\ \tilde{\underset{\sim}{V}}_e &\equiv \frac{\underset{\sim}{V}_e}{U} = \frac{1}{1+\kappa_e^2}(\tilde{x}_1 + |\kappa_e| \tilde{x}_2). \end{aligned} \tag{5.9}$$

Here the expression for $\tilde{\underset{\sim}{V}}_{ie}$, (5.8) is the exact formulation obtained from (2.6), rather than the approximation given in (4.5).

Using a digital computer, the required single and double integration in Eq. (3.10) are performed by an application of Simpson's rule. The ranges of $\mu(0 \to 1)$ and $\phi(0 \to \pi)$ are subdivided into 75 increments each. Density profiles are calculated for planes parallel and transverse to the magnetic fields, with different transport coefficients κ_i, κ_e.

Results are shown in Fig. (3.2) to (3.14) in the form of contours of constant densities. These figures clearly show the interesting features of the splitting of the inhomogeneity and the elongation of the plasma in the direction of the magnetic field. The above features are accentuated by choosing low values of the transport coefficients κ_i and κ_e.

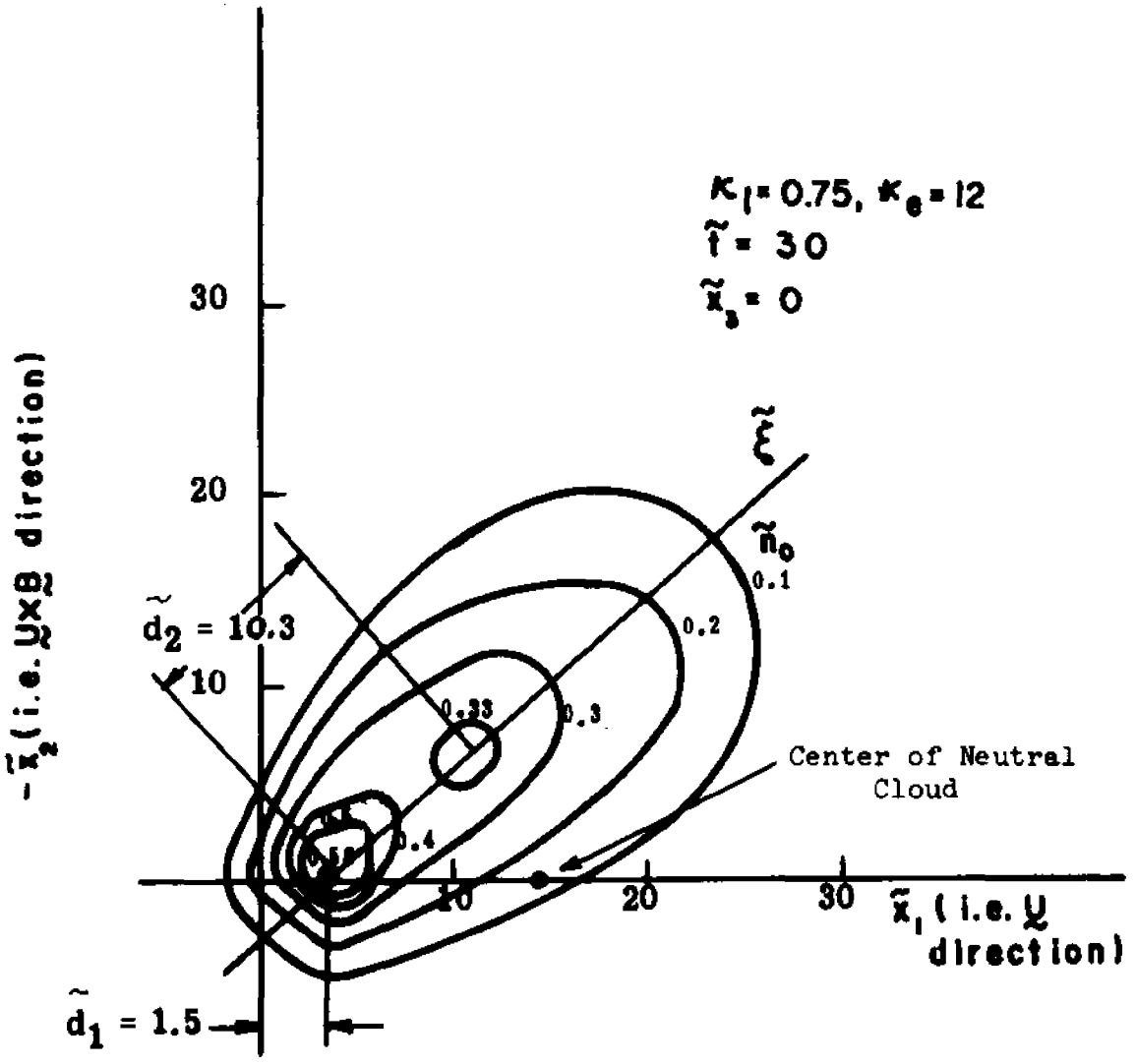

Fig. 3.2. Early Morphology ($\tilde{t} = 30$), in a Transverse Plane at $\tilde{x}_3 = 0$, Ratio $\kappa_e/\kappa_i = 16$.

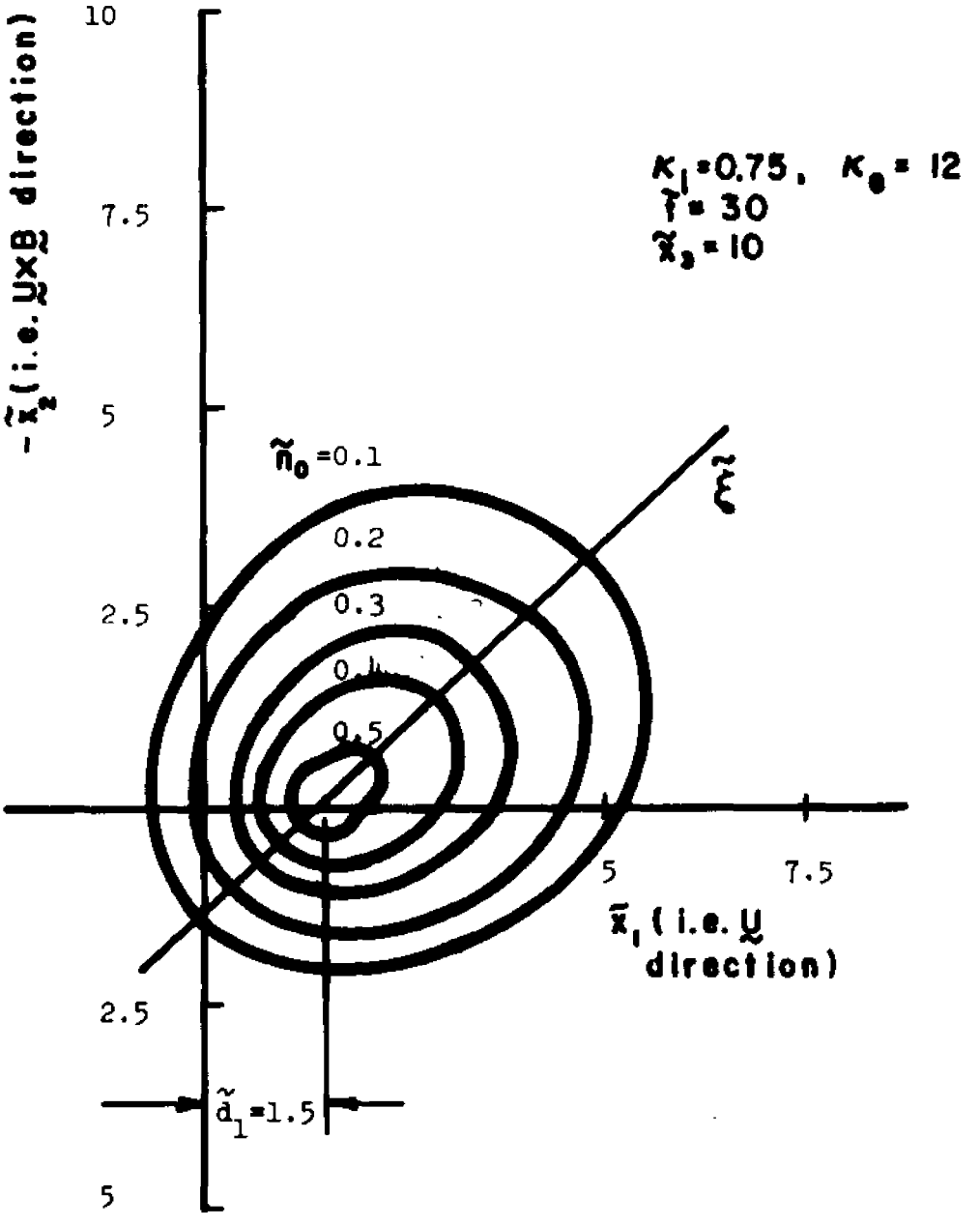

Fig. 3.3. Early Morphology ($\tilde{t}$ = 30), in a Transverse Plane at $\bar{x}_3$ = 10, Ratio κ_e / κ_i = 16.

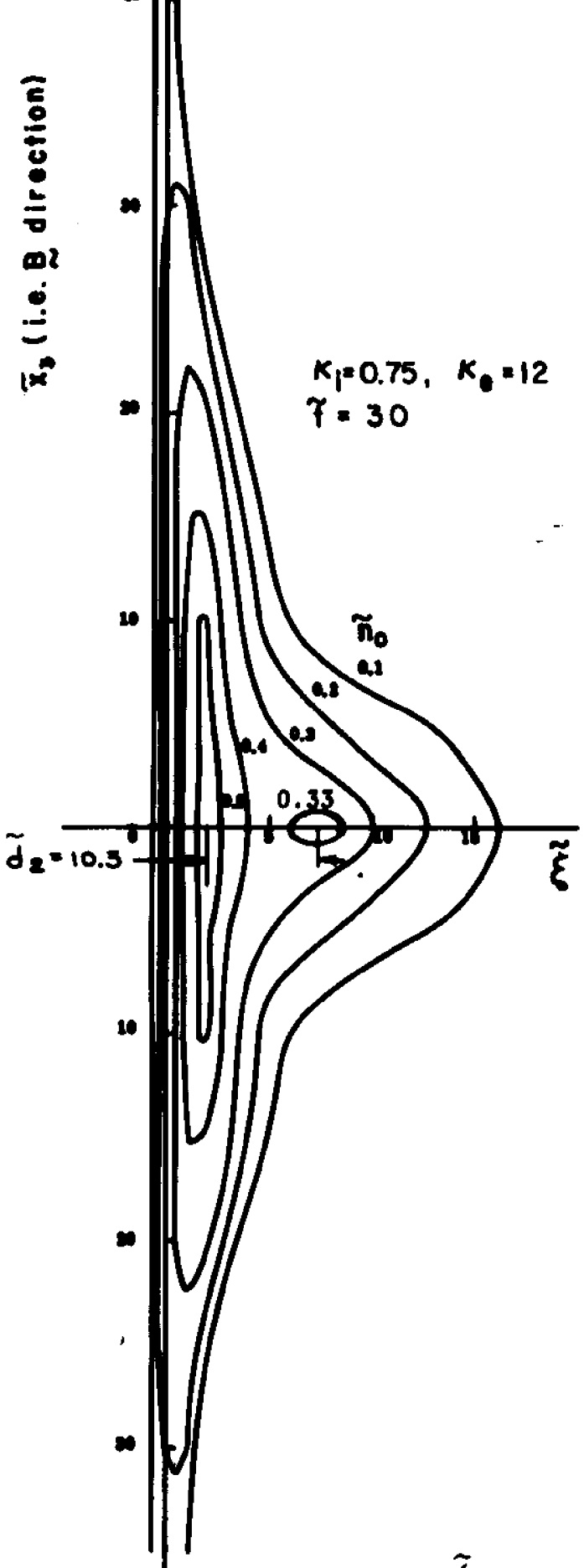

Fig. 3.4. Early Morphology ($\tilde{t}$ = 30), in the ($\tilde{\xi}$, $\tilde{x}_3$) Plane, Ratio κ_e/κ_i = 16.

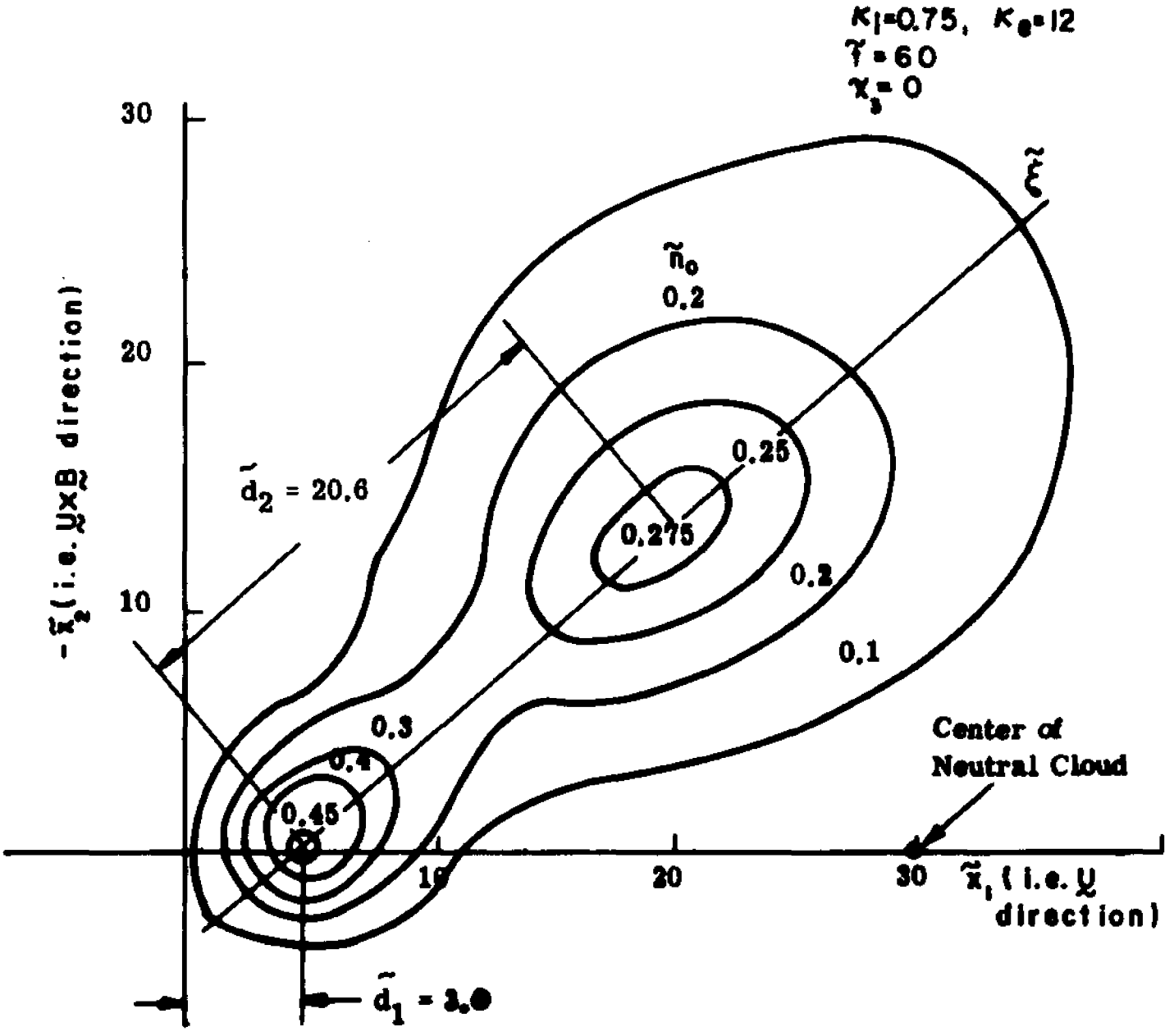

Fig. 3.5. Later Morphology ($\tilde{t}$ = 60), in the Transverse Plane at $\tilde{x}_3$ = 0, Ratio K_e/K_i = 16.

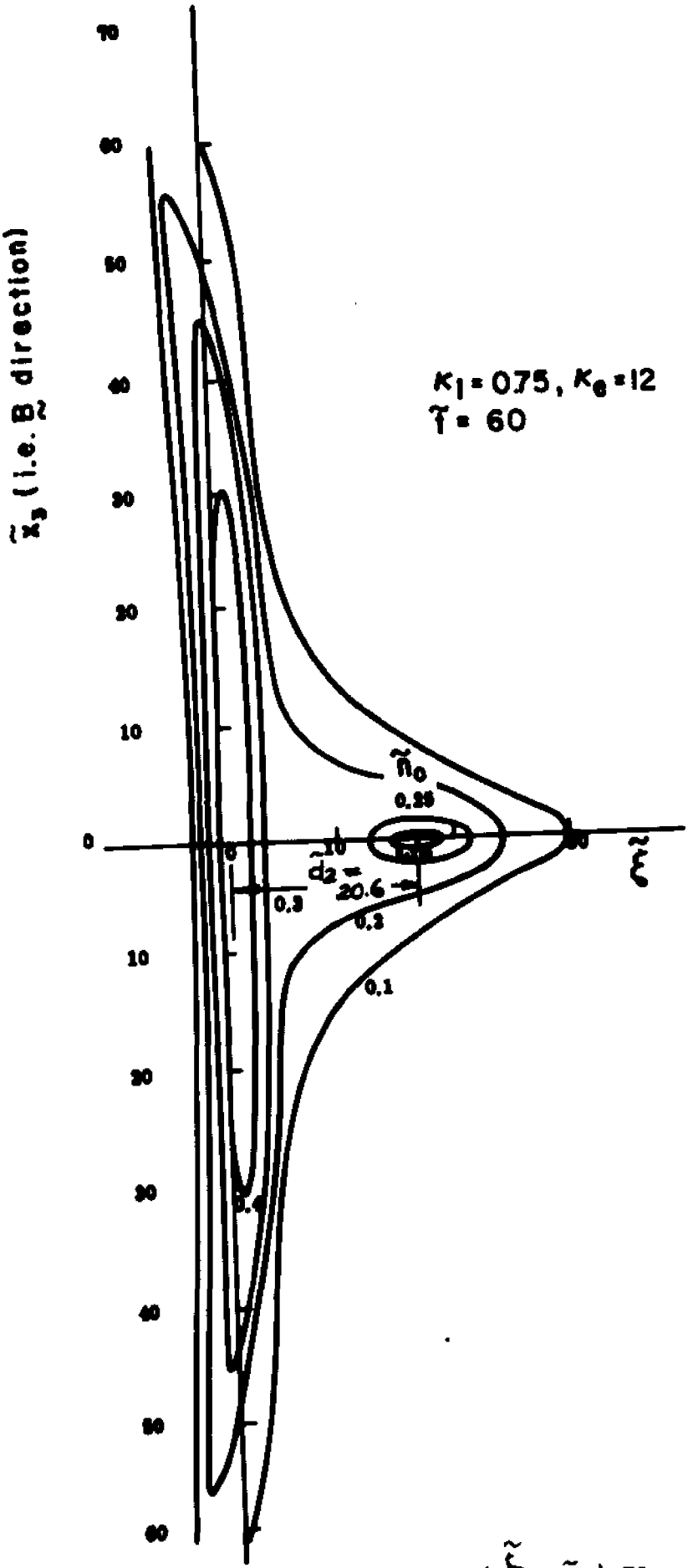

Fig. 3.6. Later Morphology ($\tilde{t} = 60$), in the ($\tilde{\xi}$, $\tilde{x}_3$) Plane, Ratio $\kappa_e/\kappa_i = 16$.

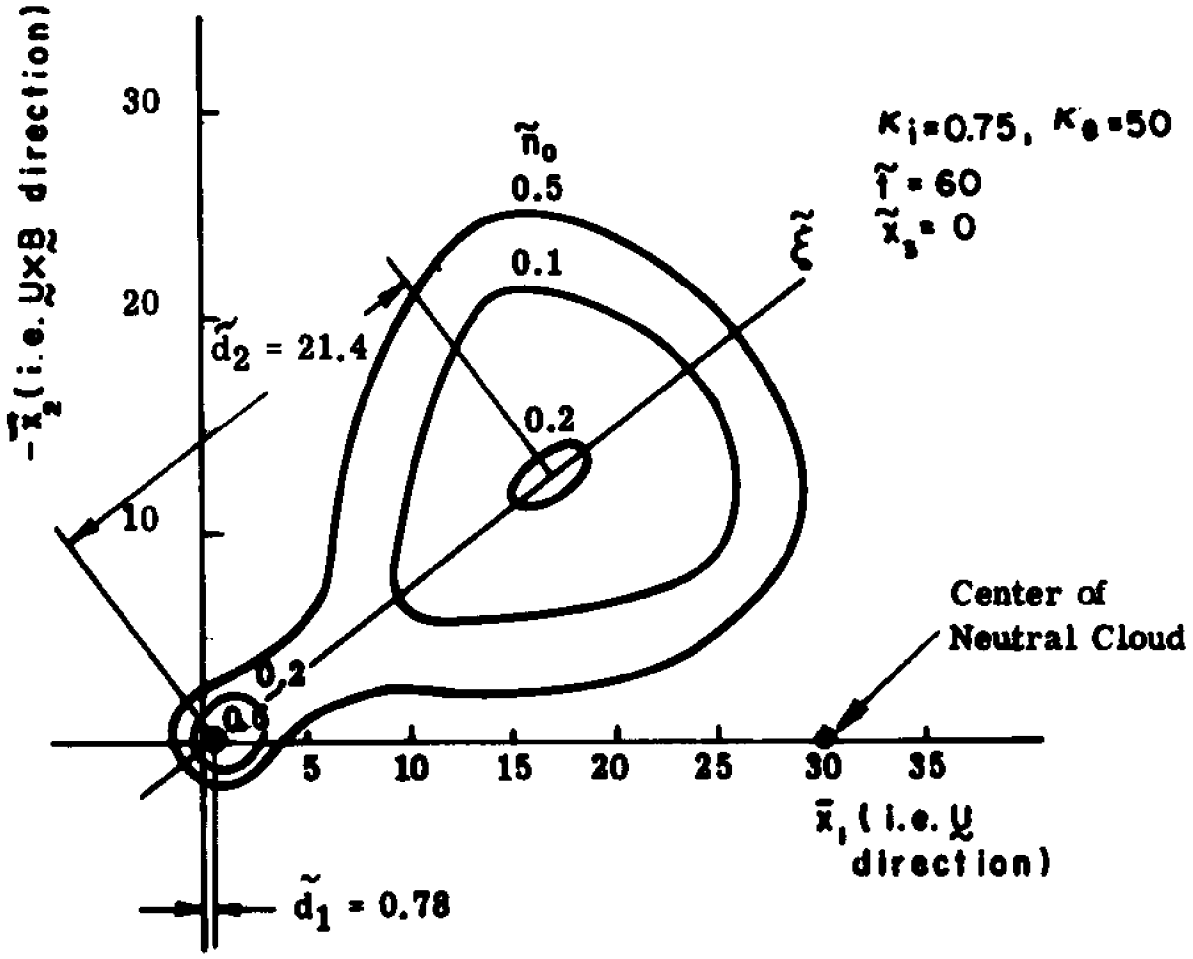

Fig. 3.7. Morphology at Higher Ratio κ_e/κ_i = 200/3, in the Transverse Plane ($\tilde{x}_1$, $\tilde{x}_2$).

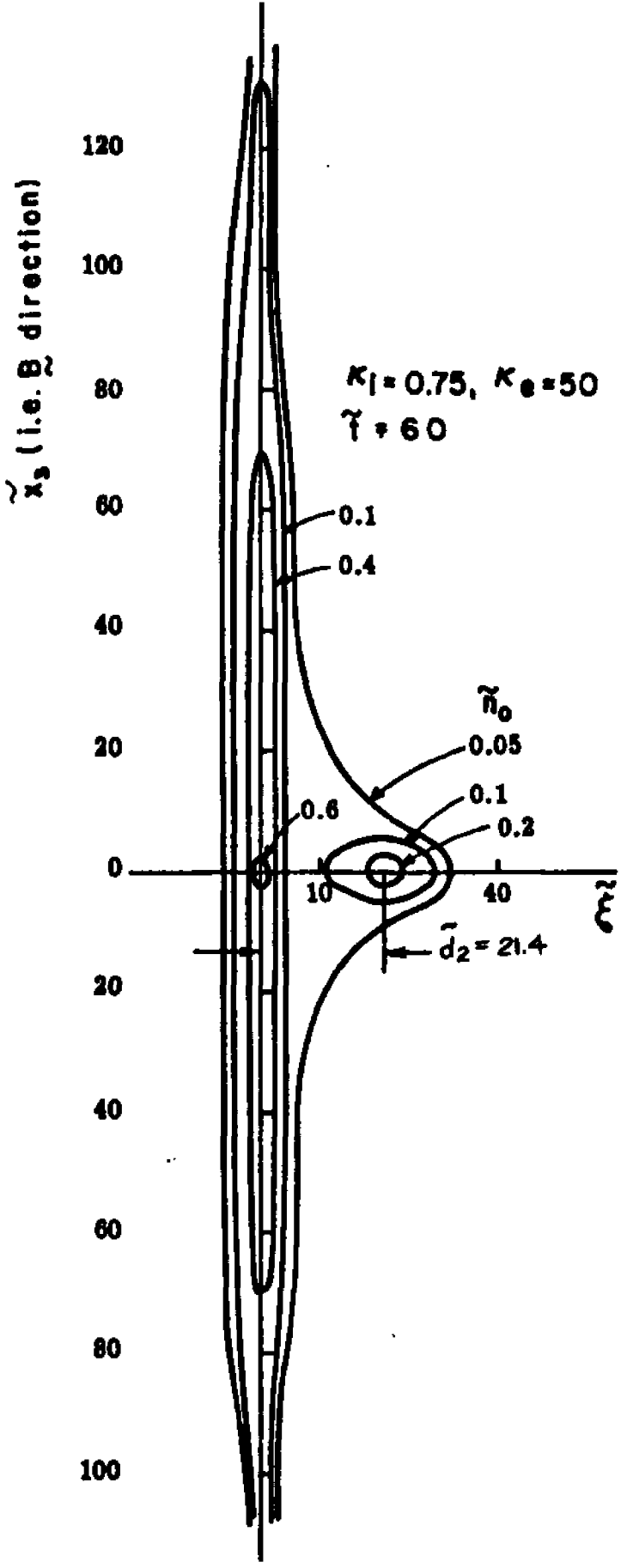

Fig. 3.8. Morphology at Higher Ratio κ_e/κ_i = 200/3, in the Parallel Plane ($\tilde{\xi}$, $\tilde{x}_3$).

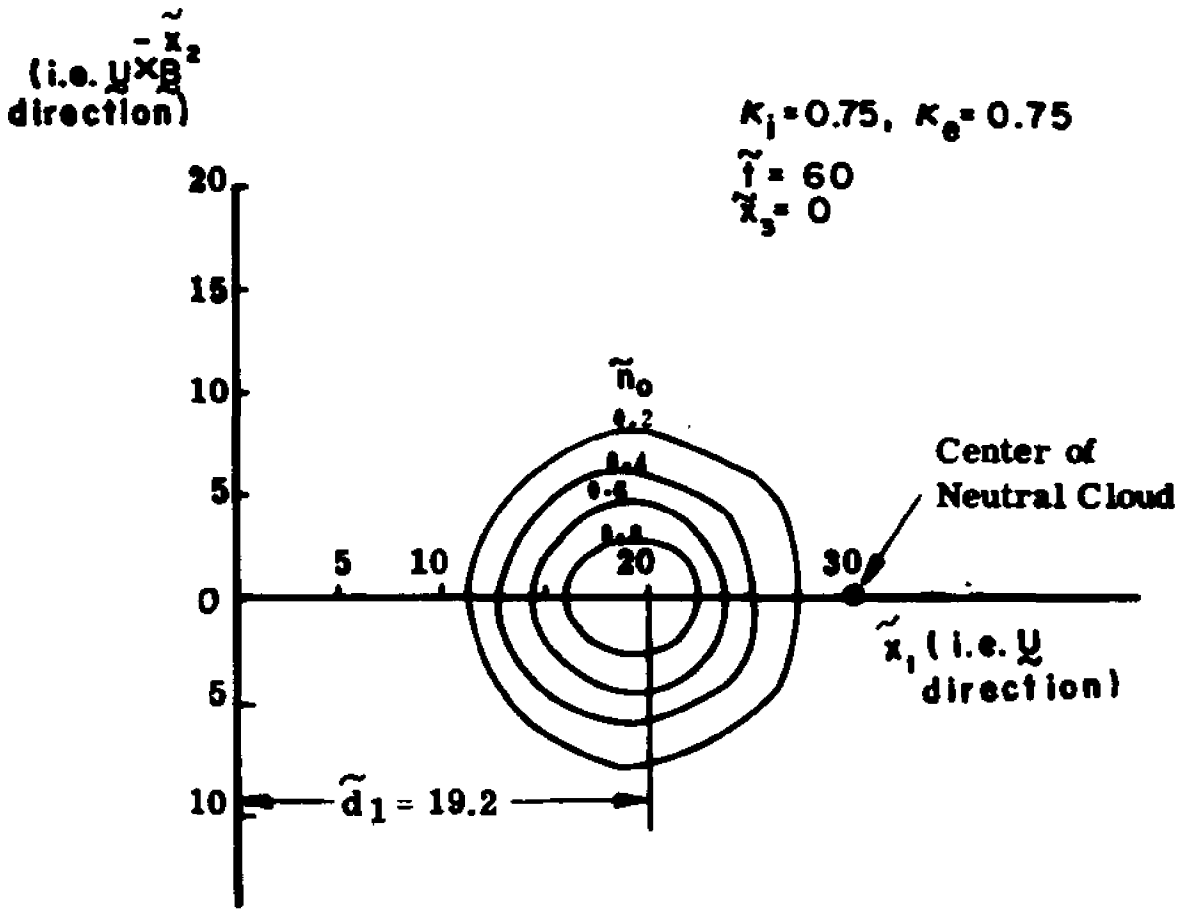

Fig. 3.9. Morphology with Equal $\kappa_i = \kappa_e$ of Small Elongation, $\ell_\parallel / \ell_\perp = 1 + \kappa_i \kappa_e = 1.56$ in the Transverse Plane $(\tilde{x}_1, \tilde{x}_2)$.

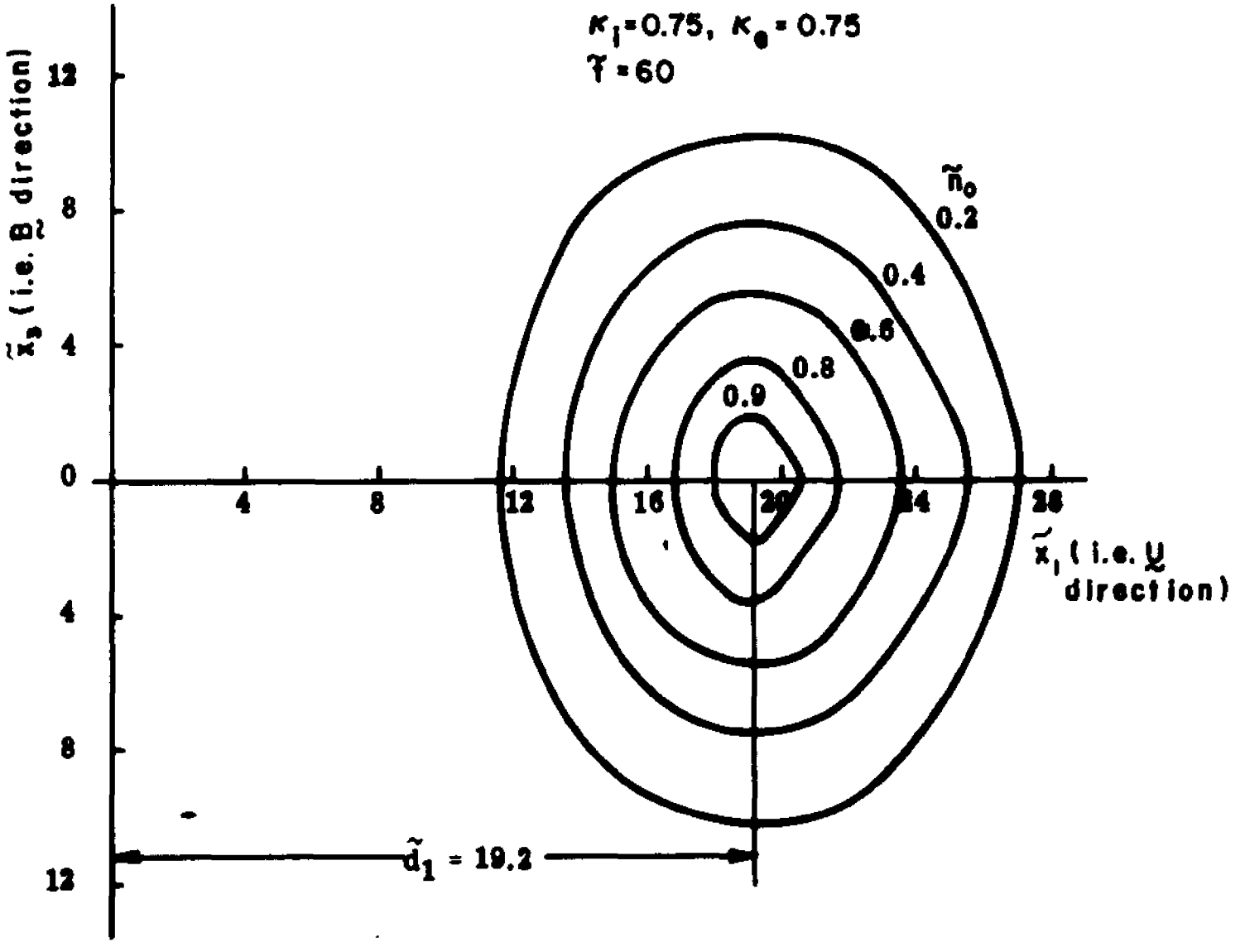

Fig. 3.10. Morphology with Equal $\kappa_i = \kappa_e$ of Small Elongation, $\ell_\parallel/\ell_\perp = 1+\kappa_i\kappa_e = 1.56$ in the Parallel Plane $(\tilde{x}_1, \tilde{x}_3)$.

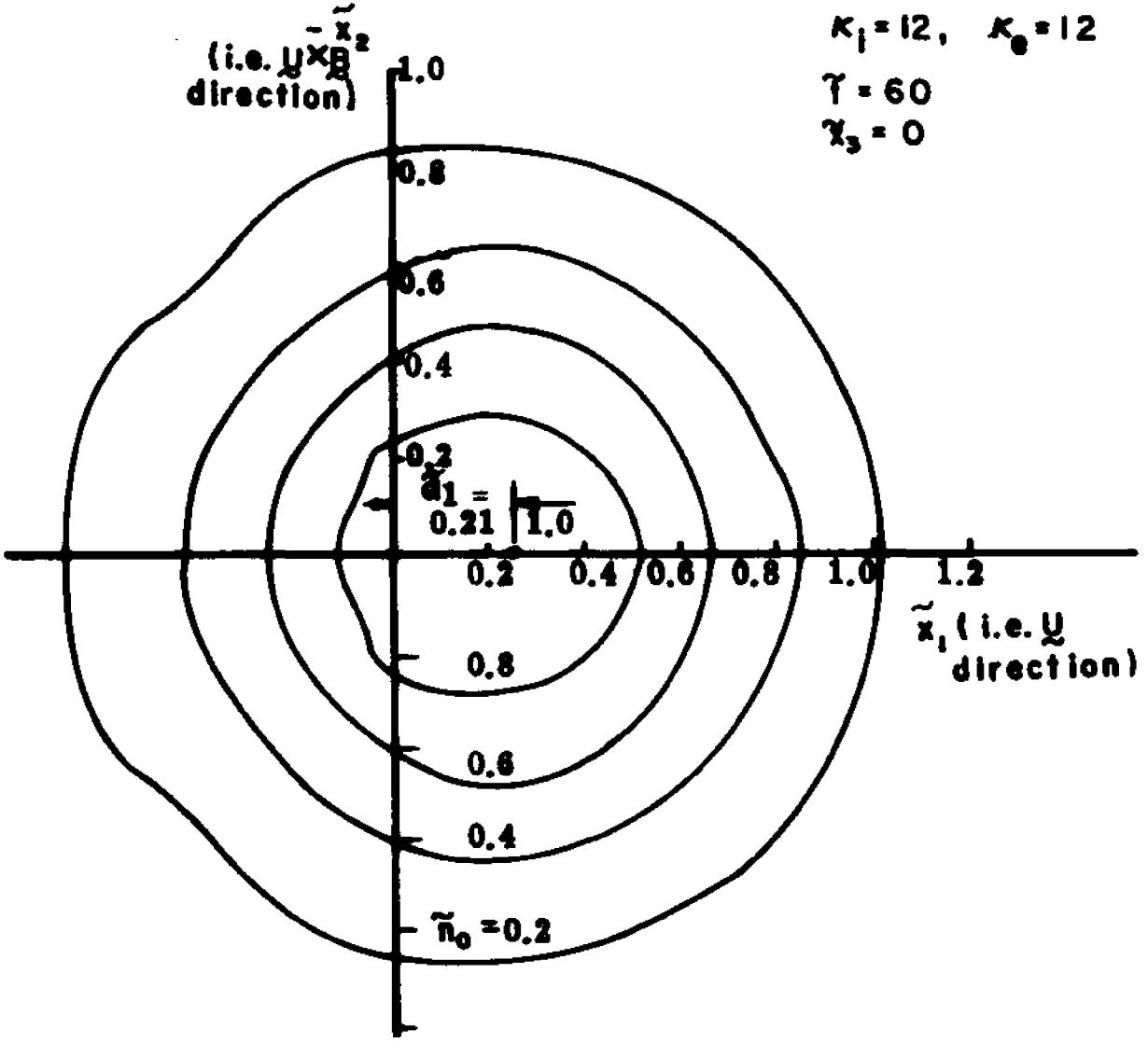

Fig. 3.11. Morphology with Equal $\kappa_i = \kappa_e$ of Large Elongation, $\ell_\parallel / \ell_\perp = 1 + \kappa_i \kappa_e = 145$, in the Transverse Plane $(\tilde{x}_1, \tilde{x}_2)$.

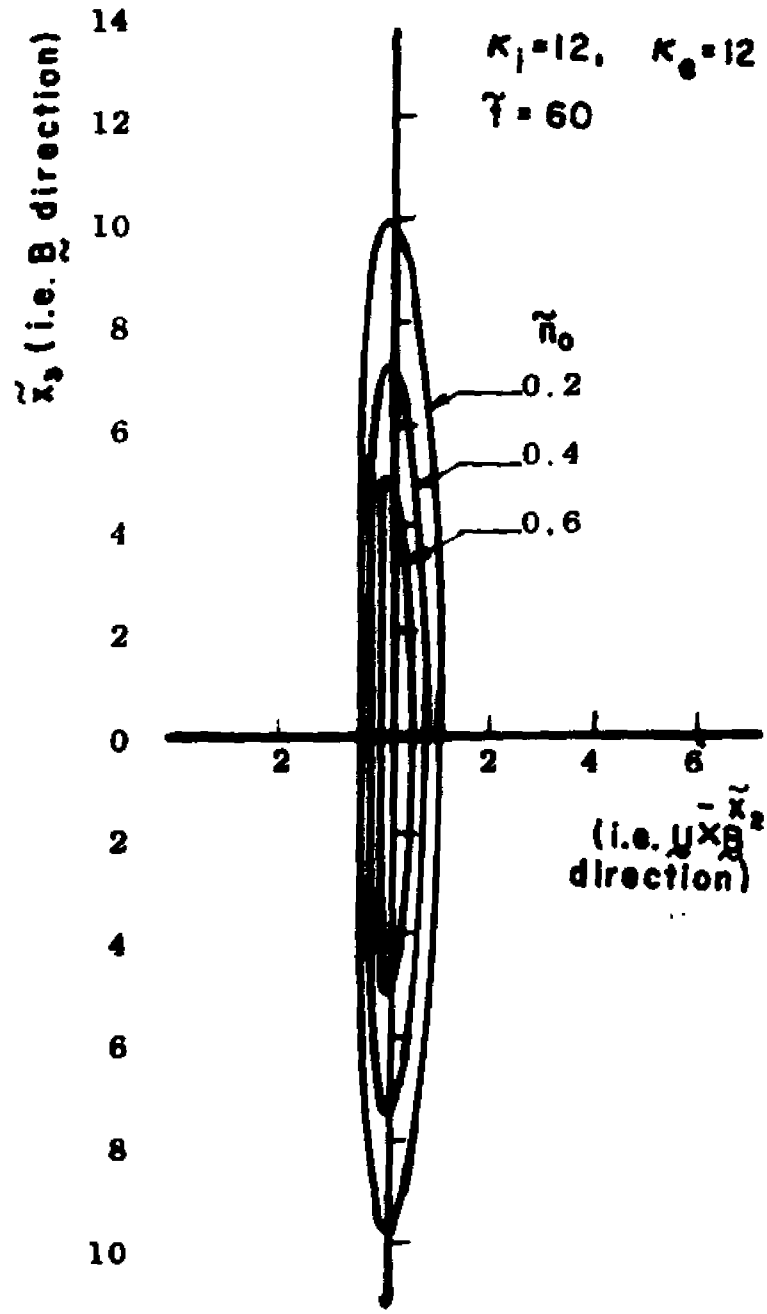

Fig. 3.12. Morphology with Equal $\kappa_i = \kappa_e$ of Large Elongation, $\ell_{\parallel}/\ell_{\perp} = 1 + \kappa_i \kappa_e = 145$, in the Parallel Plane $(\tilde{x}_2, \tilde{x}_3)$

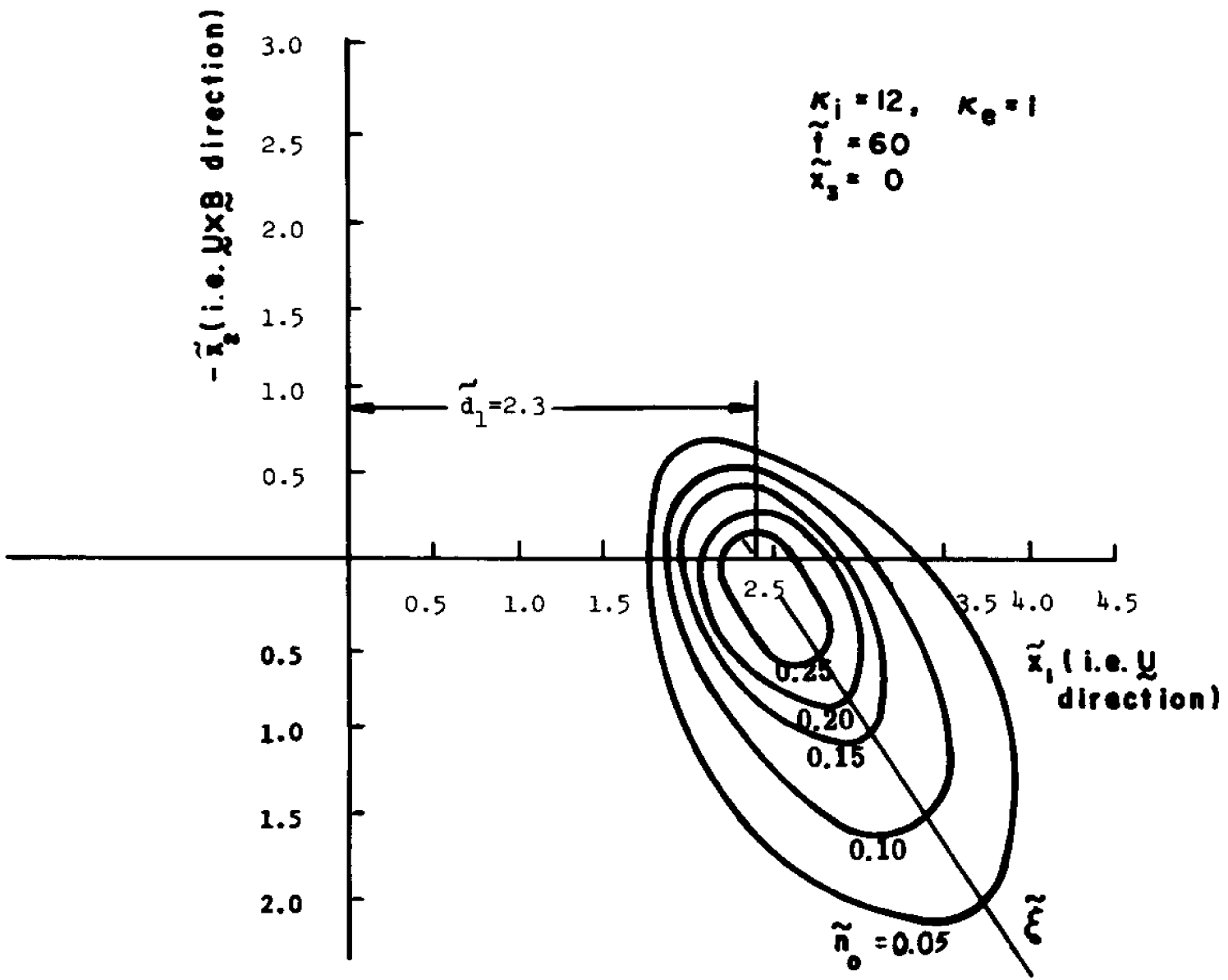

Fig. 3.13. Morphology with Small Ratio κ_e / κ_i = 1/12 in the Transverse Plane $(\tilde{x}_1, \tilde{x}_2)$.

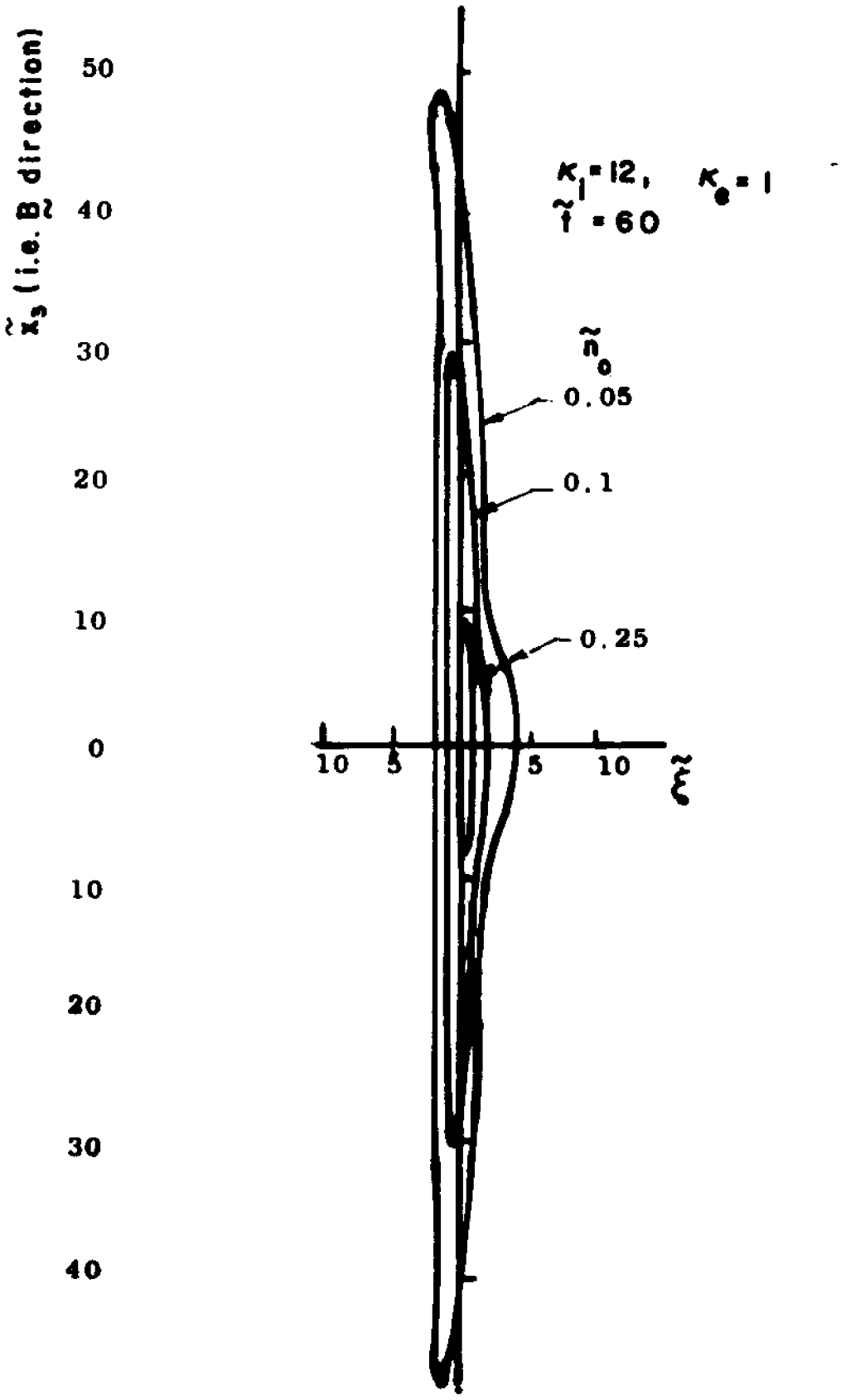

Fig. 3.14. Morphology with Small Ratio $\kappa_e/\kappa_i = 1/12$, in the Parallel Plane ($\tilde{\xi}$, $\tilde{x}_3$).

For completeness a case where $\kappa_e < \kappa_i$ has also been included. As is discussed in Chapter V, such low values of κ_i and κ_e are reasonable for turbulent plasmas. A summary of the characteristics of the cases presented is given in Table (3.1). Of particular interest are the distances d_1 and d_2, which give the separation of the two maxima, and as such, indicate the magnitude of the drift and the degree of splitting. Included in the table are also the displacements of the center of a similar neutral cloud.

The specific features of the numerical results are now discussed by means of the following figures. As mentioned earlier, the x_3- axis is chosen to be along the magnetic field, called the longitudinal direction, the x_1- axis is along the neutral wind velocity, and therefore the x_2- axis becomes parallel to

$$-\underset{\sim}{U} \times \underset{\sim}{B}/c \ .$$

The plane x_1, x_2 is called the transverse plane. The plasma diffuses more rapidly in the longitudinal direction than in the transverse direction, in view of the relationship

$$D_\perp / D_{11} \ll 1 \ .$$

As shown in Fig. (3.1), the 2 maxima develop along the axis at an angle α from the x_1- axis, with characteristic distances d_1 and d_2.

Figs.(3.2) and (3.3) represent two transverse cross sections at $\tilde{x}_3 = 0$ and $\tilde{x}_3 = 10$, respectively, while Fig. (3.4) represents a cross section in the $(\tilde{\xi}, \tilde{x}_3)$ plane. At the early time, chosen to be $\tilde{t} = 30$, the development of the second maximum is found in Fig. (3.2) at $\tilde{d}_2 = 10.3$

Table 3.1 Characteristics of the Diffusion of Plasma and Neutral Clouds

Figure No.	κ_i	κ_e	$\tilde{t}$	α, degrees	$\tilde{d}_1$	$\tilde{d}_2$	$\tilde{d}$ of neutral clouds
3.2-3.4	0.75	12.0	30	41.5	1.5	10.3	15
3.5-3.6	0.75	12.0	60	41.5	3.0	20.6	30
3.7-3.8	0.75	50.0	60	38.1	0.78	21.4	30
3.9-3.10	0.75	0.75	60	90.0	19.2	0	30
3.11-3.12	12.0	12.0	60	90.0	0.21	0	30
3.13-3.14	12.0	1.0	60	130.0	2.3	19.3	30

and is not apparent in Fig. (3.3) which is a cross section at a distance too far removed from the center for d_2 to appear. On the other hand Fig. (3.4) clearly shows the development of the second maximum as well as the elongation of the plasma along the magnetic field.

The later development of the plasma diffusion at $\tilde{t} = 60$ is given in Figs. (3.5) and (3.6) in the $(\tilde{x}_1, \tilde{x}_2)$ plane and $(\tilde{\xi}, \tilde{x}_3)$ plane respectively. These plots show a more pronounced effect of splitting of the plasma cloud into two maxima.

It is to be expected that the values κ_e and κ_i have an effect on the diffusion of the plasma. While the diffusion with the ratio $\kappa_e/\kappa_i = 16$ is represented in Figs. (3.5) and (3.6) the diffusion with a higher ratio of $\kappa_e/\kappa_i = \frac{200}{3}$ is given by Figs. (3.7) and (3.8). According to Eqs. (4.14) and (4.15), we have

$$\frac{d_2}{d_1} = \frac{\kappa_e}{\kappa_i}$$

indicating a more significant development of the 2nd maximum with a high ratio κ_e/κ_i. This is clearly shown in Fig. (3.7) with $\kappa_e/\kappa_i = \frac{200}{3}$ as compared to Fig. (3.5) with $\kappa_e/\kappa_i = 16$. Since the elongation $\ell_\parallel/\ell_\perp$ can be approximated by

$$\frac{\ell_\parallel}{\ell_\perp} = \left(\frac{D_\parallel}{D_\perp}\right)^{\frac{1}{2}} \tag{5.10}$$

and with the relationship for the ratio $\frac{D_\parallel}{D_\perp}$ given by Eq. (2.18) we obtain,

$$\frac{\ell_\parallel}{\ell_\perp} = 1 + |\kappa_i \kappa_e| \simeq \kappa_i \kappa_e \,. \tag{5.11}$$

Thus we see that the elongation is proportioned to $\kappa_i \kappa_e$. The larger elongation is shown in Fig. (3.8) with $\kappa_i \kappa_e = 37.5$ as compared to Fig. (3.6) with $\kappa_i \kappa_e = 9$.

Fig. (3.9) to (3.12) are plotted for $\kappa_i = \kappa_e$. According to Eq. (4.13), for this condition $d_2 = 0$, and no separation of maxima occurs. Since according to Eq. (5.11), the elongation is proportioned to $\kappa_i \kappa_e$ we find a small elongation of the cloud with $\ell_{\parallel}/\ell_{\perp} = 1 + \kappa_i \kappa_e = 1.56$ in Fig. (3.10) and a larger elongation with $\ell_{\parallel}/\ell_{\perp} = 145$ in Fig. (3.12).

In the above we have discussed mainly the cases with $\kappa_e \gg 1$ and $\kappa_e/\kappa_i \gg 1$ which are illustrated in Figs. (3.2) to (5.12). The fundamental feature is the development of the secondary maximum at $d_2 > 0$ in the $\tilde{\xi}$ axis. The opposite circumstance with

$$\kappa_i \gg 1 \qquad\qquad \kappa_e/\kappa_i \ll 1$$

is expected to yield a different configuration. In such a case, we have from Eq. (4.13)

$$d_2 \cong \frac{-Ut}{\sqrt{1+\kappa_e^2}} \tag{5.12}$$

which shows that the 2nd maximum develops at a negative distance d_2. A plot for $\kappa_i = 12$, $\kappa_e = 1$ for which $d_2 = -19.3$ is shown in Fig. (3.13).

Plasma inhomogeneities in the ionosphere would rarely possess the assumed properties and therefore the result of Figs. (3.13) and (3.14) are not to be found under practical circumstances but are included for completeness of the understanding of the plasma diffusion.

The important features of the diffusion process can be summarized as follows:

(i) The inhomogeneity spreads in the direction of a $\tilde{\xi}$-axis which ties the two maxima located at $\underset{\sim}{V}_{ic}(\mu=0)t$ and $\underset{\sim}{V}_{ic}(\mu=1)t$ respectively. The distance between the maxima, d_2, is given by

$$d_2 = \frac{|\kappa_i \kappa_e|(|\kappa_e| - \kappa_i)\, Ut}{(1+|\kappa_i \kappa_e|)\sqrt{(1+\kappa_i^2)(1+\kappa_e^2}},$$

see Eq. (4.13), which for $\kappa_e \gg \kappa_i$ reduces to

$$d_2 = \frac{Ut}{\sqrt{1+\kappa_i^2}}.$$

The spreading shows most distinctly in Fig. (3.5) and (3.7).

(ii) The elongation of the inhomogeneity is given by the expression

$$\ell_{\parallel}/\ell_{\perp} = 1 + |\kappa_i \kappa_e|,$$

see Eq. (5.11). Comparatively large elongations occur for plasmas with high values of κ_i and κ_e, such as shown in Fig. (3.8) and Fig. (3.12).

(iii) The diffusive spreading due to the action of an external electric field of strength $\underset{\sim}{E}_0$ is the same as that due to the action of a wind with velocity $\underset{\sim}{W}_0 = -\frac{c}{B}(\underset{\sim}{E}_0 \times \underset{\sim}{B})$ but shifted by the vector $-\underset{\sim}{W}_0$, because the plasma motion is restrained by an electric field and not by a neutral wind.

6. APPROXIMATE SOLUTION OF THE NONLINEAR DIFFUSION OF A PLASMA INHOMOGENEITY

One of the features which results from the nonlinear diffusion is the steepening of the front side of an inhomogeneity which diffuses in a neutral wind. This phenomenon has been observed in plasma experiments in the ionosphere, e.g., barium cloud experiments.

To investigate the steepening effect we consider the nonlinear diffusion equation III,(1.10) in x space.

$$(A_i + A_e)\frac{\partial n}{\partial t} = A_i(-\nabla\cdot n\underset{\sim}{V}_e + \nabla\cdot\underset{\approx}{D}_e\cdot\nabla n) + A_e(-\nabla\cdot n\underset{\sim}{V}_i + \nabla\cdot\underset{\approx}{D}_i\cdot\nabla n), \tag{6.1}$$

where the operator A_a has been defined by Eq. (1.11), or transforming to $\underset{\sim}{k}$ space and dividing by $A_i + A_e$,

$$\frac{\partial n(\underset{\sim}{k},t}{\partial t} = -\left(i\underset{\sim}{k}\cdot\underset{\sim}{\mathcal{V}} + k^2\mathcal{D}\right)n(\underset{\sim}{k},t), \tag{6.2}$$

$$\underset{\sim}{\mathcal{V}} = \frac{A_i(k)\underset{\sim}{V}_e + A_e(k)\underset{\sim}{V}_i}{A_i(k) + A_e(k)}, \tag{6.3}$$

$$\mathcal{D} = \frac{A_i(k)D_e + A_e(k)D_i}{A_i(k) + A_e(k)}, \tag{6.4}$$

$$A_a(k) = A_a^{\circ}(k) + A_a'(k). \tag{6.5}$$

The $A_a(k) = A_a^{\circ}(k) + A_a'(k)$ $A_a^{\circ}(k)$ has been defined by (2.2) and the nonlinear differential operator A_a' is evaluated from the linear solution n_o such that

$$A_a'(n_0) = \alpha_{\perp a}\, \underset{\sim}{k}_{0\perp} \cdot \nabla_\perp + \alpha_{Ha} (\underset{\sim}{k}_0 \times \nabla)_3 + \alpha_{\parallel a} (\underset{\sim}{k}_0 \cdot \nabla)_3 ,$$

where

$$\underset{\sim}{k}_0 = \frac{1}{n_0} \nabla n_0$$

is assumed small for a weak inhomogeneity so that terms in the second order of k_0 are negligible. As the nonlinear diffusion effects can be seen most easily in the transverse plane, in view of the ratio

$$\frac{\partial n}{\partial x_3} \ll \frac{\partial n}{\partial x_1}, \frac{\partial n}{\partial x_2}$$

we may assume for the investigation of the nonlinear effect that

$$\frac{\partial}{\partial x_3} = 0$$

while retaining a three dimensional geometric configuration in the gross evaluation of diffusion. It may also be assumed that the slope of the density varies slowly so that $A_a'(n_0)$ can be transformed into $\underset{\sim}{k}$ space with homogeneous transport coefficients,

$$A_a'(\underset{\sim}{k}) = i \left[\alpha_{\perp a}\, \underset{\sim}{k}_0 \cdot \underset{\sim}{k} + \alpha_H (\underset{\sim}{k}_0 \times \underset{\sim}{k})_3 \right]$$

$$= i \left[\alpha_{\perp a} (k_{01} k_1 + k_{02} k_2) + \alpha_{Ha} (k_{01} k_2 - k_{02} k_1) \right] .$$

When we assume for the plasma

$$\kappa_e \gg \kappa_i \gg 1$$

we can write according to II,(2.10)

$$\alpha_{Hi} + \alpha_{He} = \frac{ec}{B} \left[\frac{\kappa_i^2}{1+\kappa_i^2} - \frac{\kappa_e^2}{1+\kappa_e^2} \right] \cong 0$$

and obtain

$$A_i + A_e = (\alpha_{\perp i} + \alpha_{\perp e})(k^2 - i\, \underset{\sim}{k}_0 \cdot \underset{\sim}{k}) .$$

Substituting for $A_i(k)$ and $A_e(k)$, (6.3) and (6.4) become,

$$\underset{\sim}{\mathcal{V}} = \frac{\left\{-\alpha_{\perp i} k^2 + i\left[\alpha_{\perp i} \underset{\sim}{k}_0 \cdot \underset{\sim}{k} + \alpha_{H i} (\underset{\sim}{k}_0 \times \underset{\sim}{k})_3\right]\right\} \underset{\sim}{V}_e + (i \leftrightarrow e)}{(\alpha_{\perp i} + \alpha_{\perp e})(k^2 - i\, \underset{\sim}{k}_0 \cdot \underset{\sim}{k})}, \tag{6.6}$$

$$\mathcal{D} = \frac{\left\{-\alpha_{\perp i} k^2 + i\left[\alpha_{\perp i} \underset{\sim}{k}_0 \cdot \underset{\sim}{k} + \alpha_{H i} (\underset{\sim}{k}_0 \times \underset{\sim}{k})_3\right]\right\} D_{\perp e} + (i \leftrightarrow e)}{(\alpha_{\perp i} + \alpha_{\perp e})(k^2 - i\, \underset{\sim}{k}_0 \cdot \underset{\sim}{k})}. \tag{6.7}$$

Substituting for $\underset{\sim}{V}_e$ and $\underset{\sim}{V}_i$ from Eq. (4.4) and separating into real and imaginary parts, (6.6) and (6.7) become,

$$\underset{\sim}{\mathcal{V}} = \frac{\underset{\sim}{U}}{\kappa_i \kappa_e} - \frac{(\underset{\sim}{k}_0 \cdot \underset{\sim}{k})(\underset{\sim}{k}_0 \times \underset{\sim}{k})_3}{k^4 + (\underset{\sim}{k}_0 \cdot \underset{\sim}{k})^2} \frac{\underset{\sim}{U}}{\kappa_i} - \frac{(\underset{\sim}{k}_0 \cdot \underset{\sim}{k})(\underset{\sim}{k}_0 \times \underset{\sim}{k})_3}{k^4 + (\underset{\sim}{k}_0 \cdot \underset{\sim}{k})^2} \underset{\sim}{U} \times \hat{e}_3 \tag{6.8}$$

$$+ i\left[\frac{k^2 (\underset{\sim}{k}_0 \times \underset{\sim}{k})_3}{k^4 + (\underset{\sim}{k}_0 \cdot \underset{\sim}{k})^2} \frac{\underset{\sim}{U}}{\kappa_i} + \frac{k^2 (\underset{\sim}{k}_0 \times \underset{\sim}{k})_3}{k^4 + (\underset{\sim}{k}_0 \cdot \underset{\sim}{k})^2} \underset{\sim}{U} \times \hat{e}_3\right],$$

$$\mathcal{D} = D_{\perp e} + \frac{\kappa_i}{\kappa_e} D_{\perp i} - \frac{(\underset{\sim}{k}_0 \cdot \underset{\sim}{k})(\underset{\sim}{k}_0 \times \underset{\sim}{k})_3}{k^4 + (\underset{\sim}{k}_0 \cdot \underset{\sim}{k})^2} \kappa_i D_{\perp i}$$

$$+ i\, \frac{k^2 (\underset{\sim}{k}_0 \times \underset{\sim}{k})_3}{k^4 + (\underset{\sim}{k}_0 \cdot \underset{\sim}{k})^2} \kappa_i D_{\perp i}. \tag{6.9}$$

As $\underset{\sim}{k}_0$ is assumed small,

$$(\underset{\sim}{k}_0 \cdot \underset{\sim}{k})^2 \ll k^4$$

and we can neglect the $\underset{\sim}{k}_0 \cdot \underset{\sim}{k}$ term in the denominators of (6.8) and (6.9) and second order terms in $\underset{\sim}{k}_0$ in the numerator. With $\underset{\sim}{V}_\perp$ and $D_\perp$ defined by Eq. (2.14) and Eq. (2.15) such that

$$\frac{\underset{\sim}{U}}{\kappa_i \kappa_e} \cong \underset{\sim}{V}_\perp$$

and

$$D_{\perp e} + \frac{\kappa_i}{\kappa_e} D_{\perp i} = D_\perp$$

(6.8) and (6.9) simplify to,

$$\underset{\sim}{\mathcal{V}} = \underset{\sim}{V}_\perp + i \frac{(\underset{\sim}{k}_0 \times \underset{\sim}{k})_3}{k^2} \left[\frac{\underset{\sim}{U}}{\kappa_i} + \underset{\sim}{U} \times \hat{e}_3 \right] \tag{6.10}$$

and

$$\mathcal{D} = D_\perp + i \frac{(\underset{\sim}{k}_0 \times \underset{\sim}{k})_3}{k^2} \frac{\kappa_e D_\perp}{2} . \tag{6.11}$$

Substituting into (6.2), we obtain,

$$\begin{aligned} \frac{\partial n(\underset{\sim}{k}, t)}{\partial t} &= -\left\{ i \left[\underset{\sim}{k} \cdot \underset{\sim}{V}_\perp + (\underset{\sim}{k}_0 \times \underset{\sim}{k})_3 \frac{\kappa_e D_\perp}{2} \right] \right. \\ &\qquad \left. + k^2 D_\perp + (\underset{\sim}{k}_0 \times \underset{\sim}{k})_3 \left(k_z - \frac{k_i}{\kappa_i} \right) \frac{\underset{\sim}{U}}{k^2} \right\} n(\underset{\sim}{k}, t) \\ &= \left[i \left(\underset{\sim}{k} \cdot \underset{\sim}{V}_\perp + F \right) + k^2 D_\perp + P \right] n(\underset{\sim}{k}, t), \end{aligned} \tag{6.12}$$

where

$$\begin{aligned} F &= \left(k_{0_1} k_z - k_{0_z} k_1 \right) \frac{\kappa_0 D_\perp}{2} , \\ P &= \left(k_{0_1} k_z - k_{0_z} k_1 \right) \left(k_z - \frac{k_1}{\kappa_i} \right) \frac{U}{k^2} . \end{aligned} \tag{6.13}$$

The solution of Eq. (6.12) is

$$n(\underset{\sim}{k}, t) = n(\underset{\sim}{k}, 0)\, e^{-\left[i \left(\underset{\sim}{k} \cdot \underset{\sim}{V}_\perp + F \right) + \left(k^2 D_\perp + P \right) \right] t} , \tag{6.14}$$

while its inversion takes the form,

$$n(\underset{\sim}{x},t) = \frac{1}{(2\pi)^3}\int_{-\infty}^{\infty} d\underset{\sim}{k}\; n(\underset{\sim}{k},0)\, e^{i[\underset{\sim}{k}\cdot\underset{\sim}{x} - (\underset{\sim}{k}\cdot\underset{\sim}{V}_\perp + F)t] - (k^2 D_\perp + P)t} \quad . \quad (6.15)$$

This expression shows that the effects of nonlinearity are to modify the drift and diffusion by the terms F and P, respectively.

For the sake of simplicity and in consistency with the linear diffusion assumptions of Section 3, we take the inhomogeneity to be a point source at time t=o, in which case $n(\underset{\sim}{x},0)$ is represented by a δ -function corresponding in three dimensions to

$$n(\underset{\sim}{k},0) = (2\pi)^{-3} N_o ,$$

which reduces Eq. (6.15) to

$$n(\underset{\sim}{x},t) = \frac{N_o}{(2\pi)^3}\int_{-\infty}^{\infty} d\underset{\sim}{k}\; e^{i[\underset{\sim}{k}\cdot\underset{\sim}{x} - (\underset{\sim}{k}\cdot\underset{\sim}{V}_\perp + F)t] - (k^2 D_\perp + P)t} \quad . \quad (6.16)$$

The equation is brought to the same form as the linear solution, except for the additional drift term F and the diffusion term P.

It is to be remarked that the separation of the inhomogeneity into several maxima, as derived in the linear diffusion of Section 3, is due to a variable drift $\underset{\sim}{V}_\perp(\underset{\sim}{k})$ and is developed at a later time t, while the nonlinearity develops at an early time near the fundamental maximum. Therefore in contrast to the spherical coordinates, θ, ϕ and k, we now choose a new spherical coordinate system, β, ϕ and k, where β is the angle between $\underset{\sim}{k}$ and $\underset{\sim}{x}-\underset{\sim}{V}_\perp t$ and $V_\perp$ is independent of k. This system is simpler, and describes the early development with a sufficient accuracy.

Hence we write

$$d\underset{\sim}{k} = dk\, k^2 d\beta \sin\beta\, d\phi$$

and obtain

$$n(\underset{\sim}{x},t) = \frac{N_0}{(2\pi)^3}\int_0^{2\pi} d\phi \int_0^{\pi} d\beta \sin\beta \int_0^{\infty} dk\, k^2 e^{i[\underset{\sim}{k}\cdot(\underset{\sim}{x}-\underset{\sim}{V}_\perp t) - Ft] - (k^2 D_\perp + P)t}$$

$$= \frac{N_0}{(2\pi)^2}\int_{-1}^{1} d\omega\, e^{-P(\omega)t} \int_0^{\infty} dk\, k^2 e^{ik[(x-V_\perp t)\omega - F'(\omega)t] - k^2 D_\perp t}, \qquad (6.17)$$

where

$$\omega \equiv \cos\beta,$$

$$F'(\omega) = \left(k_{o_1}\sqrt{1-\omega^2} - k_{o_2}\omega\right)\frac{\kappa_e D_\perp}{2},$$

$$P(\omega) = \left[k_{o_1}(1-\omega^2) + \frac{k_{o_2}}{\kappa_i}\omega^2 - \left(\frac{k_{o_1}}{\kappa_i} + k_{o_2}\right)\omega\sqrt{1-\omega^2}\right]U.$$

Following the method of Section 3, we integrate with respect to k, and get the expression

$$\int_0^{\infty} dk\, k^2 e^{ik[(x-V_\perp t)\omega - F't] - k^2 D_\perp t} = \frac{\sqrt{\pi}}{4(D_\perp t)^{3/2}}\left[1 - \frac{(x-V_\perp t)\omega - F't}{2D_\perp t}\right] e^{-\frac{(x-V_\perp t)\omega - F't}{4D_\perp t}},$$

which leads to,

$$\tilde{n}(\underset{\sim}{x},t) = \frac{1}{2}\int_{-1}^{1} d\omega\, e^{-Pt}\left(1-2h^2\right)e^{-h^2}, \qquad (6.18)$$

where

$$h = \eta\omega - \frac{F't}{\sqrt{4D_\perp t}},$$

$$\eta = \frac{x - V_\perp t}{\sqrt{4D_\perp t}},$$

$$\tilde{n}(\underset{\sim}{x},t) = n(\underset{\sim}{x},t)\left[\frac{N_0}{8(\pi D_\perp t)^{3/2}}\right]^{-1}.$$

In order to perform the integration in (6.18), we introduce the following simplifications:

(i) Inasmuch as we are interested in the initial development of steepening due to nonlinearity, it can be assumed that k_{o_1} and k_{o_2} are small so that their second powers are negligible, permitting the series expansions of $e^{-\beta t}$ and e^{-h^2}.

(ii) The integral in (6.18) covering the limits (-1, +1) of ω requires that the integrand be an even function. This property permits neglecting the odd terms in the integrand.

With the above simplifications, and after some auxiliary calculations which are omitted, (6.18) reduces to

$$\tilde{n} = i_0 - 2\eta^2 i_2 + Ut\left\{ k_{o_1}\left[i_0 - (1+2\eta) i_2 + 2\eta i_4 \right] + k_{o_2}\left[\frac{1}{\kappa_i}\left(i_2 - 2\eta i_4 \right) + \xi\left(\eta i_2 - 2\eta^3 i_4 \right) \right] \right\}, \qquad (6.19)$$

where

$$\xi = \frac{\kappa_e}{2U}\left(\frac{D_\perp}{t}\right)^{\frac{1}{2}},$$

$$i_0 = \int_0^1 d\omega\, e^{-\eta^2\omega^2} = \frac{\sqrt{\pi}}{2\eta}\,\Phi(\eta),$$

$$i_2 = \int_0^1 d\omega\, \omega^2 e^{-\eta^2\omega^2} = \frac{1}{2\eta^2}\left[\frac{\sqrt{\pi}}{2\eta}\,\Phi(\eta) - e^{-\eta^2} \right], \qquad (6.20)$$

$$i_4 = \int_0^1 d\omega\, \omega^4 e^{-\eta^2\omega^2} = \frac{1}{2\eta^2}\left[\frac{3\sqrt{\pi}}{4\eta^3}\,\Phi(\eta) - \left(1 + \frac{3}{2\eta^2}\right) e^{-\eta^2} \right],$$

and $\Phi(\eta)$ is the error function. Upon substituting (6.20), we transform (6.19] into

$$\tilde{n} = \tilde{n}_0 + U t \nu \tag{6.21}$$

with

$$\tilde{n}_0 = e^{-\eta^2},$$

$$\nu = k_{01} I_1 + k_{02}\left(\frac{1}{\kappa_i} I_2 + \xi I_3\right),$$

$$I_1(\eta) = \frac{\sqrt{\pi}}{2\eta}\Phi(\eta)\left(1 - \frac{1}{\eta} - \frac{1}{2\eta^2} + \frac{3}{2\eta^3}\right) + \frac{e^{-\eta^2}}{2\eta^2}\left(1 - \frac{3}{2\eta}\right), \tag{6.22}$$

$$I_2(\eta) = \frac{\sqrt{\pi}}{4\eta^3}\Phi(\eta)\left(1 - \frac{3}{2\eta}\right) + \frac{e^{-\eta^2}}{\eta}\left(1 - \frac{1}{2\eta} + \frac{3}{2\eta^2}\right),$$

$$I_3(\eta) = -\frac{\sqrt{\pi}}{2\eta^2}\Phi(\eta) + \eta e^{-\eta^2}\left(1 + \frac{1}{\eta^2}\right).$$

The functions I_1, I_2 and I_3 are plotted in Fig. (3.15). For $k_{01} = k_{02} = 0$ Eq. (6.21) reduces to the Gaussian density distribution,

$$n = n_0 = \frac{N_0}{8(\pi D t)^{3/2}} e^{-\frac{(x - V_i t)^2}{4 D_i t}}, \tag{6.23}$$

which is the solution of the linear diffusion equation with constant drift and diffusion coefficient, a result which is to be expected. The variation of the function ν with η is plotted in Fig. (3.16) for

$$k_{01} = k_{02} = k_0$$

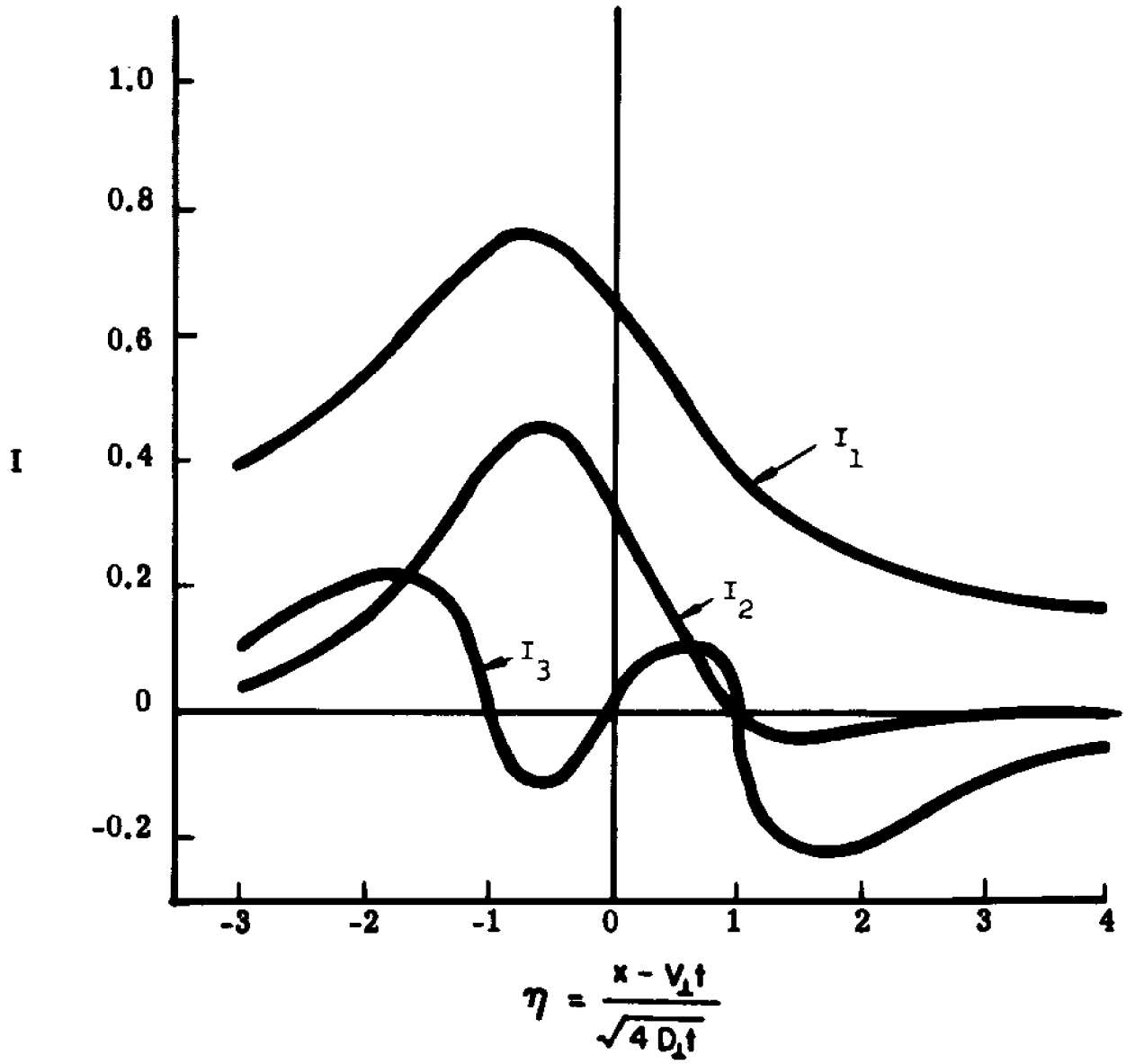

Fig. 3.15. Functions of Nonlinear Density Correction Factor

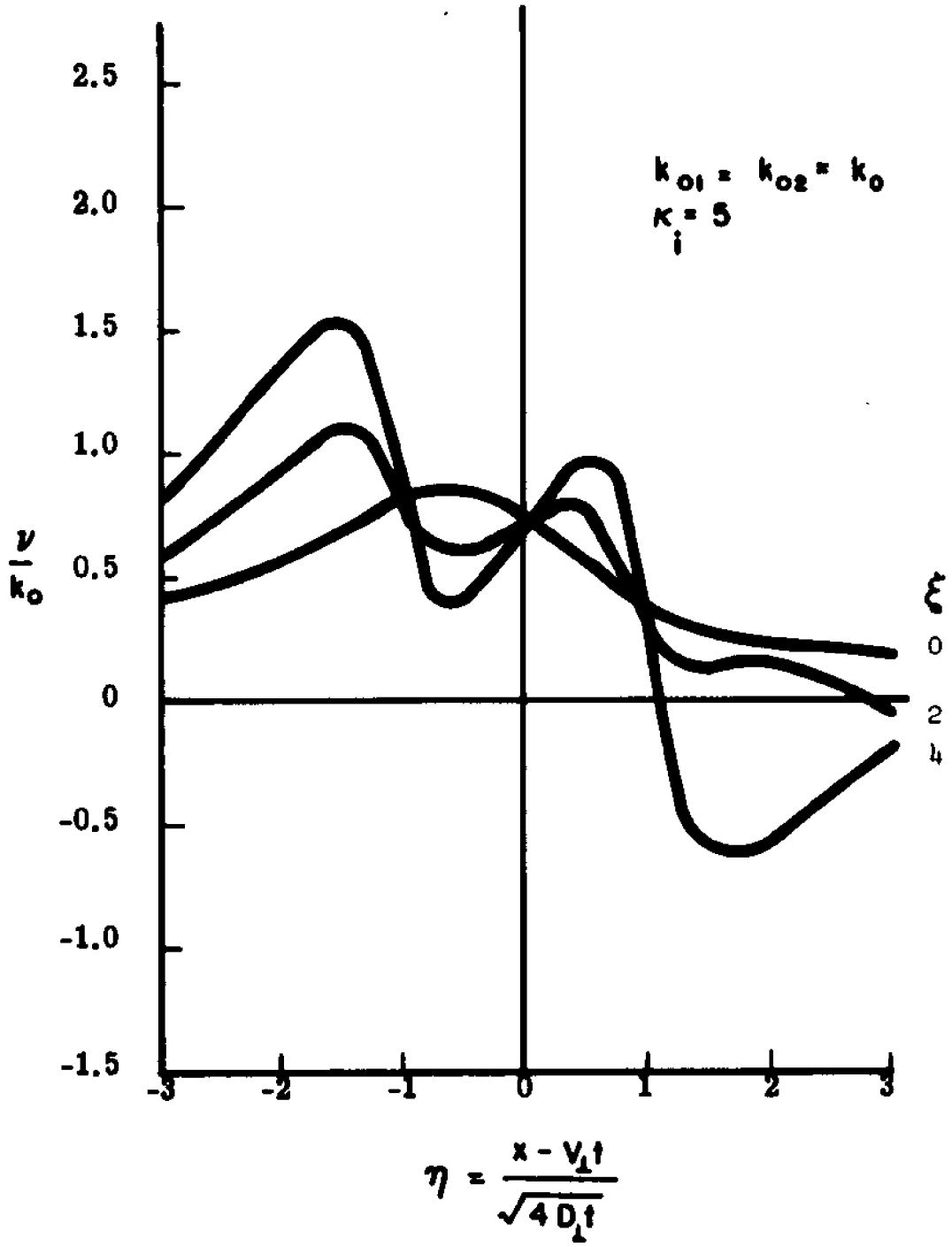

Fig. 3.16. Nonlinear Density Correction Factor

and values of ξ ranging from 0 to 4. The nonlinear density profile, $\tilde{n}$ from Eq. (6.21) is shown in Fig. (3.17) for constant $|k_0|$, corresponding to an exponential mean density distribution,

$$\tilde{n}_0 = e^{\pm |k_0| x}$$

for which there is a step change from positive to negative k_0 at $\eta = 0$ and which causes a discontinuity in the density profile. The steepening effect of the nonlinear term can be seen by comparing $\tilde{n}$ at $-\eta$ and $+\eta$. For example, at $\eta = -1$, $\tilde{n} = 0.565$ while at $\eta = +1$, $\tilde{n} = 0.287$ indicating a rapid drop in density on the front side of the inhomogeneity. The plot is for $\xi = 2$, corresponding to

$$U = 0.125 \text{ km/sec}, \quad t = 100 \text{ sec} \quad \text{and} \quad D_\perp = 0.01 \text{ km}^2/\text{sec}.$$

To illustrate the feature of steepening more clearly we take the case where the mean density is close to the Gaussian linear density distribution, for which the slope varies with position approximately as $k_0 \simeq -\eta$. Now k_0 changes direction gradually so that no discontinuity occurs. The nonlinear density profile for this case is plotted in Fig. (3.18) and shows a distinct steepening in this positive η direction.

We now examine a number of special cases, which can be derived from the general expression (6.21).

a. Case With $k_{0_1} \neq 0, k_{0_2} = 0$

This gives the density profile in the $x_2 = 0$ plane, and therefore in the y direction and reduces (6.21) to

$$v = k_{0_1} I_1. \tag{6.24}$$

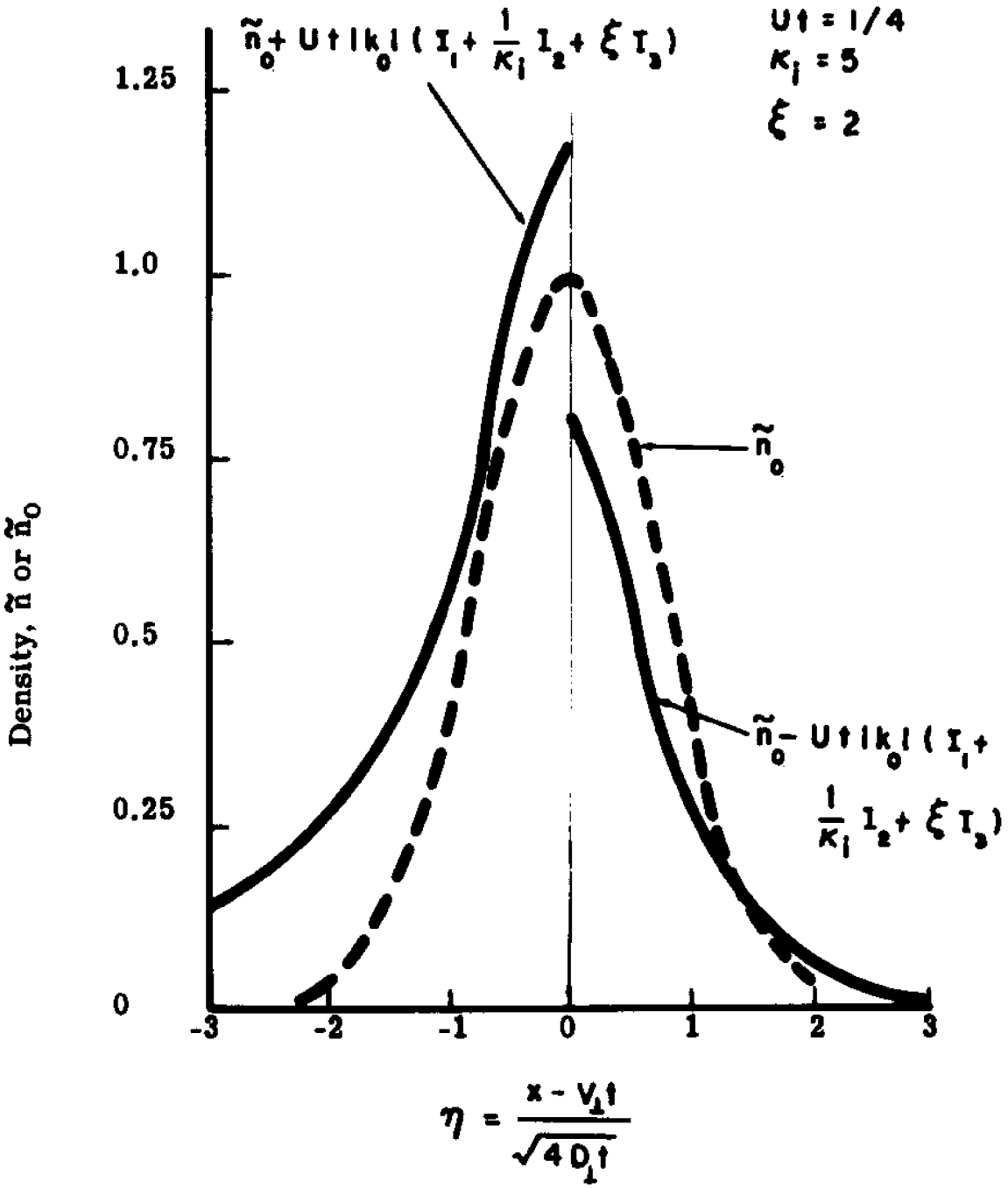

Fig. 3.17. Nonlinear Density Profile, Exponential Mean Density Distribution.

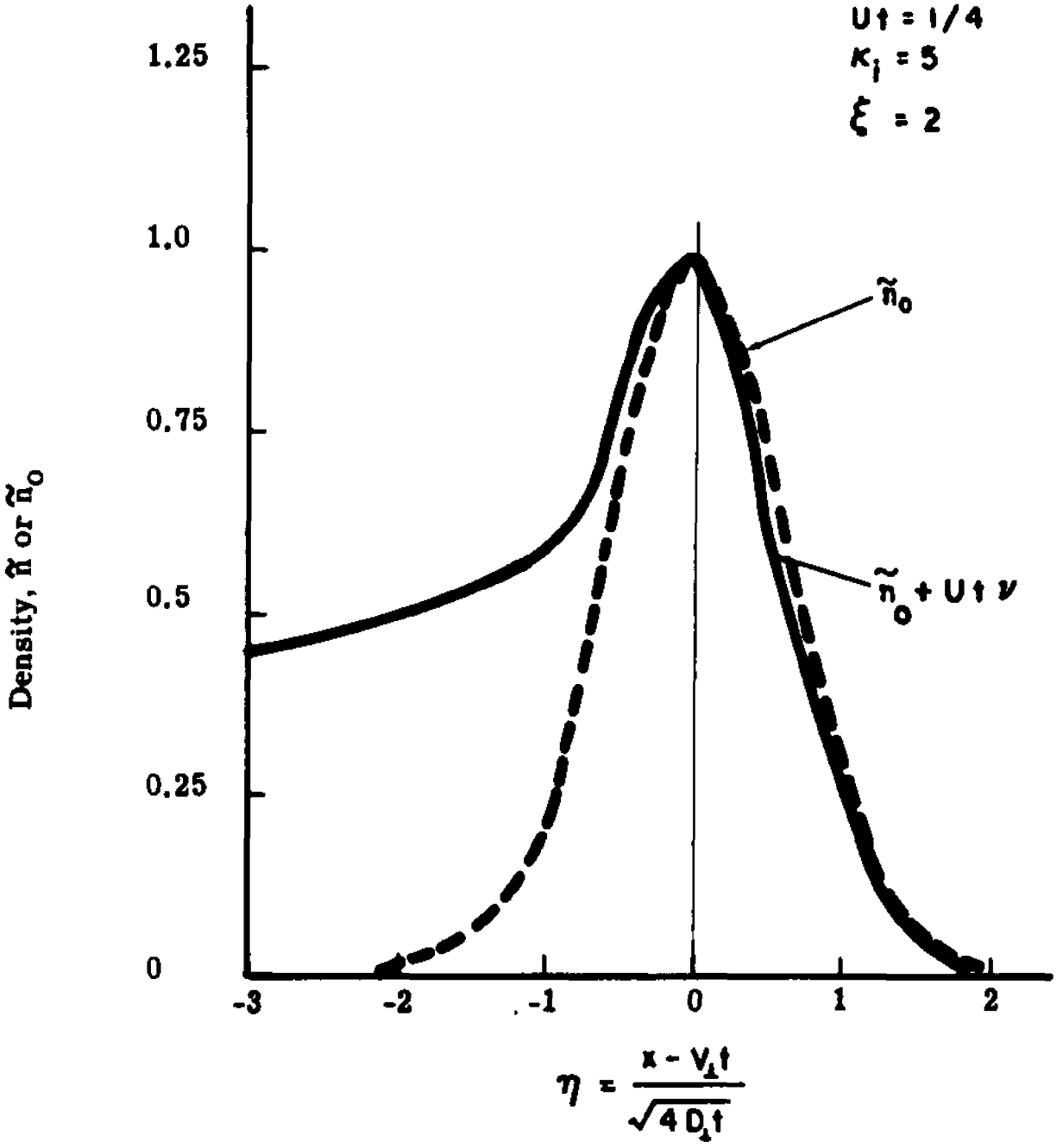

Fig. 3.18. Nonlinear Density Profile, Gaussian Mean Density Distribution.

As seen from Fig. (3.15), I_1 is positive for all η and therefore adds to the linear density $\tilde{n}_o$ for $\eta < 0$ and subtracts from $\tilde{n}_o$ for $\eta > 0$, leading to a steepening (rapid drop in density) on the $+\eta$ side facing in the x_1-direction. This effect is shown for an exponential mean density distribution in Fig. (3.19) and for a Gaussian mean density distribution in Fig. (3.20). It can be concluded that both the general case of $k_{o_1} = k_{o_2} = k_o$ and the special case $k_{o_2} = 0$ give similar features of nonlinear steepening.

To illustrate the steepening more clearly, the slope of the density profile $\left|\frac{\partial \eta}{\partial \eta}\right|$ for a Gaussian mean density distribution is plotted in Fig. (3.21) for $\eta < 0$ and $\eta > 0$. The plot shows that the larger slope and therefore the steepening occurs at $\eta > 0$ for all values of η.

b. Case With $k_{o_1} = 0$, $k_{o_2} \neq 0$, $\xi = 0$

This is the profile in the $x_1 = 0$ plane and therefore in the $-\underline{U} \times \underline{B}$ direction and reduces (6.21) to

$$v = k_{o_2}\left(\frac{1}{\kappa_i} I_2 + \xi I_3\right). \tag{6.25}$$

The nonlinear density profiles for the exponential and Gaussian mean density distributions are shown in Fig. (3.22) and (3.23), respectively. The steepening effect, while present, is not as pronounced as in the case with $k_{o_1} \neq 0$, $k_{o_2} = 0$. This can also be seen in the plot of $\left|\frac{\partial \tilde{n}}{\partial \eta}\right|$ versus η shown in Fig. (3.24).

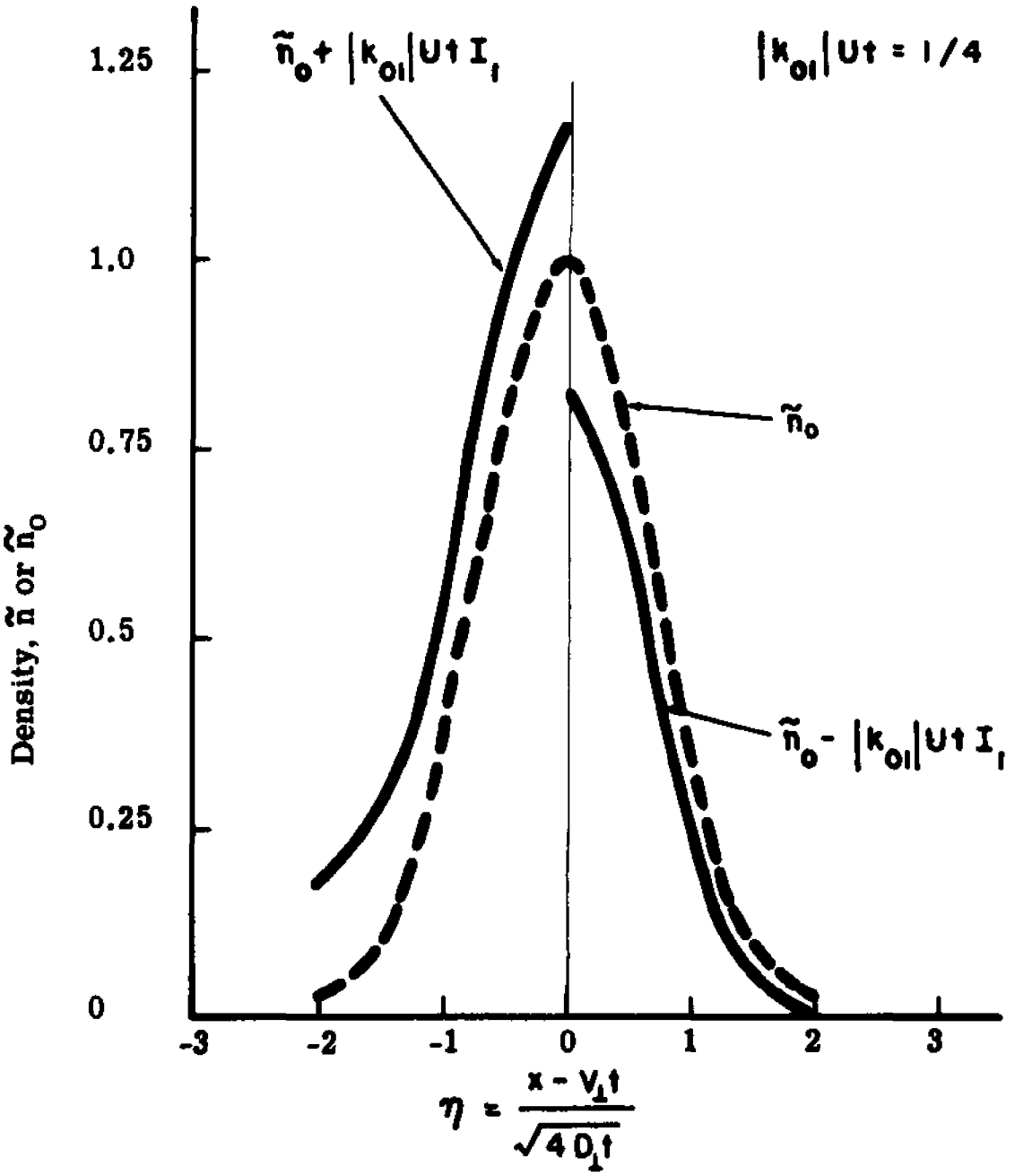

Fig. 3.19. Nonlinear Density Profile in x_2=0 Plane, Exponential Mean Density Distribution.

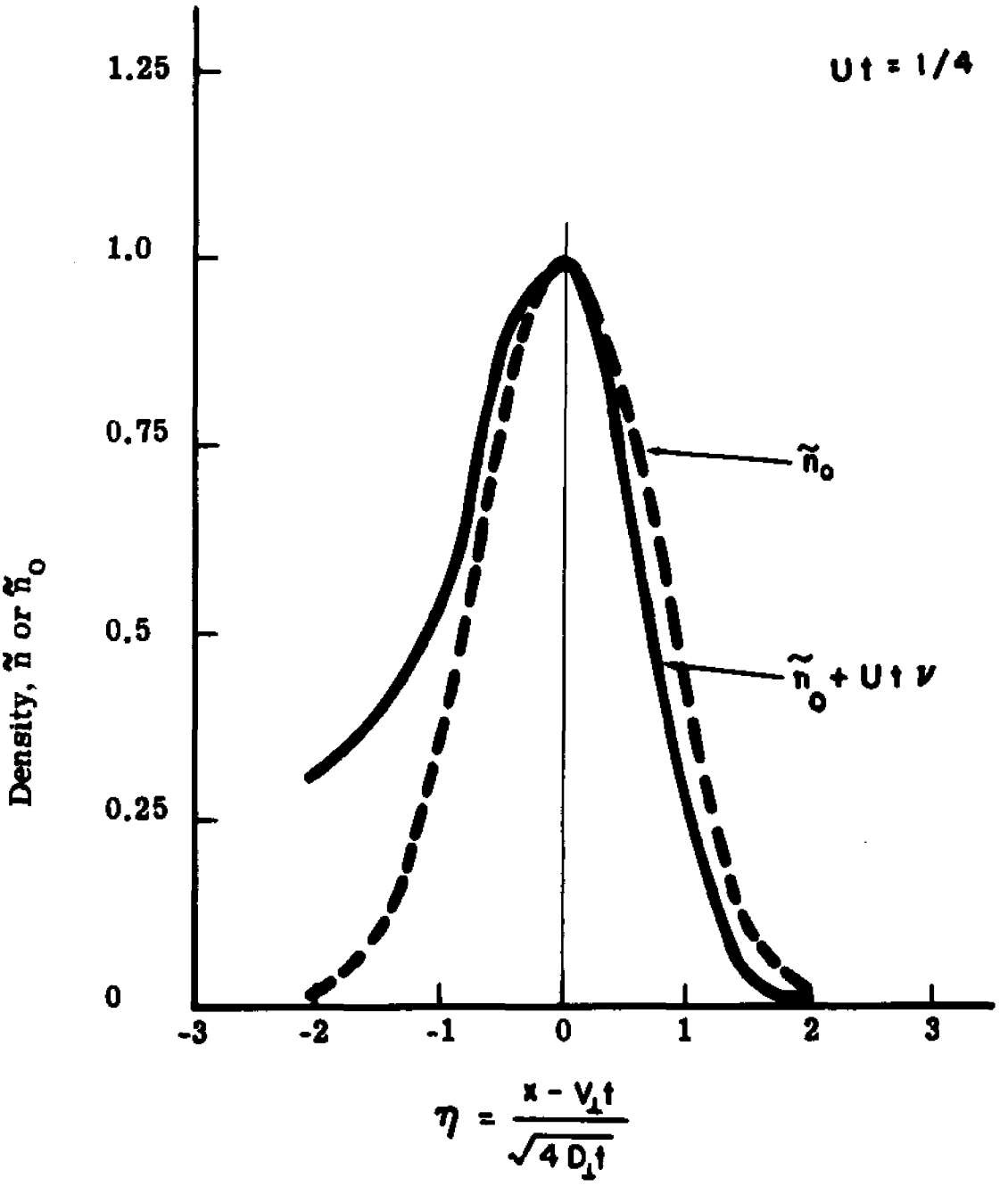

Fig. 3.20. Nonlinear Density Profile in x_2=0 Plane, Gaussian Mean Density Distribution

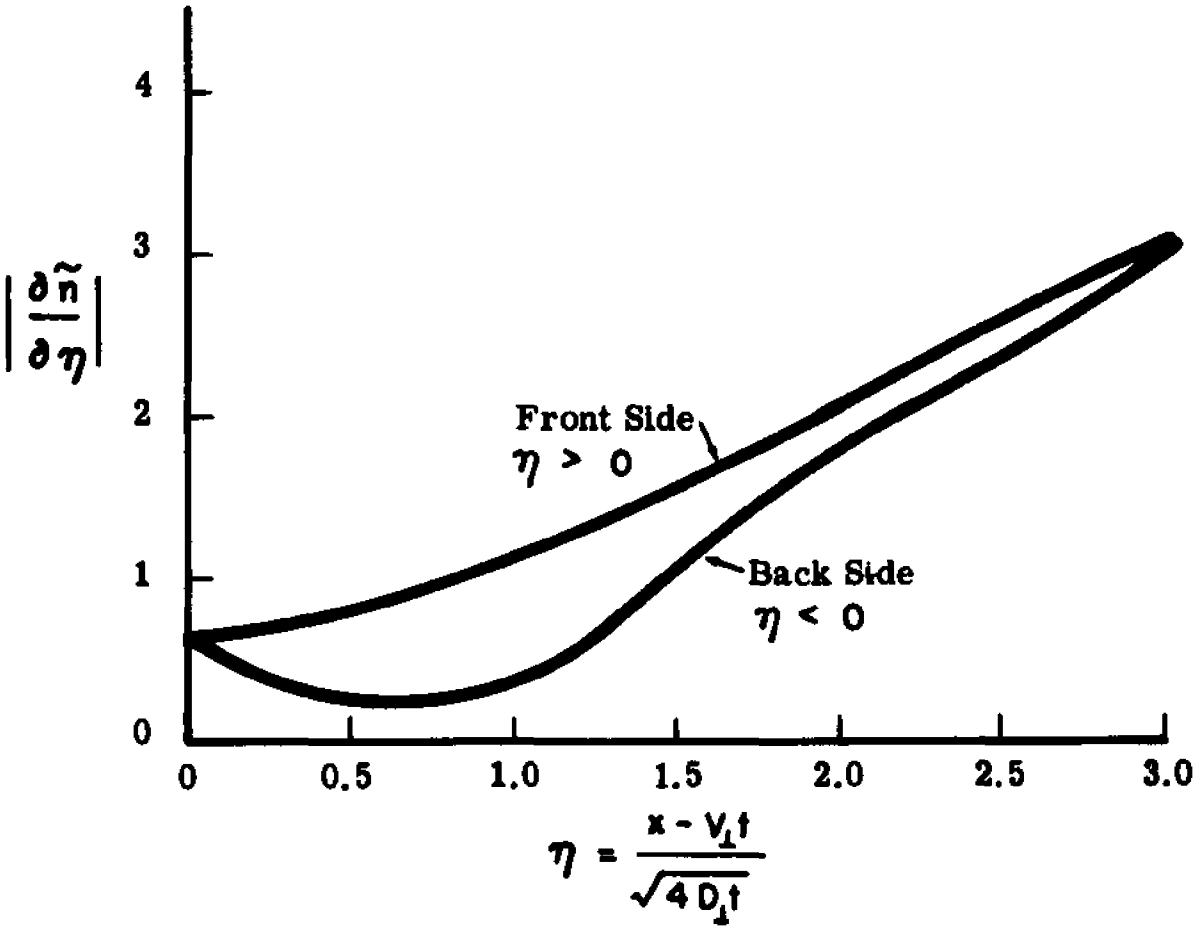

Fig. 3.21. Slopes of Front Side and Back Side of Plasma Inhomogeneity in x_2=0 Plane, Gaussian Mean Density Distrubution

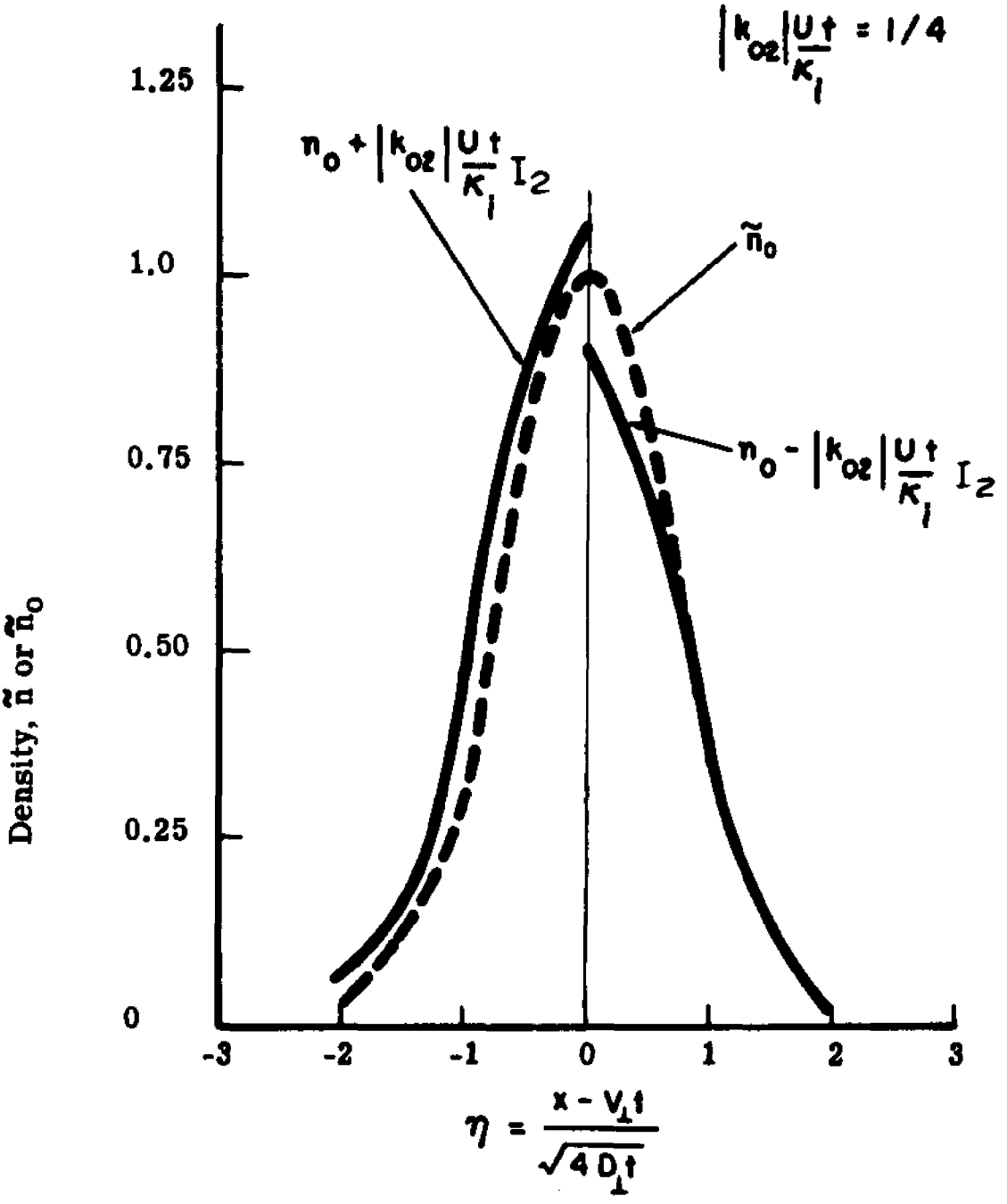

Fig. 3.22. Nonlinear Density Profile in x_1=0 Plane, Exponential Mean Density Distribution

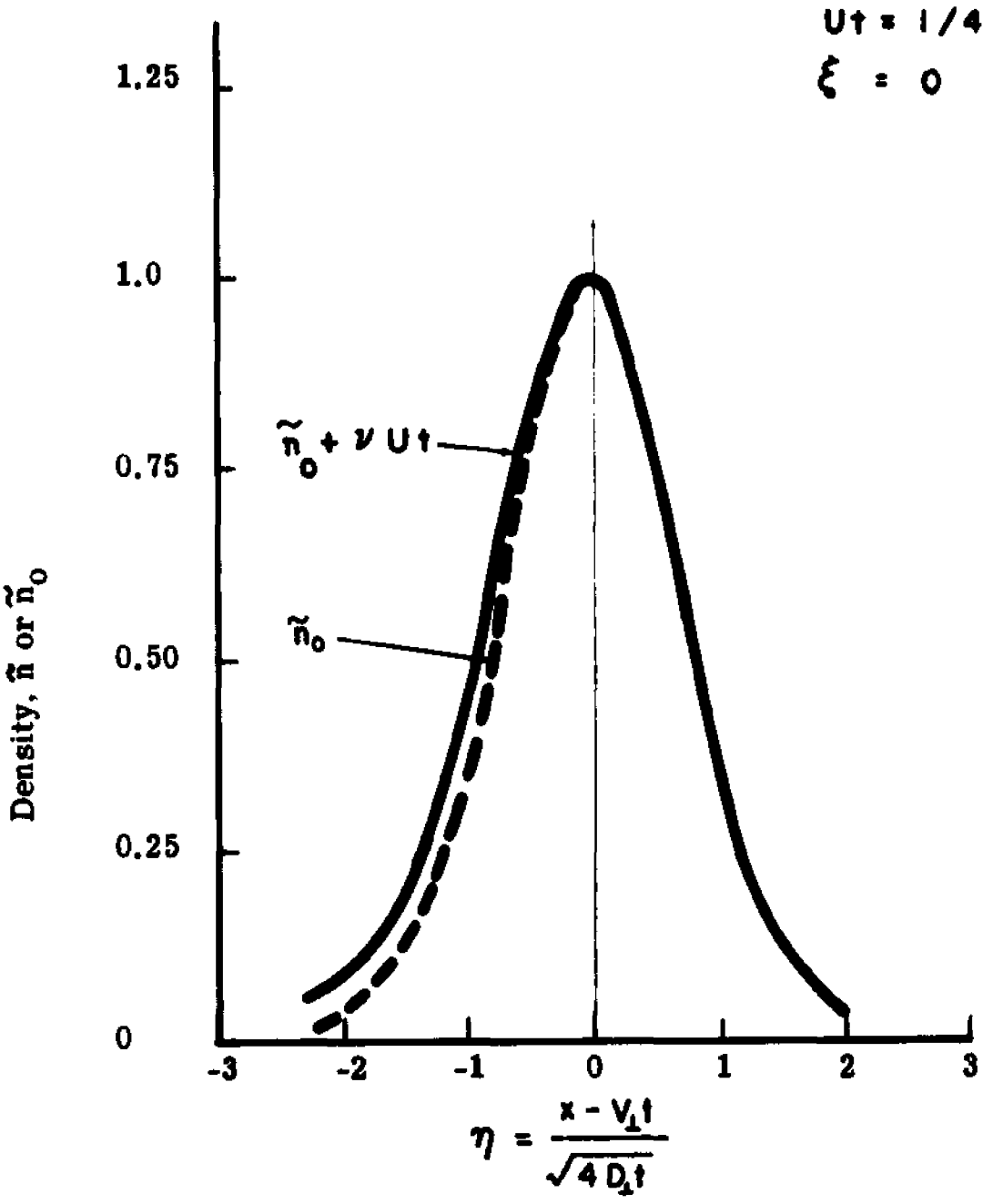

Fig. 3.23. Nonlinear Density Profile in x_1=0 Plane, Gaussian Mean Density Distribution

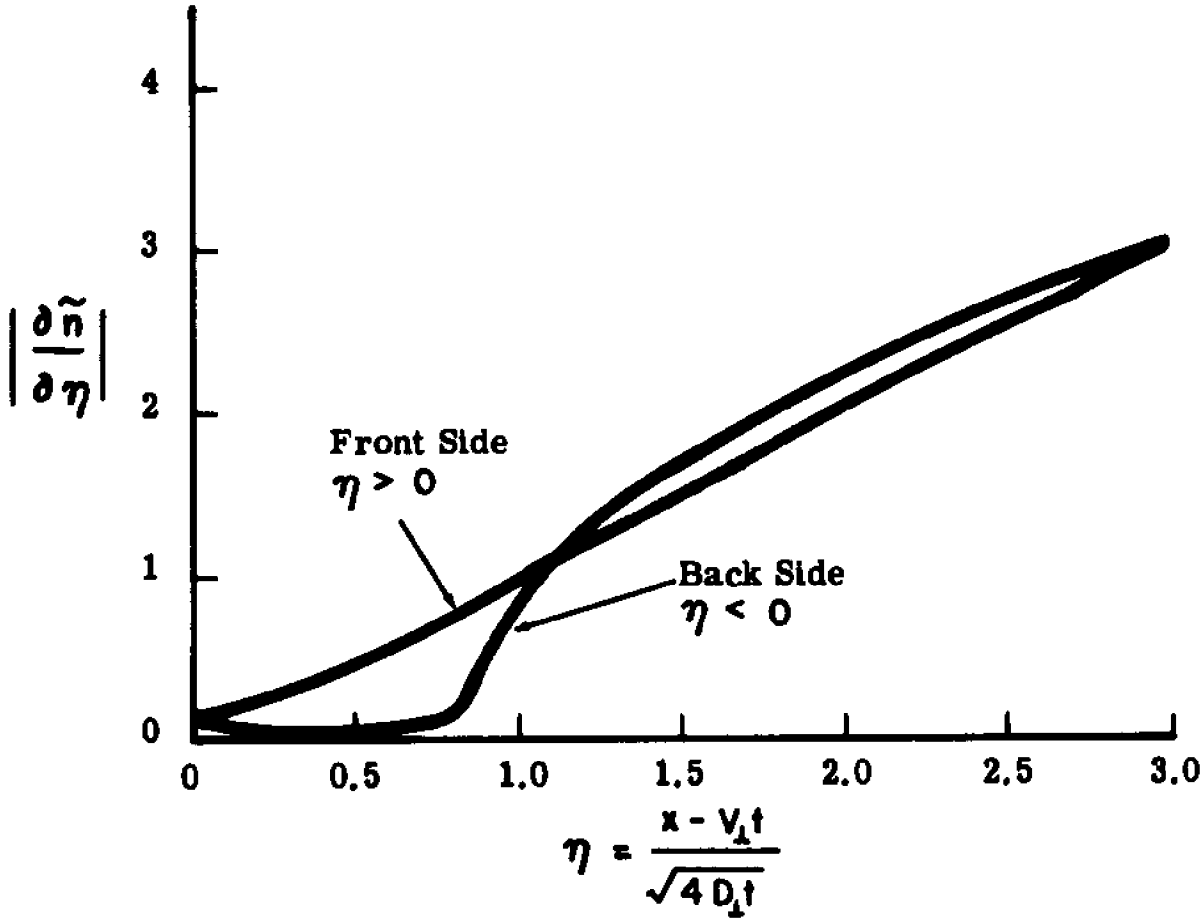

Fig. 3.24. Slopes of Front Side and Back Sides of Plasma Inhomogeneity in x_1=0 Plane, Gaussian Mean Density Distribution

c. Case With Ut = 0

For this case (6.21) reduces to

$$\nu = k_o \frac{\kappa_e}{2} \sqrt{D_\perp t}\ I_3 . \tag{6.26}$$

A plot of the nonlinear density profile is given in Fig. (3.25) and, as expected, shows no steepening. However, there is a distortion of the linear density profile, but this distortion is symmetrical about the origin.

We can conclude the following from the above analysis:

(i) The nonlinear effects arise from the Hall components of the transport coefficients. The retention of the nonlinear terms results in a density profile which shows a steeper decrease in density at the front side of the inhomogeneity. The amount of steepening increases with $k_o U t$,i.e., with wind velocity and with time, and is self-accelerating (it increases with k_o), and therefore a highly destabilizing process.

(ii) The steepening is primarily in the $\underset{\sim}{U}$ direction with only slight effects in the $-\underset{\sim}{U}\times\underset{\sim}{B}$ direction.

(iii) In the absence of a wind there is no steepening. However, there is a distortion of the linear density profile symmetrical about the center, which is proportional to $k_o \kappa_e \sqrt{D_\perp t}$.

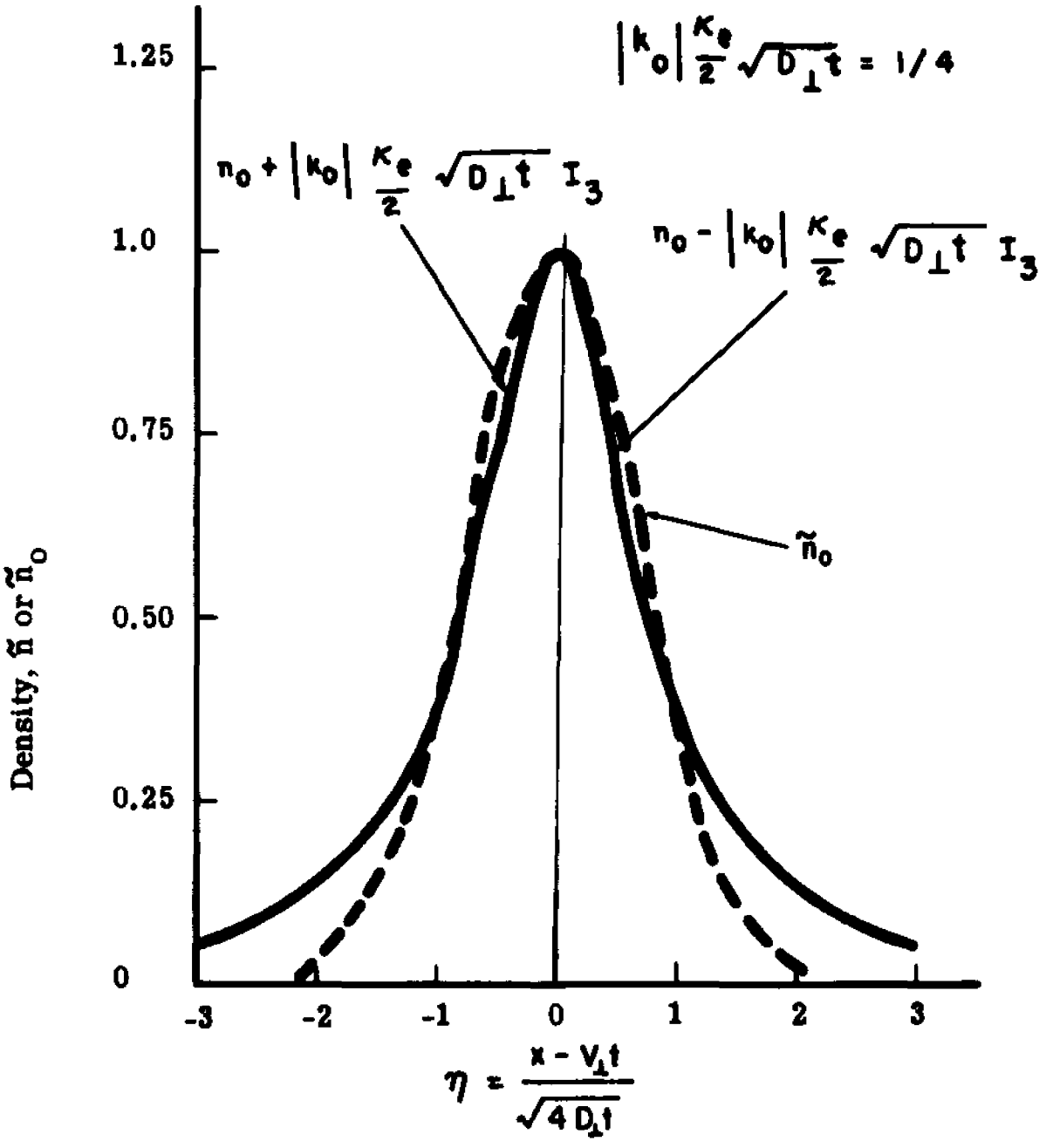

Fig. 3.25. Nonlinear Density Profile with $U t=0$, Exponential Mean Density Distribution

7. NUMERICAL SOLUTION OF THE NONLINEAR SYSTEM OF EQUATIONS OF A PLASMA INHOMOGENEITY

As the analytical solution of the nonlinear diffusion equation presented in the previous section is based on a number of simplifying assumptions, the numerical solution of the exact equation in three dimensions is undertaken. In principle it is expected that such a solution would show the features that arise from nonlinearity, such as steepening, and, in addition, those that are due to the 3 dimensional effect, such as the splitting. However, due to the long computation time required the calculations have not been carried to a point where the splitting can be seen.

To obtain a numerical solution of the nonlinear equations without approximations, it has been deemed advisable to program the system of two second order equations

$$\frac{\partial n}{\partial t} - \frac{1}{e}\nabla\cdot\underset{\approx}{\alpha}_i\cdot\nabla\phi + \nabla\cdot n\underset{\sim}{V}_i = \nabla\cdot\underset{\approx}{D}_i\cdot\nabla n, \tag{7.1}$$

$$\frac{1}{e}\nabla\cdot n\left(\underset{\approx}{\alpha}_i + \underset{\approx}{\alpha}_e\right)\cdot\nabla\phi + \nabla\cdot n\left(\underset{\sim}{V}_e - \underset{\sim}{V}_i\right) = \nabla\cdot\left(\underset{\approx}{D}_e - \underset{\approx}{D}_i\right)\cdot\nabla n \tag{7.2}$$

obtained from Eq. II,(3.20) and II,(3.21), rather than to attempt to solve a single fourth order differential equation, such as the diffusion equation III,(1.6).

The coordinates are taken to be the same as those employed previously, with the wind in the x_1-direction and the magnetic field in the x_3-direction.

For numerical solution Eq. (7.1) and (7.2) are written as finite difference equations, using the forward difference method for a nodal point located at $x_1 = h$, $x_2 = j$ and $x_3 = k$,

$$\left(\frac{\Delta n}{\Delta t}\right)_{h,j,k} = n_{h,j,k}\left[D_{\perp_i}\left(\frac{\nabla_h^2\phi}{(\Delta x_1)^2} + \frac{\nabla_j^2\phi}{(\Delta x_2)^2}\right) + D_{\parallel_i}\frac{\nabla_k^2\phi}{(\Delta x_3)^2}\right]$$

$$+ D_{\perp_i}\left(\frac{\nabla_h n}{\Delta x_1}\frac{\nabla_h\phi}{\Delta x_1} + \frac{\nabla_j n}{\Delta x_2}\frac{\nabla_j\phi}{\Delta x_2}\right) + D_{\parallel_i}\frac{\nabla_k n}{\Delta x_3}\frac{\nabla_k\phi}{\Delta x_3}$$

$$+ D_{\perp_i}\left(\frac{\nabla_h n}{\Delta x_1}\frac{\nabla_j\phi}{\Delta x_2} - \frac{\nabla_j n}{\Delta x_2}\frac{\nabla_h\phi}{\Delta x_1}\right) - V_{1_i}\frac{\nabla_h n}{\Delta x_1} - V_{2_i}\frac{\nabla_j n}{\Delta x_2}$$

$$+ D_{\perp_i}\left(\frac{\nabla_h^2 n}{(\Delta x_1)^2} + \frac{\nabla_j^2 n}{(\Delta x_2)^2}\right) + D_{\parallel_i}\frac{\nabla_k^2 n}{(\Delta x_3)^2} \qquad (7.3)$$

and

$$n_{h,j,k}\left[\left(D_{\perp_i} + D_{\perp_e}\right)\left(\frac{\nabla_h^2\phi}{(\Delta x_1)^2} + \frac{\nabla_j^2\phi}{(\Delta x_2)^2}\right)\right.$$

$$+ \frac{D_{\parallel_i} + D_{\parallel_e}}{(\Delta x_3)^2}\left(\phi_{h,j,k+1} - 2\phi_{h,j,k} + \phi_{h,j,k-1}\right)\Big] + \frac{D_{\perp_i} + D_{\perp_e}}{\Delta x_1}\left[\left(\phi_{h+1,j,k} - \phi_{h-1,j,k}\right)\right.$$

$$\left. + \frac{\nabla_j n}{\Delta x_2}\left(\phi_{h,j+1,k} - \phi_{h,j-1,k}\right)\right] + \frac{D_{\parallel_i} + D_{\parallel_e}}{\Delta x_3}\left[\frac{\nabla_k n}{\Delta x_3}\left(\phi_{h,j,k+1} - \phi_{h,j,k-1}\right)\right] + \left(D_{H_i} + D_{H_e}\right)\left[\frac{\nabla_h n}{\Delta x_1 \Delta x_2}\left(\phi_{h,j+1,k}\right.\right.$$

$$\left.\left. - \phi_{h,j-1,k}\right) - \frac{\nabla_j n}{\Delta x_2 \Delta x_1}\left(\phi_{h+1,j,k} - \phi_{h-1,j,k}\right)\right] = Q_{h,j,k}. \qquad (7.4)$$

where

Δx_m = node spacing in m direction,

Δt = time interval,

Δn = incremental density in time interval Δt,

$$D_{\perp i} = \frac{1}{4(1+\kappa_i^2)}, \qquad D_{\perp e} = \frac{1}{4(1+\kappa_e^2)},$$

$$D_{\parallel i} = \frac{1}{4}, \qquad D_{\parallel e} = \frac{|\kappa_e|}{4\kappa_i},$$

$$D_{H i} = \frac{\kappa_i}{4(1+\kappa_i^2)}, \qquad D_{H e} = -\frac{|\kappa_e|}{4(1+\kappa_e^2)},$$

$$V_{1 i} = \frac{1}{2(1+\kappa_i^2)}, \qquad V_{1e} = \frac{1}{2(1+\kappa_e^2)},$$

$$V_{2 i} = -\frac{\kappa_i}{1+\kappa_i^2}, \qquad V_{2e} = \frac{|\kappa_e|}{2(1+\kappa_e^2)},$$

$$Q_{h,j,k} = (V_{1i} - V_{1e})\frac{\nabla_h n}{\Delta x_1} + (V_{2i} - V_{2e})\frac{\nabla_j n}{\Delta x_2} + (D_{\perp e} - D_{\perp i})\left[\frac{\nabla_h^2 n}{(\Delta x_1)^2} + \frac{\nabla_j^2 n}{(\Delta x_2)^2}\right] + (D_{\parallel e} + D_{\parallel i})\frac{\nabla_k^2 n}{(\Delta x_3)^2}$$

and $\nabla_m f$ and $\nabla_m^2 f$ are the first and second derivatives with respect to m, given by

$$\nabla_m f = f_{m+1} - f_m,$$

$$\nabla_m^2 f = f_{m+1} - 2f_m + f_{m-1},$$

where

$$m = h, j, k ,$$

$$f = n, \phi .$$

Solving Eq. (7.4) for ϕ we obtain

$$\phi_{h,j,k} = \frac{1}{Y}\left[a_h \frac{\phi_{h+1,j,k}}{(\Delta x_1)^2} + a_j \frac{\phi_{h,j+1,k}}{(\Delta x_2)^2} + a_k \frac{\phi_{h,j,k+1}}{(\Delta x_3)^2} + b_h \frac{\phi_{h-1,j,k}}{(\Delta x_1)^2} + b_j \frac{\phi_{h,j-1,k}}{(\Delta x_2)^2} + b_k \frac{\phi_{h,j,k-1}}{(\Delta x_3)^2}\right] - Q_{h,j,k}, \quad (7.5)$$

where

$$Y = 2\left[\frac{D_{\perp i} + D_{\perp e}}{(\Delta x_1)^2} + \frac{D_{\perp i} + D_{\perp e}}{(\Delta x_2)^2} + \frac{D_{\parallel i} + D_{\parallel e}}{(\Delta x_3)^2}\right] + \frac{D_{\perp i} + D_{\perp e}}{n_{h,j,k}}\left[\frac{\nabla_h n}{(\Delta x_1)^2} + \frac{\nabla_j n}{(\Delta x_2)^2}\right] + \frac{D_{\parallel i} + D_{\parallel e}}{n_{h,j,k}} \frac{\nabla_k n}{(\Delta x_3)^2} + \frac{D_{\parallel i} + D_{\parallel e}}{n_{h,j,k}}\left[\frac{n_{h+1,j,k} - n_{h,j+1,k}}{\Delta x_1 \, \Delta x_2}\right] ,$$

$$a_h = \frac{D_{\perp i} + D_{\perp e}}{n_{h,j,k}} \frac{\nabla_h n}{(\Delta x_1)^2} - \frac{D_{\parallel i} + D_{\parallel e}}{n_{h,j,k}} \frac{\nabla_j n}{\Delta x_1 \Delta x_2} ,$$

$$a_j = \frac{D_{\perp i} + D_{\perp e}}{n_{h,j,k}} \frac{\nabla_j n}{(\Delta x_2)^2} - \frac{D_{\parallel i} + D_{\parallel e}}{n_{h,j,k}} \frac{\nabla_h n}{\Delta x_2 \Delta x_1} ,$$

$$a_k = \frac{D_{\parallel i} + D_{\parallel e}}{n_{h,j,k}} \frac{\nabla_k n}{(\Delta x_3)^2} ,$$

$$b_h = \frac{D_{\perp i} + D_{\perp e}}{(\Delta x_1)^2} , \qquad b_j = \frac{D_{\perp i} + D_{\perp e}}{(\Delta x_2)^2} ,$$

$$b_k = \frac{D_{\parallel i} + D_{\parallel e}}{(\Delta x_3)^2} .$$

Inasmuch as an inhomogeneity usually starts as a sphere with a Gaussian density distribution, the computation has been started with such a density distribution at time t = o, with an arbitrary peak density of 100, and a constant background density of 0.05. New density distributions are then calculated at succeeding times $t+\Delta t$ where Δt is a small time interval. Equation (7.5) is solved first for the correct ϕ at all points by an iterative procedure using the Seidel-Gauss method with scaling. In calculating ϕ, the nonlinear terms are formed from the known density distribution of the previous time step. The values of ϕ are then substituted in Eq. (7.3) and $\frac{\Delta n}{\Delta t}$ calculated. The density at time $t+\Delta t$ is then obtained from the relation

$$n_{h,j,k}(t+\Delta t) = n_{h,j,k}(t) + \left(\frac{\Delta n}{\Delta t}\right)_{h,j,k} \Delta t \,.$$

The system of equations (7.3) and (7.5) has been programmed in Fortran IV and computations started on an IBM 360/190 digital computer. The computations have been performed for a three dimensional array of 17,424 space points. For convenience the same non-dimensional time $\tilde{t}$ and scale $\tilde{x}$ devised for the linear solution and given by (5.4) are used. However, the density n is not transformed to non-dimensional form as it represents an arbitrary initial value. To maintain computational stability a small time step, $\Delta\tilde{t} = 0.015$ has been required. This has led to large amounts of computer time for comparatively small real time periods. The time development of the inhomogeneity therefore has been carried out to only a time of $\tilde{t} = 0.8$. The density profile in the x_1-direction at this time is shown in Fig. (3.26). It clearly exhibits

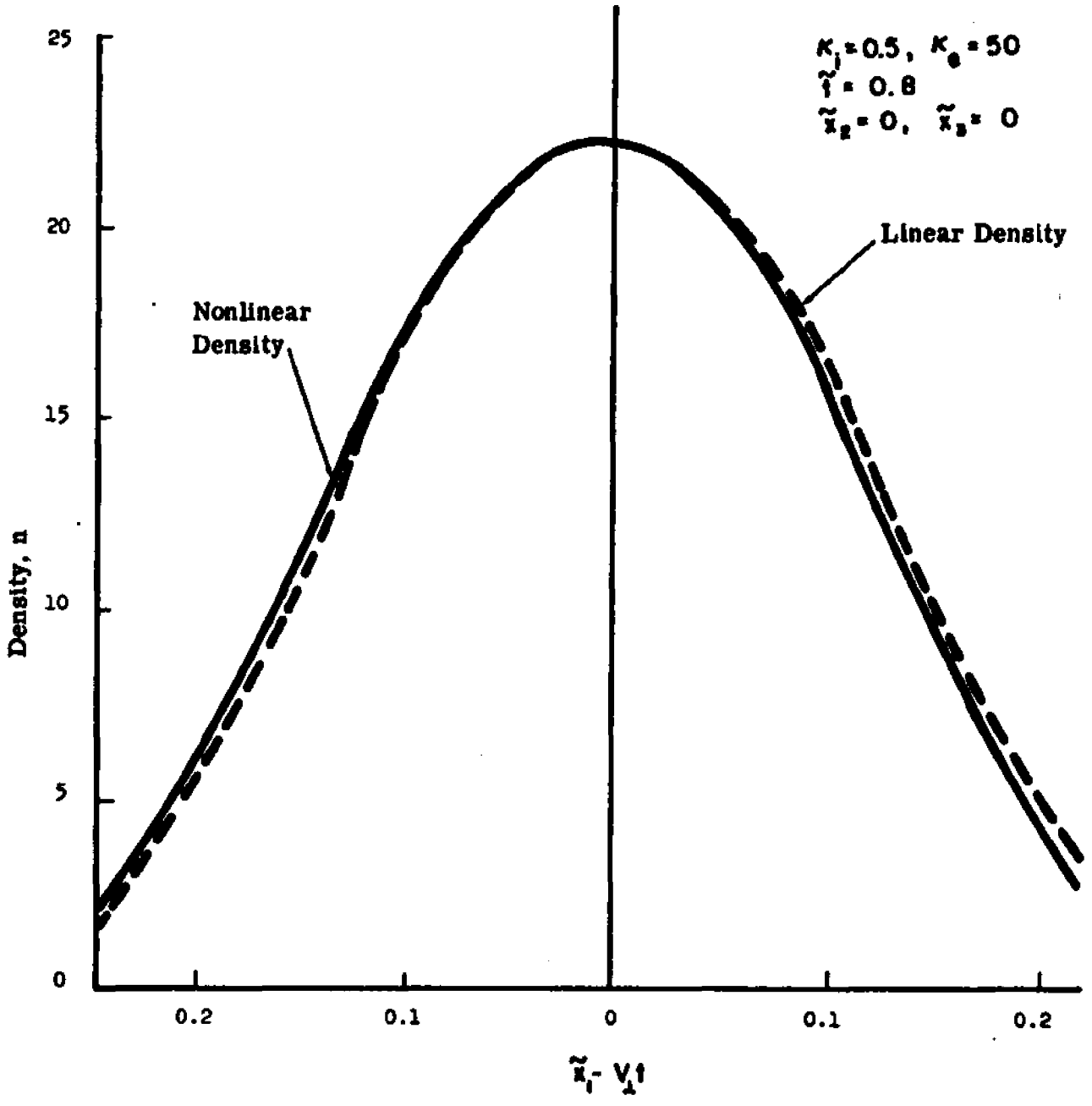

Fig. 3.26. Nonlinear Density Profile from Numerical Solution.

the steepening front in the x_1-direction in agreement with observations of ion cloud experiments.

As the computation has not been carried out for a longer time period, the splitting of the inhomogeneity is not yet apparent.

8. CONCLUSIONS

(i) The diffusion of a plasma inhomogeneity in a magnetic field, as driven by an external electric field or an atmospheric wind, is found to be governed by a fourth order nonlinear differential equation with variable ambipolar drift and variable ambipolar diffusion coefficient.

(ii) The linearized solution of the diffusion equation predicts the separation of the inhomogeneity with time, and an increase in the spread of the inhomogeneity which is proportional to the product $\varkappa_i \cdot \varkappa_e$

(iii) The diffusive effects of an external electric field of strength $\underset{\sim}{E}$ can be reduced to that of a wind with velocity $\underset{\sim}{W}_o = -\frac{c}{B}\underset{\sim}{E}_o \times \underset{\sim}{B}$ by shifted by a vector $-\underset{\sim}{W}_o$.

(iv) Analytical and numerical solutions of the nonlinear diffusion equation show that the nonlinearity leads to a steepening of the front side of the inhomogeneity. This steepening is proportional to $\varkappa_o U t$ and therefore destabilizes the plasma in the course of time.

(v) In the absence of a wind or electric field the diffusion may still be nonlinear, but the cloud remains symmetrical.

(vi) The theoretical results obtained generally agree with observations during tests with artificial plasma clouds.

Chapter IV

Theory of Striations

1. INTRODUCTION

Striations are a manifestation of the instability of plasmas and have been observed in aurora and in barium releases in the upper atmosphere. In the barium experiments striations appear about 10 minutes after release, usually at the edge of the plasma cloud closest to the neutral cloud, because that edge is unstable on the basis of drift instability.

Theories explaining the appearance of striations due to plasma instability, have been reported by several investigators [20-25], who showed that a plasma in a magnetic field is unstable if an electric field exists perpendicular to the magnetic field and the density gradient is in the same direction as the electric field. Because of the presence of crossed electric and magnetic fields this phenomenon has been called the E x B instability[32], the crossed field instability, or the density induced drift instability. Its basic mechanism arises from the unequal drift of ions and electrons in crossed electric and magnetic fields. The drift instability mechanism has been suggested by Hasegawa[33] to explain the appearance of striations in aurora. More recently Cunnold[34] has postulated that a similar type of instability in the F layers of the ionosphere can be caused by a temperature gradient as well as a density

gradient. The present theory of drift instability is developed from a new approach, using a fourth order diffusion equation including dissipations. This theory is more general and systematic than others. The results are compared with observations of striations in artificially released plasma clouds.

2. BASIC EQUATIONS OF PERTURBATION

Consider the fourth order diffusion equation, derived in Eq. III,(1.6) for a plasma in a magnetic field and with a neutral wind or an external electric field, rewritten as,

$$\left(\nabla\cdot n\underset{\approx}{\alpha}_i\cdot\nabla\right)\left[\frac{\partial n}{\partial t}+\left(\underset{\sim}{V}_e\cdot\nabla n-\nabla\cdot\underset{\approx}{D}_e\cdot\nabla n\right)\right]$$

$$+\left(i\leftrightarrow e\right)=0, \tag{2.1}$$

where $(i\leftrightarrow e)$ represents similar terms obtained by interchanging the subscripts i and e. The notations used are

$$\underset{\sim}{V}_a=\underset{\approx}{K}_a\cdot\left(\frac{c}{B}\underset{\sim}{E}_0+\underset{\sim}{U}\times\hat{e}_B\right)+\underset{\sim}{U}, \tag{2.2}$$

$$\underset{\approx}{\alpha}_a=\frac{e_a c}{B}\underset{\approx}{K}_a, \tag{2.3}$$

$$\underset{\approx}{D}_a=\frac{kT_a}{e^2}\underset{\approx}{\alpha}, \tag{2.4}$$

$$\underset{\approx}{K}_a = \begin{vmatrix} K_{a_\perp} & K_{a_H} & 0 \\ -K_{a_H} & K_{a_\perp} & 0 \\ 0 & 0 & K_{a_\parallel} \end{vmatrix} , \tag{2.5}$$

$$K_{a_\parallel} = \mathcal{K}_a ,$$

$$K_{a_\perp} = \frac{\mathcal{K}_a}{1+\mathcal{K}_a^2} , \tag{2.6}$$

$$K_{a_H} = \frac{\mathcal{K}_a^2}{1+\mathcal{K}_a^2} ,$$

$$\mathcal{K}_a = \frac{\Omega_a}{\nu_a^*} ,$$

$$\Omega_a = \frac{e_a B}{m_a c} . \tag{2.7}$$

where m_a is the electron or ion mass, ν_a^* is the effective frequency, the subscript a refers to ions $(\quad)_i$ or electrons $(\quad)_e$, $\underset{\sim}{U}$ is the neutral wind velocity, $\underset{\sim}{E}_0$ is an external field, $\underset{\sim}{B}$ is the magnetic field, c is the speed of light, e_a is the electron or ion charge, $\hat{e}_B$ is a unit vector in the direction of the magnetic field. The density n is composed of two parts

$$n = n_0 + n' \tag{2.8}$$

including a background density n_0 , and a perturbation n' .

Substitution of (2.8) into (2.1) yields,

$$\nabla\cdot\left(n_o\underset{\sim}{\underset{\approx}{\alpha}}_i\cdot\nabla\right)\left[\frac{\partial n'}{\partial t}+\left(\underset{\sim}{V}_e\cdot\nabla n'-\nabla\cdot\underset{\sim}{\underset{\approx}{D}}_e\cdot\nabla n'\right)\right]$$
$$+\nabla\cdot\left(n'\underset{\sim}{\underset{\approx}{\alpha}}_i\cdot\nabla\right)\left[\frac{\partial n_o}{\partial t}+\left(\underset{\sim}{V}_e\cdot\nabla n_o-\nabla\cdot\underset{\sim}{\underset{\approx}{D}}_e\cdot\nabla n_o\right)\right]$$
$$+\left(i\leftrightarrow e\right)=0\,. \tag{2.9}$$

3. DISPERSION RELATION

To study the stability of the plasma from Eq. (2.9), we assume that n' is of the form,

$$n'=n_o e^{-i(\omega t-\underset{\sim}{k}\cdot\underset{\sim}{x})} \tag{3.1}$$

in the plane transverse to the magnetic field, where ω is the oscillation frequency, a complex number, and $\underset{\sim}{k}$ is the wave number of the excitation, a real number. It is now required to find the so called dispersion relation, which is a relation between ω and $\underset{\sim}{k}$. The background density n_o is expressed as a function of $\underset{\sim}{x}$ and t, which, for the sake of simplicity, is written as an exponential function

$$n_o=N_o e^{\underset{\sim}{k}_o\cdot\left(\underset{\sim}{x}-\underset{\sim}{V}_\perp t\right)}\,. \tag{3.2}$$

Here $\underset{\sim}{V}_\perp$ is the ambipolar drift in two dimensions given by III,(2.14),

$$\underset{\sim}{V}_\perp = \frac{\alpha_{\perp i}\underset{\sim}{V}_e + \alpha_{\perp e}\underset{\sim}{V}_i}{\alpha_{\perp i} + \alpha_{\perp e}} , \tag{3.3}$$

N_o is the constant peak density, and $\underset{\sim}{k}_o$ is the density gradient

$$\underset{\sim}{k}_o = \frac{\nabla n_o}{n_o} .$$

The approximate exponential shape of the cloud as expressed by (3.2) is not a poor simulation of the actual Gaussian cloud at least for a small region. As before, we assume that the magnetic field is in the x_3-direction and the ambipolar drift velocity $\underset{\sim}{V}_\perp$ in the x_1-direction. Substitution of (3.1) and (3.2) into Eq. (2.9) for two dimensions yields

$$\begin{aligned}\alpha_{\perp i} P_\perp \left(\underset{\sim}{k}_o \cdot \underset{\sim}{V}_\perp + i\omega\right) - \left(\alpha_{\perp i} P_\perp + \alpha_{H i} P_H\right)\Big[\left(i\underset{\sim}{k} + \underset{\sim}{k}_o\right)\cdot\underset{\sim}{V}_e \\ - L_\perp^2 D_{\perp e}\Big] - \left(\alpha_{\perp i} Q_\perp - \alpha_{H i} P_H\right)\Big[\underset{\sim}{k}_o \cdot \underset{\sim}{V}_e \\ - \left(k_{o_1}^2 + k_{o_2}^2\right) D_{\perp e}\Big] + \left(i \leftrightarrow e\right) = 0 ,\end{aligned} \tag{3.4}$$

where

$$\begin{aligned}P_\perp = 2\left(k_{o_1}^2 + k_{o_2}^2\right) - \left(k_1^2 + k_2^2\right) \\ + 3i\left(k_1 k_{o_1} + k_2 k_{o_2}\right)\end{aligned}$$

and

$$Q_\perp = 2\left(k_{o_1}^2 + k_{o_2}^2\right) + i\left(k_1 k_{o_1} + k_2 k_{o_2}\right)$$

$$P_H = i\left(k_{o_1} k_2 - k_{o_2} k_1\right)$$

$$L_\perp^2 = k_{o_1}^2 + k_{o_2}^2 - k_1^2 - k_2^2 + 2i\left(k_1 k_{o_1} + k_2 k_{o_2}\right).$$

As the exitations in the ionosphere are bound to be large, we can assume

$$k_0 \ll k$$

and neglect higher powers of k_{o_1} or k_{o_2} than the first. With this simplification the frequency ω from (3.4) becomes

$$\omega = \underset{\sim}{k}\cdot\left(\underset{\sim}{V}_\perp + \frac{P_H}{P_\perp}\underset{\sim}{V}_H\right) + i L_\perp^2\left(D_\perp + \frac{P_H}{P_\perp} D_H\right)$$

$$= \underset{\sim}{k}\cdot\underset{\sim}{V}_\perp + \left(k_{o_1} k_2 - k_{o_2} k_1\right) D_H - \left(k_{o_1} k_1 + k_{o_2} k_2\right) 2 D_\perp + i\left[\frac{k_{o_2} k_1 - k_{o_1} k_2}{k^2}\, k\cdot\underset{\sim}{V}_H - k^2 D_\perp\right], \qquad (3.5)$$

where

$$\underset{\sim}{V}_H = \frac{\alpha_{Hi}\,\underset{\sim}{V}_e + \alpha_{He}\,\underset{\sim}{V}_i}{\alpha_{\perp i} + \alpha_{\perp e}}\,, \tag{3.6}$$

$$D_\perp = \frac{\alpha_{\perp i}\,D_{\perp e} + \alpha_{\perp e}\,D_{\perp i}}{\alpha_{\perp i} + \alpha_{\perp e}}\,, \tag{3.7}$$

$$D_H = \frac{\alpha_{Hi}\,D_{\perp e} + \alpha_{He}\,D_{\perp i}}{\alpha_{\perp i} + \alpha_{\perp e}}\,. \tag{3.8}$$

Equation (3.5) is the desired dispersion relation in terms of the ambipolar drift $V_\perp$, the Hall drift $\underset{\sim}{V}_H$, the ambipolar diffusion coefficient $D_\perp$ and the Hall diffusion coefficient D_H.

By letting

$$\omega = \omega_0 + i\gamma \tag{3.9}$$

we can obtain the oscillation frequency ω_0 from the real part of (3.5) and the growth rate γ from the imaginary part. According to the definition (3.1), the instability corresponds to $\gamma > 0$, i.e., the amplitude of the oscillations grow with time while for $\gamma < 0$ any oscillations will damp out.

We now investigate the amplitude and growth rate for two special cases, one where the plasma inhomogeneity is driven by a neutral

wind, with

$$\underset{\sim}{U} \neq 0 \; ; \qquad \underset{\sim}{E}_0 = 0$$

and the other where the inhomogeneity is driven by an external electric field, with

$$\underset{\sim}{U} = 0 \; ; \qquad \underset{\sim}{E}_0 \neq 0 \; .$$

4. OSCILLATIONS IN A PLASMA INHOMOGENEITY IN A NEUTRAL WIND $(\underset{\sim}{U} \neq 0, \underset{\sim}{E}_0 = 0)$

For this case, from III,(4.6)

$$\underset{\sim}{V}_\perp = \frac{\underset{\sim}{U}}{1 + |\kappa_i \kappa_e|}$$

and by substituting for the drift velocities $\underset{\sim}{V}_i$ and $\underset{\sim}{V}_e$, from III,(4.4) in (3.6), we obtain the Hall drift,

$$\underset{\sim}{V}_H = - \frac{U}{\kappa_i} \hat{x}_1 + U \hat{x}_2 \; , \qquad (4.1)$$

where $\hat{x}_1$ and $\hat{x}_2$ are the unit vectors in the x_1 and x_2 direction, respectively. A substitution of (4.1) in Eq. (3.5) yields,

$$\omega = \frac{k_1 U}{1 + |\kappa_i \kappa_e|} + (k_{01} k_2 - k_{02} k_1) D_H - (k_{01} k_1 + k_{02} k_2) z D_\perp + i \left[\frac{k_{02} k_1 - k_{01} k_2}{k^2} \left(k_2 - \frac{k_1}{\kappa_i} \right) U - k^2 D_\perp \right] . \qquad (4.2)$$

To simplify, we take the case where $k_{o_1} = k_{o_2}$ and consider two directions for k. First we let

$$\text{(i)} \quad k_1 \neq 0 \quad , \quad k_2 = 0 \, ,$$

whereupon from (4.2) we obtain

$$\omega_o = k \left[\frac{U}{1 + |\kappa_i \kappa_e|} - k_o \left(D_H + 2 D_\perp \right) \right] , \tag{4.3}$$

$$\gamma = - \frac{k_o U}{\kappa_i} - k^2 D_\perp \, . \tag{4.4}$$

Equation (4.3) shows that the oscillation frequency ω_o is proportional to k while Eq. (4.4) shows that for instability we require that

$$- \frac{k_o U}{\kappa_i} > k^2 D_\perp \, . \tag{4.5}$$

Condition (4.5) can only occur on the front side of the inhomogeneity where $k_o < 0$.

Next we consider the case where

$$\text{(ii)} \quad k_1 = 0 \quad ; \quad k_2 \neq 0 \, ,$$

so that (4.2) reduces to

$$\omega_o = k k_o \left(D_H - 2 D_\perp \right) \tag{4.6}$$

and

$$\gamma = -k_0 U - k^2 D_\perp \,, \tag{4.7}$$

which shows that the frequency again is proportional to k and that the instability can only occur on the front side of the inhomogeneity.

5. OSCILLATIONS IN A PLASMA INHOMOGENEITY IN AN EXTERNAL ELECTRIC FIELD ($\underset{\sim}{U} = 0$, $\underset{\sim}{E}_0 \neq 0$)

When there is an external electric field $\underset{\sim}{E}_0$ in the x_2-direction the inhomogeneity drifts in the x_1-direction with an ambipolar drift derived from III,(4.20) as,

$$\underset{\sim}{V}_\perp = \frac{E_0 c}{B} \hat{x}_1 \,. \tag{5.1}$$

A substitution of the drift velocities $\underset{\sim}{V}_i$ and $\underset{\sim}{V}_e$ from Eq. III,(4.16) in (3.6) leads to the Hall drift

$$\underset{\sim}{V}_H = -\frac{E_0 c}{B} \hat{x}_2 \,, \tag{5.2}$$

which upon substitution in (3.5) yields,

$$\omega = k_1 \frac{E_0 c}{B} + (k_{01} k_2 - k_{02} k_1) D_H - (k_{01} k_1 + k_{02} k_1) 2 D_\perp$$
$$+ i \left[\frac{k_{01} k_2 - k_{02} k_1}{k^2} k_2 \frac{E_0 c}{B} - k^2 D_\perp \right] . \tag{5.3}$$

Again taking $k_{o_1} = k_{o_2}$ and examining two specific directions for k, for

(i) $k_1 \neq 0 \qquad k_2 = 0$,

we obtain

$$\omega_o = k\left[\frac{E_o c}{B} - k_o\left(D_H + D_\perp\right)\right], \tag{5.4}$$

$$\gamma = -k^2 D_\perp , \tag{5.5}$$

which shows that the oscillation frequency is proportional to k and that there can be no instability as γ is always negative.

(ii) For the second case, $k_1 = 0$, $k_2 \neq 0$

and (5.3) reduces to

$$\omega_o = k k_o \left(D_H - 2D_\perp\right), \tag{5.6}$$

$$\gamma = k_o \frac{E_o c}{B} - k^2 D_\perp . \tag{5.7}$$

The frequency, according to (5.6), is again proportional to k while from (5.7), an instability condition requires that

$$k_o \frac{E_o c}{B} > k^2 D_\perp , \tag{5.8}$$

a condition that can only occur on the side of the inhomogeneity where $x < V_\perp t$.

6. CRITICAL WAVE NUMBER DIVIDING A STABLE AND UNSTABLE OSCILLATION

As an application of the theory of oscillations developed above, the dispersion relation (4.7) is plotted in Fig. (4.1) for typical values of an artificial plasma inhomogeneity in an atmospheric wind in the ionosphere, about 10 minutes after release:

$$\begin{aligned} U &= 0.1 \ km/sec, \\ D_\perp &= 0.001 \ km^2/sec., \\ r_\perp &= 10 \ km \end{aligned} \tag{6.1}$$

Here r is the radius of the inhomogeneity in the transverse direction. The value of k_0 at the leading edge of the inhomogeneity where the striations start can be estimated as,

$$k_0 \cong -\frac{1}{r_\perp/2} = -0.2 \ km^{-1} \tag{6.2}$$

and the critical wave number k_s which separates a stable oscillation from an unstable one is obtained by setting $\gamma = 0$ in (4.7), which yields,

$$k_s = \left(\frac{-k_0 U}{D_\perp}\right)^{\frac{1}{2}} . \tag{6.3}$$

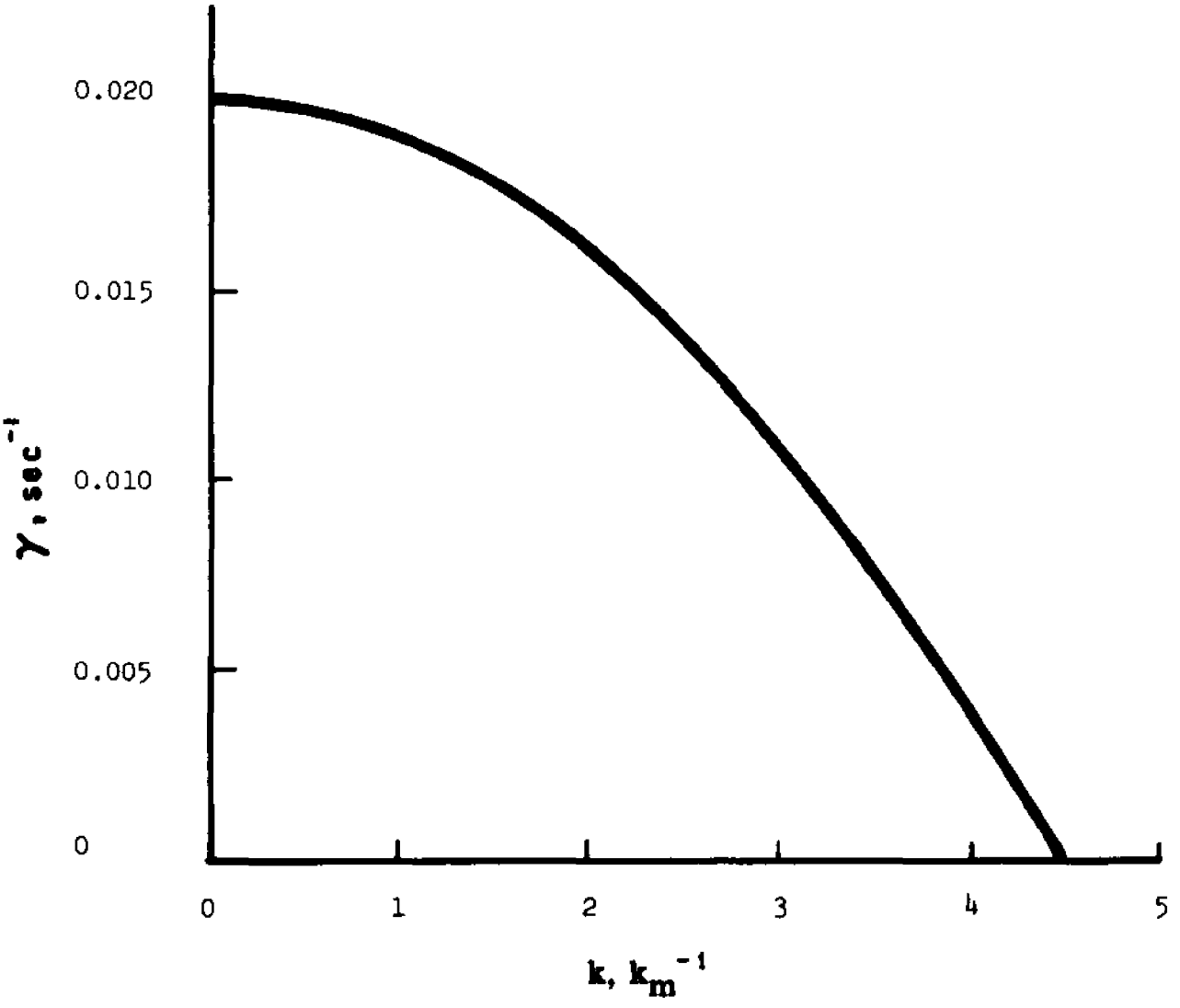

Fig. 4.1. Dispersion Relation, Plasma Inhomogeneity in Neutral Wind.

With the constants of (6.1) and (6.2),

$$k_s = 4.5 \ km^{-1}$$

and the wave length ℓ_s corresponding to the critical wave number then is,

$$\ell_s = \frac{2\pi}{k_s} = 1.4 \ km \ .$$

This distance is in good agreement with observed widths of striations in plasma clouds, which are of the order of 1 km.

7. CONCLUSIONS

The theory of striations developed above leads to the following results.

(i) The amplitude of the oscillations is proportional to the exitation wave number k, for small k_0.

(ii) Unstable oscillations in plasma inhomogeneities in a neutral wind develop at the leading edge, which is the side with a negative mean density gradient. The molecular dissipation dampens the growth so that a positive growth corresponds to the condition

$$k_0 U > k^2 D_\perp \ ,$$

see (6.3). The problem of instability caused by a wind drift is studied in Section 4.

(iii) The instability of a plasma inhomogeneity in an external field is studied in Section 5. The growth occurs at wave numbers smaller than a critical value k_s such that

$$\frac{k_0 E_{oc}}{B} > k' D_1 .$$

As the Hall drift V_H, which causes the instability is in the direction of the electric field only exitation modes in that (x_2-direction) direction are effective in causing instabilities.

(iv) Results obtained above agree with artificial cloud experiments.

Chapter V

Theory of Turbulence Generated by Drift Instability in a Plasma Inhomogeneity

1. INTRODUCTION

In previous chapters, the larger and intermediate scale plasma motions, characterized by diffusion and striations were analyzed. Now we turn our attention to the small scale fluctuations in a plasma inhomogeneity, i.e., to turbulence.

As pointed out in Chapter I, the effects of turbulence have been observed in artificial barium cloud experiments where the morphology of the cloud did not follow classical diffusion laws. In addition, recent experiments in beam-plasma interactions[35], turbulent heating[36], diffusion in porous media and stochastic acceleration of particles in plasma have shown the importance of the role of turbulent processes in determining the transport properties and physical features of plasmas.

The effects of turbulence on plasmas are two-fold:

(i) In most problems of turbulent transport, it is necessary to enter into the study of the structure of turbulence, e.g., the turbulent spectral distributions of plasma kinetic energy, plasma density, and of electric field fluctuations.

(ii) The turbulent motions introduce new transport coefficients, called anomalous or eddy transport coefficients and consequently modify the diffusion of a plasma inhomogeneity.

These two topics are covered in this chapter. A theory on the structure of turbulence is presented first, followed by a study of the effects of turbulence on the transport properties of a plasma inhomogeneity.

2. STRUCTURE OF TURBULENCE

In this section, a simple theory on the structure of turbulence is given, while experimental results are presented in the following section. Turbulence in a plasma inhomogeneity results from energy input deriving from a mean density gradient and a non-uniform electric field within the plasma inhomogeneity as well as from the effects of turbulence in the background atmosphere in which the inhomogeneity is embedded. This analysis only treats the self-generating plasma turbulence.

As seen in Chapter IV, an inhomogeneous plasma can be unstable to a drift. This instability may lead to turbulence. In view of the presence of the non-linear mode coupling, the flow of energy across a turbulent spectrum covers the full sequence of production, inertia and dissipation subranges in the universal part of the spectrum.

Theories on plasma turbulence are mostly confined to weak turbulence[26] for the sake of the simplicity of treatment. But the turbulent motions, as observed in atmospheres and laboratories, often belong to strong turbulence. The simplest model is the isotropic and homogeneous hydrodynamic turbulence, for which dimensional methods are known to predict certain spectral laws, verifiable by experiments, e.g., the Kolmogoroff law. Most analytical theories have not yet been able to predict this law in a satisfactory manner.

The more complicated problem of plasma turbulence cannot fruitfully resort to the above analytical methods. For this reason, Tchen[31] has proposed a repeated cascade method. Since the mathematical details are still cumbersome, we shall present in the present work, a simplified model. This offers an opportunity to discuss certain fundamental mechanism of turbulent processes in plasma, and at the same to propose a dimensional theory.

a. Fundamental Equations

As a mathematical model, an inhomogeneous plasma can be described by a system of two equations governing density and electric field. Those equations have been derived for a low frequency plasma by Eq. II,(3.29) and II,(3.30) and can be written as,

$$\frac{\partial n}{\partial t} + \nabla \cdot n \underset{\sim}{w} = D \nabla^2 n , \tag{2.1}$$

$$\nabla \cdot n \underset{\sim}{u} = \lambda \nabla^2 n , \tag{2.2}$$

$$\underset{\sim}{w} = \frac{c}{B}\left(\underset{\sim}{E}_o - \nabla\phi\right) \times \hat{e}_B \,, \tag{2.3}$$

$$\underset{\sim}{u} = \frac{c}{B}\left(\underset{\sim}{E}_o - \nabla\phi\right) + \underset{\sim}{U} \times \hat{e}_B \,, \tag{2.4}$$

where n is the plasma density, ϕ is an electric field potential, $\underset{\sim}{U}$ is the neutral wind velocity, $\underset{\sim}{E}_o$ is an external electral field, B is the magnetic field strength, c is the speed of light, D and λ are diffusion coefficients and $\hat{e}_B$ is a unit vector in the direction of the magnetic field.

For the sake of simplification, the structure of turbulence will be studied in the plane transverse to the magnetic field, and therefore Eq. (2.1) and (2.2) will be considered in two dimensions. The variables n , $\underset{\sim}{u}$, and $\underset{\sim}{w}$ can be decomposed into a mean value denoted by a bar and a fluctuation denoted by a prime, such as

$$n = \bar{n} + n' \quad . \tag{2.5}$$

This leads to

$$\begin{aligned}
\underset{\sim}{\bar{u}} &= \frac{c}{B}\left(\underset{\sim}{E}_o - \nabla\bar{\phi}\right) + \underset{\sim}{U} \times \hat{e}_B \,, \\
\underset{\sim}{u'} &= -\frac{c}{B}\nabla\phi' \,, \\
\underset{\sim}{\bar{w}} &= \frac{c}{B}\left(\underset{\sim}{E}_o - \nabla\bar{\phi}\right) \times \hat{e}_B \,, \\
w' &= \underset{\sim}{u'} \times \hat{e}_B \,,
\end{aligned} \tag{2.6}$$

where $\underset{\sim}{E}_o$ and $\underset{\sim}{U}$ are mean environmental quantities, $\bar{n}$ and $\bar{\phi}$ are mean values of the plasma inhomogeneity and n' and ϕ' are

fluctuations representative of the plasma turbulence. Substituting in the equations for total motion and subtracting the averaged equation for mean motion we obtain the equations for the fluctuations of plasma turbulence as follows:

$$\frac{\partial n'}{\partial t} + \underset{\sim}{\bar{w}} \cdot \nabla n' = -\underset{\sim}{w}' \cdot \left(\nabla \bar{n} + \nabla n' \right) + D \nabla^2 n' ,$$

$$\underset{\sim}{\bar{u}} \cdot \nabla n' = - \underset{\sim}{u}' \cdot \left(\nabla \bar{n} + \nabla n' \right) + \lambda \nabla^2 n' . \qquad (2.7)$$

It is now necessary to find expression for the fluctuations n' and ϕ' in terms of the mean quantities. This is accomplished by application of the cascade theory described below.

b. Cascade Method

To simplify the analysis, instead of the more rigorous repeated cascade method[31], the less cumbersome method of single cascade[30] for study of the spectral structure of hydrodynamic and plasma turbulence will be applied to the dynamic system, Eq. (2.7) for plasma turbulence. For this purpose, each of the fluctuating quantities is decomposed into two groups, one representing the large scale fluctuations, denoted by the superscript (^{o}) and another group representing the small scale fluctuations identified by subscript ($_{1}$), such that

$$\underset{\sim}{u}' = \underset{\sim}{u}^{o} + \underset{\sim}{u}^{(1)} . \qquad (2.8)$$

In accordance with the mixing length hypothesis, as introduced by Boussinesq[41] in studying turbulent motion, the two groups are associated with different mixing lengths, which can be incorporated into the Fourier components, such that for example, for the decomposition of $\underset{\sim}{u}'$, the component with the large scale is

$$\underset{\sim}{u}^{\circ}(\underset{\sim}{x},t) = \int_{0}^{k} d\underset{\sim}{k}\, e^{i\underset{\sim}{k}\cdot\underset{\sim}{x}}\, \underset{\sim}{u}'(\underset{\sim}{k},t)$$

and the other part with fine scales is

$$\underset{\sim}{u}^{(1)}(\underset{\sim}{x},t) = \int_{k}^{\infty} d\underset{\sim}{k}\, e^{i\underset{\sim}{k}\cdot\underset{\sim}{x}}\, \underset{\sim}{u}'(\underset{\sim}{k},t)\,,$$

or alternately that $\underset{\sim}{u}^{\circ}(\underset{\sim}{x},t)$ transforms into $\underset{\sim}{u}^{\circ}(\underset{\sim}{k},t)$ and $\underset{\sim}{u}'(\underset{\sim}{x},t)$ into $\underset{\sim}{u}'(\underset{\sim}{k},t)$. The large scale components are associated with wave number ranging from 0 to k and the small scale components with wave numbers ranging from k to ∞ .

As a quasi-stationary process, the large scales form a macroscopic background, prescribing the initial conditions for the motion of the smaller scales. The smaller scales move more randomly in the framework of the macroscopic background, and as a result of the statistical effect of fluctuations, shape up certain transport properties in the background medium. An ensemble average screens between the two entities.

The cascade ensemble averages, denoted by $< >$ are determined by means of cascade distribution functions which determine the relation

between the cascade ensemble average applicable to a quasi-homogeneous system and the global ensemble average applicable to a homogeneous system. The cascade system is not a series of perturbations of decreasing amplitude as in an iteration procedure, but is a series of physical processes. The rank $\mathcal{U}^o$ represents a field velocity in the portion of the spectrum between wave numbers zero and k and contributes to the kinetic energy. The transfer of energy across the spectrum is represented by a higher order correlation, called transfer functions in Fourier space, which in analogy with the molecular viscosity in the theories of gases, divide the spectrum into a vorticity portion and a portion of smaller scales representing eddy viscosity. The two portions interact in a cascade mechanism. The dividing wave number k can be considered an independent variable in an integral equation. It is then necessary to empirically postulate the formal structure of eddy viscosity, in order to reduce the transfer function which has the form of a triple correlation explicity in terms of the spectral distribution. In this study, the structure of the eddy viscosity has been derived on the basis of the physical significance of the particular function and a dimensional formulation. As a solution, power law spectra are found for the universal range of turbulence. In the context of spectral structure, the turbulent motion belongs to a quasi-stationary process, in which the large scale motions are considered relatively macroscopic, bulky and inert, while the smaller scales are more random and swift. Such a picture has already been incorporated in early treatments by Boussinesq, Richardson, Reynolds, and Lorentz.[43]

Upon applying the method of cascade decomposition and its rules of screening, the dynamical system Eq. (2.7) can be transformed into a cascade system for the large scale fluctuations by means of convolution integrals,

$$\frac{\partial n^{\circ}(\underset{\sim}{k})}{\partial t} + \int_{-\infty}^{\infty} d\underset{\sim}{k}' \, i\underset{\sim}{k}' \cdot \underset{\sim}{\bar{w}}(\underset{\sim}{k}-\underset{\sim}{k}') n^{\circ}(\underset{\sim}{k}')$$

$$= \int_{-\infty}^{\infty} d\underset{\sim}{k}' \, i\underset{\sim}{k}' \left[w^{\circ}(\underset{\sim}{k}-\underset{\sim}{k}') \bar{n}(\underset{\sim}{k}') + \langle \underset{\sim}{w}'(\underset{\sim}{k}-\underset{\sim}{k}') n'(\underset{\sim}{k}') \rangle \right] - D k^2 n^{\circ}(\underset{\sim}{k}), \tag{2.9}$$

$$\int_{-\infty}^{\infty} d\underset{\sim}{k} \, i\underset{\sim}{k}' \cdot \underset{\sim}{\bar{u}}(\underset{\sim}{k}-\underset{\sim}{k}') n^{\circ}(\underset{\sim}{k}')$$

$$= \int_{-\infty}^{\infty} d\underset{\sim}{k}' \, i\underset{\sim}{k}' \cdot \left[\underset{\sim}{u}^{\circ}(\underset{\sim}{k}-\underset{\sim}{k}') \bar{n}(\underset{\sim}{k}') + \langle \underset{\sim}{u}'(\underset{\sim}{k}-\underset{\sim}{k}') n'(\underset{\sim}{k}') \rangle \right] - \lambda k^2 n^{\circ}(\underset{\sim}{k}). \tag{2.10}$$

The equation for the time development of the small scale function is

$$\frac{\partial n'}{\partial t} + \int_{-\infty}^{\infty} d\underset{\sim}{k}' \, i\underset{\sim}{k}' \cdot \underset{\sim}{w}^{\circ}(\underset{\sim}{k}-\underset{\sim}{k}') n'(\underset{\sim}{k}')$$

$$= \int_{-\infty}^{\infty} d\underset{\sim}{k}' \, i\underset{\sim}{k}' \cdot \underset{\sim}{w}'(\underset{\sim}{k}-\underset{\sim}{k}') n^{\circ}(\underset{\sim}{k}') - D k^2 n'(\underset{\sim}{k}), \tag{2.11}$$

In Eq. (2.9) and (2.11) the second term is a convection term which can be neglected for locally homogeneous turbulence.

c. Turbulent Transport Functions

The density n_o and the electric field $\underset{\sim}{u}^\circ$ are governed by the cascade system, Eq. (2.9) to (2.11) from which the equations for the development of the spectral distributions can be derived. These so-called "equations of spectral balance" give the density and field spectral distributions

$$< n^\circ(\underset{\sim}{k},t)n^\circ(-\underset{\sim}{k},t) >$$

and

$$< \underset{\sim}{u}^\circ(\underset{\sim}{k},t)\ \underset{\sim}{u}^\circ(-\underset{\sim}{k},t) > .$$

As several transport processes are involved in the dynamical system (2.9) to (2.11), the equations of spectral balance will contain other similar correlations which are categorized as transport functions. These turbulent transport processes are controlled by eddy mixing, and therefore will call for "eddy diffusivities" of density and field fluxes. The time evolution of the density spectrum

$$< n^\circ(\underset{\sim}{k})\, n^\circ(-\underset{\sim}{k}) > \qquad (2.12)$$

is obtained by multiplying Eq. (2.9) by $n^\circ(-\underset{\sim}{k})$ and averaging. By neglecting the convection term this leads to

$$\frac{\partial}{\partial t}\langle n^{\circ}(\underset{\sim}{k})\, n^{\circ}(-\underset{\sim}{k})\rangle = -\int_{-\infty}^{\infty} d\underset{\sim}{k}'\, i k_j \ll w_j^{\circ}(\underset{\sim}{k}-\underset{\sim}{k}') n^{\circ}(-\underset{\sim}{k})\rangle^{\circ}\, \bar{n}(\underset{\sim}{k}')\rangle$$

$$-\int_{-\infty}^{\infty} d\underset{\sim}{k}'\, i k_j \ll w_j^{(1)}(\underset{\sim}{k}-\underset{\sim}{k}')\, n^{(1)}(\underset{\sim}{k}')^{(1)}\rangle\, n^{\circ}(-\underset{\sim}{k})\rangle$$

$$- D\underset{\sim}{k}\langle n^{\circ}(\underset{\sim}{k})\, n^{\circ}(-\underset{\sim}{k})\rangle^{\circ} + (\underset{\sim}{k} \to -\underset{\sim}{k}) \,. \qquad (2.13)$$

The notation $\underset{\sim}{k} \to -\underset{\sim}{k}$ represents the complex conjugate part, obtained by replacing $\underset{\sim}{k}$ by $-\underset{\sim}{k}$.

Integrating over all wave numbers contributing to rank ($^{\circ}$), i.e., covering the spectrum in the range of wave numbers 0 to k we obtain

$$\frac{1}{2}\frac{\partial}{\partial t}\int_0^{\infty} dk\, G(k) = S_n^{\circ} - T_n^{\circ} - D_n^{\circ} \,, \qquad (2.14)$$

where G(k) is the density spectrum defined by

$$G(k) = \chi^{\circ}\langle n^{\circ}(\underset{\sim}{k})\, n^{\circ}(-\underset{\sim}{k})\rangle^{\circ}$$

and χ° is the ensemble length separating the zero order and first order rank, and S_n°, T_n° and D_n° are called production, transfer and dissipation functions, respectively, and are defined as follows:

$$S_n^{\circ} = -\iint_0^{k} d\underset{\sim}{k}\, d\underset{\sim}{k}'\, i k_j' \chi^{\circ} \ll w_j^{\circ}(\underset{\sim}{k}-\underset{\sim}{k}') n^{\circ}(-\underset{\sim}{k})\rangle \bar{n}(\underset{\sim}{k}')\rangle \,, \qquad (2.15)$$

$$T_n^\circ = \iint_0^k d\underset{\sim}{k}\, d\underset{\sim}{k}'\, i k_j' \chi^\circ \ll w_j^{(1)}(\underset{\sim}{k}-\underset{\sim}{k}') n^{(1)}(\underset{\sim}{k}') > n^\circ(-\underset{\sim}{k}) > \quad , \tag{2.16}$$

$$D_n^\circ = D \int_0^k d\underset{\sim}{k}\; k^2 \chi^\circ < n^\circ(\underset{\sim}{k})\, n^\circ(-\underset{\sim}{k}) > \quad . \tag{2.17}$$

It is understood that each of the above expressions has a complex conjugate which after integration has the same value.

Multiplying Eq. (2.10) by $n^\circ(-\underset{\sim}{k})$, neglecting the convection term and averaging, an equation for the field energy analagous to Eq. (2.14) is obtained:

$$0 = S_\phi^\circ - T_\phi^\circ - D_\phi^\circ \quad , \tag{2.18}$$

where S_ϕ° , T_ϕ° , and D_ϕ° are production, transfer and dissipation functions respectively, governing the field spectrum. They are defined as follows:

$$S_\phi^\circ = -\iint_0^k d\underset{\sim}{k}\, d\underset{\sim}{k}'\, i k_j' \chi^\circ < u_j^\circ(\underset{\sim}{k}-\underset{\sim}{k}')\, n^\circ(-\underset{\sim}{k}) > \bar{n}(\underset{\sim}{k}') \quad , \tag{2.19}$$

$$T_\phi^\circ = \iint_0^k d\underset{\sim}{k}\, d\underset{\sim}{k}'\, i k_j' \chi^\circ \ll u_j^{(1)}(\underset{\sim}{k}-\underset{\sim}{k}')\, n^{(1)}(\underset{\sim}{k}') > n^\circ(-\underset{\sim}{k}) > \quad , \tag{2.20}$$

$$D_\phi^\circ = \lambda \int_0^k d\underset{\sim}{k}\; k^2 \chi^\circ < n^\circ(\underset{\sim}{k})\, n^\circ(-\underset{\sim}{k}) > \quad . \tag{2.21}$$

d. Functions for Density Spectrum

A spectrum can be divided into a non-universal range, which depends on particular boundary conditions or generating agents and a universal range governed exclusively by the transport functions, Eq. (2.15) to (2.17) and (2.19) to (2.21) at large wave numbers.

The production function, S_n°, given by Eq. (2.15) governing the intensification of the turbulent density fluctuations is controlled by the strength of the local mean density gradient, $\nabla \bar{n}$. The large scale density fluctuation, n°, in the cascade ensemble average of Eq. (2.15) can also be expressed in terms of the mean density gradient $\nabla \bar{n}$ by a relaxation frequency ω such that

$$\eta^{\circ} \cong \left\langle \frac{w^{\circ}}{\omega} \right\rangle \cdot \nabla \bar{n} \tag{2.22}$$

and that S_n° of Eq. (2.15) can be written as

$$S_n^{\circ} = \eta^{\circ} \bar{J}, \tag{2.23}$$

where

$$\bar{J} = \langle (\nabla \bar{n})^2 \rangle$$

and

$$\eta^{\circ} = \left\langle \frac{w_j \cdot w_j}{\omega} \right\rangle^{\circ}$$

is called the eddy viscosity, as it is a measure of the turbulent fluctuations. $\eta_{\circ}$ is isotropic and has the dimensions ℓ^2/t or energy/relaxation frequency.

The transfer function T_n° given by Eq. (2.16) represent the transfer of energy from the larger to the smaller scale fluctuations. As such, it is the product of two turbulent terms. This can be seen from Eq. (2.16) where we replace the n' component of the cascade ensemble average by an expression analogous to Eq. (2.22) so that

$$\eta^{(1)} \simeq \left\langle \frac{\underline{w}'}{w} \right\rangle \cdot \nabla n^{\circ} .$$

Therefore T_n° can be approximated by

$$T_n^{\circ} = \eta^{(1)} J^{\circ} ,$$

where

$$J_o = \langle (\nabla n_o)^2 \rangle$$

$$= 2 \int_0^k dk' \, k'^2 G(k') \qquad (2.24)$$

and

$$\eta^{(1)} = \left\langle \frac{\underline{w}_o' \cdot \underline{w}_1'^{(1)}}{w} \right\rangle = w\ell .$$

Analogous to the density spectrum a spectral distribution F(k), for the field energy can be defined as,

$$\tfrac{1}{2} \langle (w')^2 \rangle = \int_0^{\infty} dk \, F(k) . \qquad (2.25)$$

As a result,

$$\eta^{(1)} \simeq \ell (kF)^{\frac{1}{2}} \simeq k^{-\frac{1}{2}} F^{\frac{1}{2}} .$$

The dissipation function given by Eq. (2.17) represents the dissipation of the turbulent energy in the small scale eddies, i.e., at the high wave numbers. As such, it consists of a molecular diffusion coefficient D and a turbulent gradient represented by J^o, such that:

$$D_m^o = D J^o. \tag{2.26}$$

e. Functions for Field Spectrum

In a manner similar to the expressions derived for the density spectral functions, there is a corresponding set of functions for the field spectrum, defined by Eq. (2.19) to (2.21), involving the velocity $\underset{\sim}{u}$ instead of $\underset{\sim}{w}$. The production function (2.19) now takes the form:

$$S_\phi^o = \eta_{12}^o \bar{J}, \tag{2.27}$$

where

$$\eta_{12}^o = -\left\langle \frac{u_i^o w_i^o}{\omega} \right\rangle .$$

Inasmuch as $\underset{\sim}{w} = \underset{\sim}{u} \times \hat{e}_\theta$, η_{12}^o is anisotropic and

$$\begin{aligned} \eta_{12}^o &= -\left\langle \frac{u_i u_j}{\omega} \right\rangle \\ &= -\left\langle \frac{\eta_{11}^o}{\omega} \right\rangle \frac{\partial \bar{u}_2}{\partial x_1} - \left\langle \frac{\eta_{22}^o}{\omega} \right\rangle \frac{\partial \bar{u}_1}{\partial x_2} \\ &= -\nu^o \Gamma_{12}, \end{aligned} \tag{2.28}$$

where

$$\Gamma_{12} = \frac{\partial \bar{u}_2}{\partial x_1} + \frac{\partial \bar{u}_1}{\partial x_2}$$

and

$$\nu^o = \frac{\eta^o}{\omega} .$$

Here ν^0 is called the eddy diaperaion and has the dimension ℓ^2 and as such is independent of F. We can now write

$$S_\phi^0 = \nu^0 \Gamma_{12} \bar{J}$$

and similarly

$$T_\phi^0 = \nu^{(1)} \Gamma_{12} J_{12}^0 ,$$

$$D_\phi^0 = \lambda J .$$

As

$$S_n^0 - S_n(k^0 = \infty) = \eta^{(1)} \bar{J}$$

and

$$S_\phi^0 - S_\phi(k^0 = \infty) = \nu^{(1)} \Gamma_{12} J^0 ,$$

we can substitute in Eq. (2.14) and (2.18) to obtain:

$$\eta^{(1)} \bar{J} + \eta^{(1)} J^0 + D J^0 = D J , \tag{2.29}$$

$$\Gamma_{12} \left(\nu^{(1)} \bar{J} + \nu^{(1)} J^0 \right) + \lambda J^0 = \lambda J . \tag{2.30}$$

As the plasma consists of ions and electrons, two diffusivities D and λ determine the dissipations D_n and D_ϕ. The plasma is represented by a mean density gradient $\bar{J}$ and the gradient of the mean electric field, Γ_{12}. The eddy viscosity $\eta^{(1)}$ controls the transfer of density from small to large wave numbers across the

spectrum in a homogeneous field, while the eddy dispersion $\nu^{(1)}$ controls a similar transfer in the gradient of the field.

f. Power Laws for Inertial Subrange

The power laws for the spectral distributions F and G are obtained by means of dimensional analysis and physical arguments. Each subrange of the universal spectrum represents a different physical process and therefore may lead to different relationships or power laws for the spectral distributions.

The inertial subrange is the simplest as it is governed by the transfer function alone. All other subranges require the flow from one process to another along each spectrum or between the two spectra. The inertial subrange is characterized by the mode coupling alone with a constant transfer across each spectrum. Neglecting the production and dissipation functions, the equations of spectral balance, Eq. (2.29) and (2.30) degenerate to

$$\eta^{(1)} J^{\circ} = D J , \tag{2.31}$$

$$\Gamma_{12} \nu^{(1)} J^{\circ} = \lambda J . \tag{2.32}$$

By eliminating J° we obtain

$$\frac{\eta^{(1)}}{\nu^{(1)}} = \Gamma_{12} \frac{D}{\lambda} . \tag{2.33}$$

On the left hand side only $\nu^{(1)}$ is neither a function of F or G and $\eta^{(1)}$ is a function of F; therefore F is dependent on k with $\Gamma_{12} D/\lambda$

as a parameter. With this parameter it follows from dimensional considerations that

$$F = c_1 \left(\frac{T_{12} D}{\lambda}\right)^n k^{-m}, \tag{2.34}$$

where c_1 is a dimensionless constant.

The dimensions of F, $T_{12} D/\lambda$ and k are ℓ^3/t, $1/t$ and $1/\ell$, respectively. Therefore, from Eq. (2.34),

$$\frac{\ell^3}{t^2} = \left(\frac{1}{t}\right)^n \ell^m,$$

which leads to

$$n = 2, \qquad m = 3$$

and therefore

$$F = c_1 \left(\frac{T_{12} D}{\lambda}\right)^2 k^{-3}. \tag{2.35}$$

To derive the spectral law for the density spectrum G we examine the spectral balances Eq. (2.31) and (2.32). Equation (2.31) contains the parameter $\eta^{(1)}$, a function of F, and can therefore not be used to derive G. On the other hand, Eq. (2.32) is a more direct form appropriate for the dimensional analysis as it puts the parameter $\lambda J/T_{12}$ into evidence. This parameter is a constant while of the remaining parameters of Eq. (2.32), $\nu^{(1)}$ is not a function of G, while J^o is a function of G, as shown by Eq. (2.24). For the purpose of dimensional analysis of the

spectral law we put

$$G = c_2 \left(\frac{\lambda J}{\Gamma_{12}}\right)^n k^{-m} \tag{2.36}$$

where c_2 is a dimensionless constant.

The dimensions of G, $\lambda J/\Gamma_{12}$ and k are $n^2\ell$, n^2 and ℓ^2, respectively. Therefore, from Eq. (2.36)

$$n^2\ell = (n^2)^n \ell^m,$$

which leads to

$$n = 1, \qquad m = 1$$

and therefore

$$G = c_2 \left(\frac{\lambda J}{\Gamma_{12}}\right) k^{-1}. \tag{2.37}$$

g. Power Laws for the Production Subrange

In the production subrange molecular dissipations are not effective, so that the terms DJ^* and λJ° can be eliminated from Eq. (2.29) and (2.30). In this range $\bar{J} \gg J^\circ$ so that the spectral balance equations can be reduced to

$$\eta^{(1)} \bar{J} = D\bar{J}, \tag{2.38}$$

$$\Gamma_{12} \nu^{(1)} \bar{J} = \lambda \bar{J}. \tag{2.39}$$

As above, by dividing one equation by the other we obtain the same expression as Eq. (2.33) and by the same dimensional arguments obtain the same F spectrum as above

$$F = c_1 \left(\frac{\Gamma_{12} D}{\lambda}\right)^2 k^{-3}. \tag{2.40}$$

To obtain G we differentiate Eq. (2.39) which contains only parameters that are functions of G and k with respect to k and obtain

$$\Gamma_{12} \bar{J} \frac{d v^{(1)}}{d k} = 0 \tag{2.41}$$

and note that the only constant in this equation is $\bar{J}$, leading to

$$G = c_3 (\bar{J})^n k^{-m}.$$

The dimensions of $\bar{J}$ are n^2/ℓ^2 so that

$$n^2 \ell = \left(n^2/\ell^2\right)^n \ell^m,$$

which leads to,

$$n = 1 \quad , \quad m = 3$$

and therefore

$$G = c_3 \bar{J} k^{-3}. \tag{2.42}$$

h. Power Laws for the Dissipation Subrange

In the dissipation subrange the nonlinear mode transfers are dissipated by molecular diffusion. In this region, the production function

can be neglected so that the system of equations, Eq. (2.29) and (2.30) reduces to

$$J^{o}\left(\eta^{(1)}+D\right) = DJ, \tag{2.43}$$

$$J^{o}\left(\Gamma_{12}v^{(1)}+\lambda\right) = \lambda J \tag{2.44}$$

Dividing the two equations gives

$$\frac{\eta^{(1)}+D}{v^{(1)}\Gamma_{12}+\lambda} = \frac{D}{\lambda}\,. \tag{2.45}$$

The dissipation region is characterized by large wave numbers to justify the assumption

$$J^{o} \cong J \tag{2.46}$$

and

$$\left(\Gamma_{12}v^{(1)}+\lambda\right) = \lambda\,. \tag{2.47}$$

Substitution of (2.47) in (2.45) leads to

$$\frac{\eta^{(1)}}{v^{(1)}} = \frac{\Gamma_{12}D}{\lambda}\,.$$

This expreasion is the same as Eq. (2.33) and therefore F is the same as (2.35)

$$F = c_1\left(\frac{\Gamma_{12}D}{\lambda}\right)^{2}k^{-3}. \tag{2.48}$$

To obtain G, in view of the flow of the energy from the inertia subrange into the dissipation subrange, we write (2.44) in its differential form:

$$\frac{dJ^{\circ}}{dk}\left(\Gamma_{12}v^{(1)}+\lambda\right)+J^{\circ}\Gamma_{12}\frac{dv^{(1)}}{dk}=0. \tag{2.49}$$

Substituting Eq. (2.46) and (2.47) in Eq. (2.49) yields

$$\frac{dJ^{\circ}}{dk}\lambda+J\Gamma_{12}\frac{dv^{(1)}}{dk}=0. \tag{2.50}$$

From this expression it is seen that the governing parameter is

$$\frac{J\Gamma_{12}}{\lambda}$$

with dimensions n^2/ℓ^4. The density spectrum therefore is,

$$G=c_4\left(\frac{J\Gamma_{12}}{\lambda}\right)^n k^{-m}$$

which has the dimensions

$$n^2\ell=(n^2/\ell^4)^n\ell^m.$$

This leads to

$$n=1, \qquad m=5$$

and therefore

$$G=c_4\left(\frac{J\Gamma_{12}}{\lambda}\right)k^{-5}. \tag{2.51}$$

i. Critical Wave Numbers

A critical wave number separating the production and inertia subranges is given by the ratio

$$\left(\frac{J^o}{J}\right)_{k=k_s} = 1$$

with J^o determined by the inertial spectrum (2.32). This leads to

$$k_s = \left(\frac{\Gamma_{12}\,\bar{J}}{\lambda J}\right)^{\frac{1}{2}}. \tag{2.52}$$

The critical wave number separating the inertia and dissipation subranges is obtained from an equilibrium condition between the transfer and dissipation functions,

$$\left(\eta^{(1)}\right)_{k=k_\lambda} = D.$$

This leads to

$$k_\lambda = \left(\frac{\Gamma_{12}}{\lambda}\right)^{\frac{1}{2}}. \tag{2.53}$$

3. EXPERIMENTAL SPECTRA

Plasma drift turbulence is observed in the ionosphere as well as in plasma laboratory experiments. In the laboratory, field spectra have been measured by means of Langmuir probes and density spectra by means

of microwave scattering. An example of a field spectrum observed in Zeta experiments is shown in Fig. (5.1), while a density spectrum obtained in these experiments[31] is shown in Fig. (5.2). A density spectrum of emissions from a beam plasma interaction[35] is given in Fig. (5.3). The k^{-3} law for the field spectrum and the k^{-1}, k^{-5} laws derived for the density spectrum as predicted by Eq. (2.35), (2.37) and (2.51) can be seen in these figures. Although the abscissa are plotted in frequencies, the spectra are in wave numbers, as the plasmas are moving inhomogeneities with constant drift.

4. EFFECTS OF TURBULENCE ON TRANSPORT PROPERTIES AND DIFFUSION

a. General Considerations

As pointed out in Section I, 2, there exists a discrepancy of several orders of magnitude between the measured rates of diffusion in the ionosphere, and values predicted by existing theories. Hence a new transport theory is needed, based upon a new mechanism, which includes the effects of stochastic fluctuations or micro-perturbations, i.e. microturbulence waves and instability in addition to molecular collisions. In diffusion phenomena at altitudes below 50 km, the collisional mechanism is dominant, so that the turbulent effects need not be considered. On the other hand at altitudes above 100 km the turbulent effects become important. Evidence of the existence of the collisionless mechanism is also seen from tests conducted by NASA at high altitudes (near 12 earth

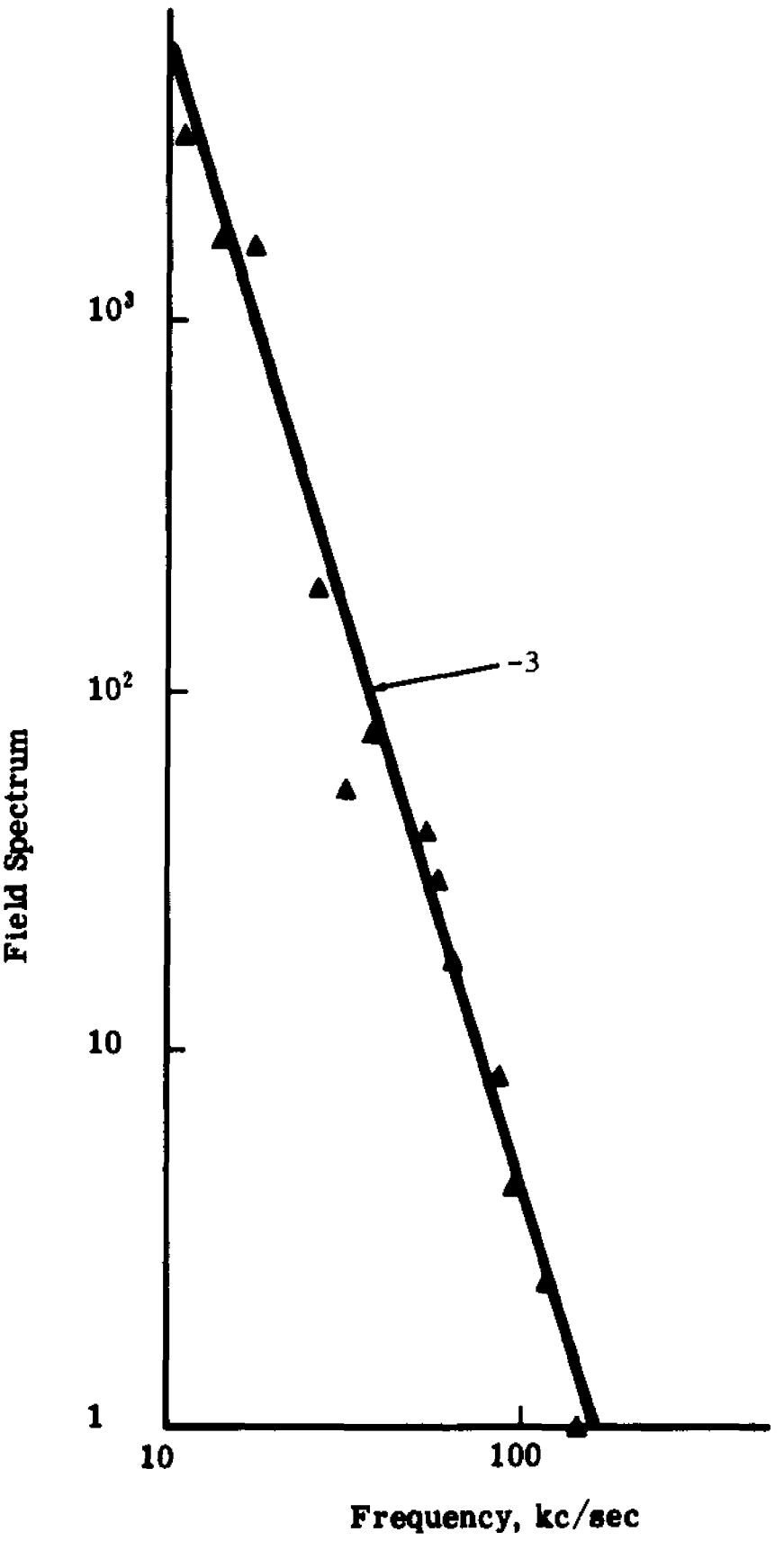

Fig. 5.1. Spectrum of Electric Field Fluctuations in Zeta (from Ref. 31).

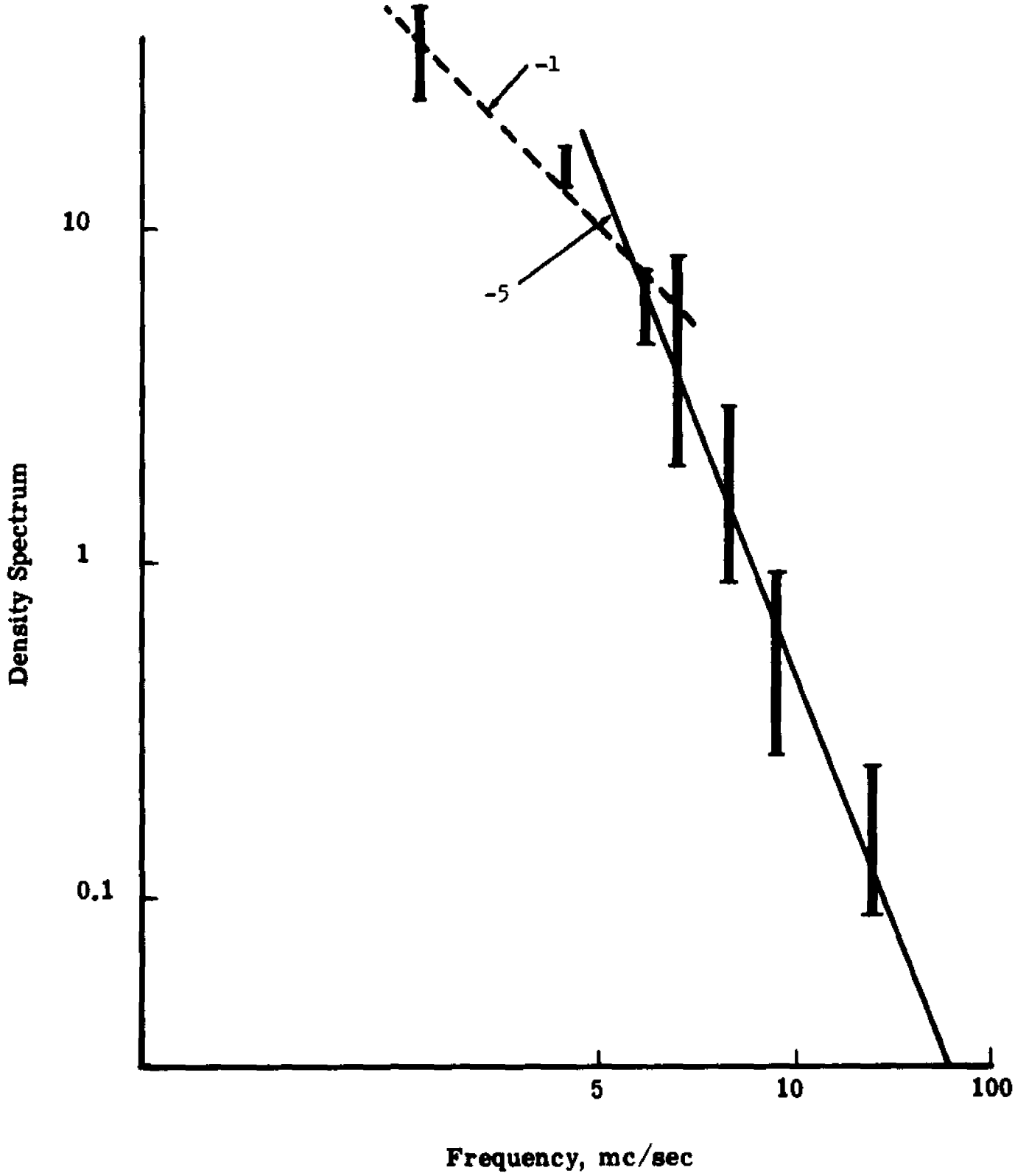

Fig. 5.2. Spectrum of Density in Zeta (From Ref. 31).

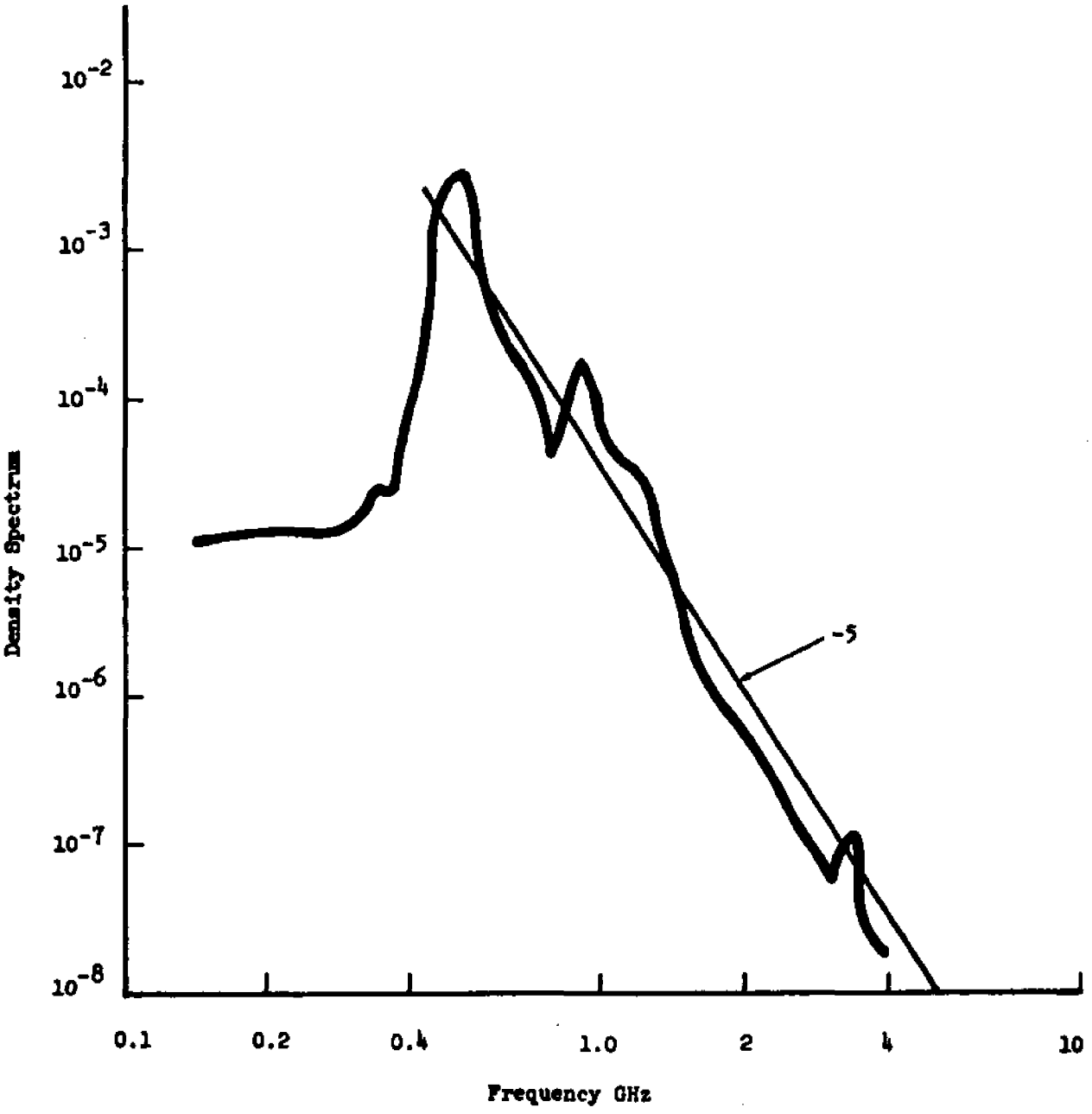

Fig. 5.3. Density Spectrum of Emissions From a Beam-Plasma Interaction (Data Rearranged from Ref. 35).

radii), where barium has been released from satellites in regions where the molecular collisions are absent.[44] The tests show that the cloud still diffuses. This diffusion of collisionless nature is also found in laboratory experiments.[20,23]

To obtain valid results for plasma in the ionospheric region (100 to 250 km) the transport coefficients must be reformulated to include both collisional and turbulent diffusion mechanisms. This tends to increase the diffusion in the perpendicular direction and decrease the growth in the longitudinal direction, in agreement with experimental observations.

The transport coefficients are derived from the fundamental equations given in Chapter II for the motion of a plasma inhomogeneity, i.e., the continuity and momentum equations (II,1.1) and (II,1.2) which when written without the subscript a, denoting ions and electrons are,

$$\frac{\partial n}{\partial t} + \nabla \cdot (n \underset{\sim}{v}) = 0 \tag{4.1}$$

and

$$\begin{aligned} mn\left(\frac{\partial \underset{\sim}{v}}{\partial t} + \underset{\sim}{v} \cdot \nabla \underset{\sim}{v}\right) &= -k \nabla nT + mn \underset{\sim}{g} \\ &+ ne\left(\underset{\sim}{E} + \underset{\sim}{v} \times \underset{\sim}{B}/c\right) - mn\nu_n \left(\underset{\sim}{v} - \underset{\sim}{U}\right) \\ &+ mn\nu \nabla^2 \underset{\sim}{v} \end{aligned} \tag{4.2}$$

Here m is the mass, v the velocity, T the temperature, e the electric charge, ν the kinematic viscosity, ν_n the collision frequency with the neutrals, $\underset{\sim}{E}$ the electric field, $\underset{\sim}{g}$ the acceleration of gravity and k is Boltzmann's constant. Following the practice of treatments in theories of turbulent motion, the total motion, as governed by Eq. (4.1) and (4.2), is decomposed into a mean, or background part, denoted by a bar, and a fluctuation, denoted by a prime as follows,

$$\begin{aligned} \underset{\sim}{v} &= \bar{\underset{\sim}{v}} + \underset{\sim}{v}' , \\ n &= \bar{n} + n' , \\ T &= \bar{T} + T' , \\ \underset{\sim}{E} &= \bar{\underset{\sim}{E}} + \underset{\sim}{E}' . \end{aligned} \tag{4.3}$$

The effects of the fluctuation n' arising from the terms

$$m n \frac{d\underset{\sim}{v}}{dt} , \quad n e (\underset{\sim}{E} + \underset{\sim}{v} \times \underset{\sim}{B}/c) , \quad m n \nu_n (\underset{\sim}{v} - \underset{\sim}{U})$$

and

$$m n \nu \nabla^2 \underset{\sim}{v}$$

are negligible. Therefore, without much error n can be replaced by $\bar{n}$ in these terms and Eq. (4.2) reduced to

$$m\,\bar{n}\,\frac{d\underset{\sim}{v}}{dt} = -\,k\,\nabla\cdot T n + m\,n\,\underset{\sim}{g}$$
$$+\,\bar{n}e\,(\underset{\sim}{E} + \underset{\sim}{v}\times\underset{\sim}{B}/c) - m\bar{n}\,\nu_n\,(\underset{\sim}{v}-\underset{\sim}{U})$$
$$+\,m\bar{n}\,\nu\,\nabla^2\underset{\sim}{v}\ . \qquad (4.4)$$

This approximation is customarily known as the Boussinesq approximation for gravity waves where the fluctuation of density resides only with the gravity and pressure terms. With this approximation the dynamical equations for mean motion and the fluctuations can be derived.

b. Dynamic Equations for the Mean Motion

By taking the average of Eq. (4.1) and (4.4) the equations of momentum and continuity for the mean motion are obtained:

$$\frac{\partial\bar{n}}{\partial t} + \nabla\cdot\bar{n}\,\underset{\sim}{\bar{v}} = -\,\nabla\cdot\overline{n'\underset{\sim}{v}'} \qquad (4.5)$$

and

$$\frac{D\underset{\sim}{\bar{v}}}{Dt} = \underset{\sim}{\bar{L}} - \nu_n\left(\underset{\sim}{\bar{v}}-\underset{\sim}{U}\right) + \nu\nabla^2\underset{\sim}{\bar{v}} - \overline{(\underset{\sim}{v}'\cdot\nabla)\underset{\sim}{v}'}$$
$$-\,\frac{v_{th}^2}{\bar{n}\bar{T}}\left[\overline{n'\nabla T'} + \overline{T'\nabla n'}\right]\ . \qquad (4.6)$$

Here

$$\frac{D}{Dt} \equiv \frac{\partial}{\partial t} + \bar{\underset{\sim}{v}} \cdot \nabla ,$$

$$\bar{\underset{\sim}{L}} = \frac{e}{m}\left(\underset{\sim}{E} + \bar{\underset{\sim}{v}} \times \underset{\sim}{B}/c\right) - v_{th}^2\left(\frac{\underset{\sim}{e}_g}{\bar{H}} + \frac{\nabla \bar{T}}{\bar{T}} + \frac{\nabla \bar{n}}{\bar{n}}\right) ,$$

$$v_{th}^2 = \left(\frac{k\bar{T}}{m}\right)^{\frac{1}{2}} , \qquad (4.7)$$

$$\underset{\sim}{e}_g = (0, 0, 1) ,$$

$$\bar{H} = \frac{k\bar{T}}{mg} .$$

Subtracting Eq. (4.6) from Eq. (4.4) results in the momentum equation for the fluctuations, written in a simplified form by keeping the forcing terms only:

$$\frac{D\underset{\sim}{v}'}{Dt} = \underset{\sim}{L}' - \left(\underset{\sim}{v}' \cdot \nabla\right)\bar{\underset{\sim}{v}} , \qquad (4.8)$$

$$\underset{\sim}{L}' = \frac{e}{m}\left(\underset{\sim}{E}' + \underset{\sim}{v}' \times \underset{\sim}{B}/c\right) - v_{th}^2\left(\frac{\underset{\sim}{e}_g}{\bar{H}}\frac{n'}{\bar{n}} + \frac{\nabla \bar{T}}{\bar{T}}\frac{n'}{\bar{n}} + \frac{\nabla \bar{n}}{\bar{n}}\frac{T'}{\bar{T}}\right) .$$

The continuity equation for the density fluctuation n' can be obtained by subtracting Eq. (4.5) from Eq. (4.1), and takes the simplified form,

$$\frac{Dn'}{Dt} = -\underset{\sim}{v}' \cdot \nabla \bar{n} \,. \tag{4.9}$$

Similarly, the temperature fluctuation T' is governed by

$$\frac{DT'}{Dt} = -\underset{\sim}{v}' \cdot \nabla \bar{T} \,. \tag{4.10}$$

It can be seen that the mean variables $\bar{n}$ and $\underset{\sim}{\bar{v}}$ are governed by Eq. (4.5) and (4.6) and that these expressions contain the statistical effects of fluctuations as determined by Eq. (4.8) to (4.10).

c. Eddy Transport Phenomena

The correlations in Eq. (4.5) and (4.6) are the statistical effects of the fluctuations on the mean motions and represent eddy transports. They will be accounted for by retaining, as an approximation, the forcing terms only, such as $\nabla \underset{\sim}{\bar{v}}$, $\nabla \bar{T}$, $\nabla \bar{n}$, and $\underset{\sim}{e}_g$. The stochastic terms of Eq. (4.5) and (4.6) then become the following:

$$\begin{aligned}
-\frac{1}{\bar{n}}\,\overline{n'\underset{\sim}{v}'} &= \frac{1}{\nu_m}\left(D_{nv}\cdot\nabla\right) + D_{nn}\frac{\nabla\bar{T}}{\bar{T}} + D_{nT}\frac{\nabla\bar{n}}{\bar{n}} + \frac{\underset{\sim}{e}_g}{\bar{H}}D_{nn}\,, \\
-\nabla\cdot\overline{n'\underset{\sim}{v}'} &= \frac{\bar{n}}{\nu_m}\left(\psi_{nv}\,\underset{\sim}{\bar{v}} + \psi_{nn}\bar{T} + \psi_{nT}\,\bar{n} + \psi_{nn}\,z\right), \\
-\overline{(\underset{\sim}{v}'\cdot\nabla)\underset{\sim}{v}'} &= \psi_{vv}\,\underset{\sim}{\bar{v}} + \psi_{nv}\,\bar{T} + \psi_{Tv}\,\bar{n} + \psi_{nv}\,z, \\
-\frac{\nu_m^2}{\bar{n}\bar{T}}\,\overline{n'\nabla T'} &= e_{nv}\,\bar{T} \quad , \quad -\frac{\nu_m^2}{\bar{n}\bar{T}}\,\overline{T'\nabla n'} = e_{Tv}\,\bar{n}\,.
\end{aligned} \tag{4.11}$$

In order to simplify the writing, the following transport operators have been introduced:

$$\psi_{nn}\bar{T} = v_{th}\nabla\cdot\left[\frac{1}{\bar{T}}D_{nn}\nabla\bar{T}\right], \qquad \psi_{T\underset{\sim}{v}}\bar{n} = v_{th}\nabla\left[\frac{1}{\bar{n}}D_{T\underset{\sim}{v}}\cdot\nabla\bar{n}\right],$$

$$\psi_{nT}\bar{n} = \frac{v_{th}}{\bar{n}}\nabla\cdot\left[D_{nT}\nabla\bar{n}\right], \qquad \psi_{n\underset{\sim}{v}}\bar{T} = v_{th}\nabla\left[\frac{1}{\bar{T}}D_{n\underset{\sim}{v}}\cdot\nabla\bar{T}\right],$$

$$\psi_{nv}\bar{\underset{\sim}{v}} = \nabla\cdot\left[D_{n\underset{\sim}{v}}\cdot\nabla\bar{\underset{\sim}{v}}\right], \qquad \psi_{\underset{\sim}{v}\underset{\sim}{v}}\underset{\sim}{v} = \nabla\cdot\left[D_{\underset{\sim}{v}\underset{\sim}{v}}\cdot\nabla\bar{\underset{\sim}{v}}\right], \tag{4.12}$$

$$\psi_{nn}z = v_{th}\nabla\cdot\left[\frac{1}{\bar{n}}D_{nn}\nabla z\right], \qquad \psi_{n\underset{\sim}{v}}z = v_{th}\nabla\left[\frac{1}{\bar{n}}D_{n\underset{\sim}{v}}\cdot\nabla z\right],$$

$$\mathcal{C}_{nv}\bar{T} = v_{th}\nabla\left[\frac{1}{\bar{T}}K_{n\underset{\sim}{v}}\nabla\bar{T}\right], \qquad \mathcal{C}_{T\underset{\sim}{v}}\bar{n} = v_{th}\nabla\left[\frac{1}{\bar{n}}K_{T\underset{\sim}{v}}\cdot\nabla\bar{n}\right],$$

which contain eddy diffusivities of the form

$$K_{fg} = \frac{v_{th}^2}{f_0 g_0}\int_0^\infty d\tau\ \overline{f'(0)\,g'(\tau)},$$

$$D_{fg} = \frac{v_{th}^2}{f_0 g_0}\int_0^\infty d\tau\ \overline{f'(0)\,g'(\tau)}\ \cos\Omega\tau, \tag{4.13}$$

where f', g' represent the fluctuations v', n', T', and f_0, g_0 are representative of the mean quantities such that if f', g' = n', T' then f_0, $g_0 = \bar{n}$, $\bar{T}$, etc. The presence of the term $\cos\Omega\tau$ in D_{fg} is due to

the integration along the orbit of the particle in the magnetic field B, with $\Omega = eB/mc$, the gyrofrequency. The conjugate term with the factor $\sin \Omega\tau$ has been dropped in view of the odd nature of the integrand, which leads to no contributions in the integration from $-\infty$ to $+\infty$.

d. Turbulent Transport Coefficients

By substituting the stochastic terms of (4.11), we transform Eq. (4.5) and (4.6) into

$$\frac{\partial \bar{n}}{\partial t} + \nabla \cdot \bar{n} v = \psi_n , \tag{4.14}$$

$$\frac{D\bar{\underset{\sim}{v}}}{Dt} = \bar{\underset{\sim}{L}} - \nu_n \left(\bar{\underset{\sim}{v}} - \underset{\sim}{U} \right) + \underset{\sim}{\psi}_v , \tag{4.15}$$

where

$$\psi_n \equiv \frac{\bar{n}}{v_{th}} \left[\psi_{n\underset{\sim}{v}} \bar{\underset{\sim}{v}} + \psi_{nn} \bar{T} + \psi_{nT} \bar{n} + \psi_{n\underset{\sim}{z}} \right] ,$$

$$\underset{\sim}{\psi}_v \equiv \left(\psi_{\underset{\sim}{v}\underset{\sim}{v}} + \nu \nabla^2 \right) \bar{\underset{\sim}{v}} + \left(\psi_{n\underset{\sim}{v}} + \varrho_{n\underset{\sim}{v}} \right) \bar{T} + \left(\psi_{T\underset{\sim}{v}} + \varrho_{T\underset{\sim}{v}} \right) \bar{n} + \psi_{n\underset{\sim}{z}} .$$

By comparing II,(1.1) and II,(1.2) for the laminar motion with the corresponding equations (4.14) and (4.15) for the turbulent motion it can be seen that the dissipative term in the momentum equation II,(1.2) depends on $\bar{\underset{\sim}{v}}$ only, and that the continuity equation II,(1.1) does not even have a dissipative term, while the new Eqs. (4.14) and (4.15) have their dissipation depend on all transferable mean quantities, $\bar{\underset{\sim}{v}}$, $\bar{T}$ and $\bar{n}$.

As was done in Chapter II, we can simplify the momentum equation (4.15) by dropping the inertia terms on the left hand side. Also, we make a further simplification by replacing all the velocity dissipations by a friction term such that

$$\underset{\sim}{\mathscr{V}}_v = -\nu_f \left(\bar{\underset{\sim}{v}} - \underset{\sim}{U} \right), \tag{4.16}$$

where ν_f is a collisionless or turbulent dissipation frequency. The momentum equation (4.15) then reduces to

$$0 = \underset{\sim}{L} - \nu_o \left(\bar{\underset{\sim}{v}} - \underset{\sim}{U} \right), \tag{4.17}$$

where

$$\nu_o \equiv \nu_n + \nu_f$$

is an effective dissipation frequency. At high altitudes where $\nu_f \gg \nu_n$, the turbulent value is

$$\begin{aligned} \kappa_a &= \Omega / \nu_o \\ &= \Omega / (\nu_n + \nu_f) \\ &\cong \Omega / \nu_f , \end{aligned} \tag{4.18}$$

which is smaller than the laminar value

$$\kappa_a = \frac{\Omega}{\nu_n} \,. \tag{4.19}$$

This difference between the above two values will change the transport coefficients and diffusion characteristics of a plasma inhomogeneity considerably.

Solving (4.17) for $\bar{\underset{\sim}{v}}$ as in Chapter II and substituting in the continuity equation (4.14) we obtain a turbulent equation analogous to the laminar equation II,(3.2),

$$\frac{\partial \bar{n}}{\partial t} + \nabla \cdot (\bar{n}\, \underset{\sim}{U}) + \nabla \cdot \frac{\bar{n}\, \underset{\approx}{\alpha}}{e} \cdot \left(-\nabla \phi + \bar{\underset{\approx}{E}}^{*}\right)$$

$$= \nabla \cdot \underset{\approx}{D} \cdot \nabla \bar{n} + \psi_n \,, \tag{4.20}$$

where ψ_n is an additional term due to turbulent effects. If we assume an isothermal plasma and neglect gravity effects, and further assume that derivatives higher than the fourth order are negligible, we can approximate,

$$\nabla \cdot \underset{\approx}{D} \cdot \nabla \bar{n} + \psi_n \tilde{=} \nabla \cdot \left(\underset{\approx}{D} + \underset{\approx}{D}_{nt}\right) \cdot \nabla \bar{n} \,, \tag{4.21}$$

reducing the equation to the same form as II,(3.2) except for the magnitude of the transport coefficient D, which now contains an eddy diffusivity $\underset{\approx}{D}_{nt}$.

The theoretical values of the turbulent transport coefficients which include the effects of fluctuations can be obtained from an evaluation of the transport operators and eddy diffusivities given by (4.12) and (4.13). Measurements in the atmosphere have given a value of 0.5-5 for κ_i and a value of 50-200 for κ_e. Those values are considerably smaller than the laminar values of $\kappa_i = 50$ and $\kappa_e = 2 \times 10^4$. Such an anomaly is due to the effects of turbulent fluctuations in the transport mechanism.

It is to be remarked that an analytical theory of the turbulent transport properties can be formulated on the basis of the spectral structure of turbulence. A spectral theory has been developed in Section 2 of this Chapter which will confirm the above phenomenological considerations of the anomalous transport.

Additional evidence of the above mentioned anomalous transport can be seen from the following:

(i) The experimentally observed rate of drift of the plasma inhomogeneity can be explained on the basis of lower effective values of κ_i and κ_e. As derived in Section III,4, the fundamental and secondary maxima of a plasma inhomogeneity after time t have moved a distance

$$d_1 \simeq \frac{Ut}{\kappa_i \kappa_e} , \tag{4.22}$$

$$d_2 \simeq \frac{Ut}{\sqrt{1+\kappa_i^2}} . \tag{4.23}$$

From a barium cloud experiment[12] at 195 km with U = 0.1 km/sec and t = 678 sec., we observe d_1 = 0.35 km and d_2 = 35 km. Using these values, we find from (4.22) and (4.23) the turbulent values

$$\mathcal{K}_i = 2 \quad , \quad \mathcal{K}_e = 100$$

in contrast to the laminar values

$$\mathcal{K}_i = 50 \quad , \quad \mathcal{K}_e = 2 \times 10^4 .$$

Therefore it can be concluded that the above experiment supports the turbulent expression of $\mathcal{K}_a$, given by (4.18) and not the laminar expression (4.19).

(ii) The phenomenon of the separation of a plasma inhomogeneity has been observed in many releases at altitudes between 185 and 200 km. In Section III,4 it is shown that this phenomenon can occur only for values of $\mathcal{K}_i$ that are not too much larger than 1, which again indicates the necessity to include turbulent effects in the transport properties.

5. CONCLUSIONS

(i) It is known that turbulence can be generated by drift instability in a plasma inhomogeneity. Based upon the fundamental equations governing the density and the electric field of an inhomogeneous plasma, a dimensional theory is developed to study the spectral distributions of density and field for a turbulent plasma inhomogeneity. The dimensional theory agrees with the more complicated

analytical theory of Tchen, for the present purpose of elucidating phenomenologically the plasma nonlinear interactions processes,

(ii) After decomposing the equations into those for mean motion and those for fluctuations, the method of single cascade was applied to formulate the nonlinear turbulent transport coefficients. An energy balance then led to the spectral relations, from which, by means of dimensional arguments, the spectral laws governing the spectral distributions for field and density, F and G have been derived. Over the entire universal range of the spectrum

$$F = \left(\frac{\Gamma_{12} D}{\lambda}\right)^2 k^{-3},$$

while G follows a different law for each subrange. For the production subrange,

$$G \approx \bar{J} k^{-3};$$

for the inertial subrange,

$$G \approx \frac{\lambda J}{\Gamma_{12}} k^{-1};$$

and for the dissipation subrange,

$$G \approx \frac{J \Gamma_{12}}{\lambda} k^{-5}.$$

(iii) From the fundamental equations of an inhomogeneous plasma transport coefficients are derived and involve correlation functions. Those turbulent effects are experimentally found important in certain

ionospheric regions such as the F_2 region. The inclusion of turbulent effects leads to anomalous diffusion rates in the longitudinal and transverse magnetic field directions, which are in better agreement with observed values than results based upon a laminar theory.

Chapter VI

General Conclusions

1. SUMMARY OF METHODS AND RESULTS

This chapter summarizes the principal aspects of the research which has been presented in the preceding chapters.

As an investigation of the dynamics of a plasma inhomogeneity its overall motion has been studied in three phases corresponding to large, intermediate and small scale motion, typified by diffusion, striations and turbulence, respectively. The research has emphasized the development of theoretical interpretations and predictions for explaining anomalous features in the evolution of plasma inhomogeneities under the action of magnetic, electric and wind forces. This has been accomplished by the inclusion of a variable ambipolar drift, nonlinearities and turbulent effects in the dynamics of the plasma inhomogeneity.

The theoretical investigation of the motion in the inhomogeneity is based on the fundamental equations governing ions and electrons, the continuity, momentum and Maxwell equations. By resolving these equations we reduce to a system of two equations containing the density and the self-consistent field as unknowns, and the conductivity and the diffusivity tensors as transport coefficients. The conductivity tensor is a function of density and thereby introduces nonlinearities.

The system of equations can be reduced to a single diffusion equation with the density the only unknown. This single equation is a fourth order nonlinear partial differential equation with variable ambipolar drift and variable ambipolar diffusion coefficient. A linearized solution of the diffusion equation, obtained by means of a Fourier transform, shows that under certain conditions the inhomogeneity separates into two parts, a feature which has been observed in barium cloud experiments. A requirement for splitting is that the transport coefficient $\mathcal{K}_i$ be not too large, which is in agreement with the results obtained by including the effects of turbulence in the formulation of the transport coefficients. Density plots for linear plasma over a range of $\mathcal{K}_i$ and $\mathcal{K}_e$ are obtained by means of a computerized calculation.

The nonlinear diffusion equation is solved analytically, by assuming small density gradients in the linear terms. The solution consists of the linear density and a correction term due the nonlinearities. In agreement with barium cloud experiments, results show that a steepening occurs, i.e., the density falls off rapidly, on the side of the inhomogeneity that faces in the direction of a neutral wind. A numerical solution of the exact three dimensional nonlinear diffusion equation, performed on a digital computer, also shows this steepening.

The development of striations is predicted from an instability analysis based on the nonlinear diffusion equation, at the edge of the plasma inhomogeneity facing a neutral cloud, which is also the side where steepening occurs, in agreement with observations during artificial

cloud experiments. The numerical value of the wave length of a stable oscillation obtained from the theory agrees with observed values of about 1 km.

Turbulent spectra for the density and energy distribution functions of a drift instability generated turbulence are obtained by means of a dimensional theory based on a simplified model using the single cascade method. The energy distribution function, F, follows the k^{-3} law over the entire universal spectrum, while the density spectral function G, follows the k^{-3}, k^{-1} and k^{-5} laws, for the production, inertial and dissipative subranges, respectively. The spectral laws are confirmed by experiments with Zeta and with beam-plasma interactions.

As an application of turbulent theory, the turbulent transport coefficients for a plasma inhomogeneity are formulated by including in addition to the molecular dissipation, collisionless dissipations resulting from turbulent fluctuations in density, velocity and temperature. The effect of these fluctuations on the mean motion can be expressed in terms of stochastic correlations between the various fluctuating quantities. The effect of this turbulence is to reduce the rate of diffusion of the inhomogeneity in a direction parallel to the magnetic field and increase it in a transverse direction, in agreement with observations of barium cloud diffusions.

2. SUGGESTIONS FOR FUTURE WORK

Additional studies that could contribute to a better understanding of the diffusion process of plasma inhomogeneities are among the

following:

(i) The effect of temperature gradients on diffusion and instability phenomena can be investigated. Temperature gradients, similar to density gradients, provide driving forces that induce additional diffusion mechanisms and instabilities.[34]

(ii) Ion and electron mass interchange with the background can be included. In the present analysis, it has been assumed that the flow of ion and electrons to and from the surroundings is small. Actually, electron currents exist in the ionosphere which may transport charged particles from ionospheric regions (such as the F layer) to the inhomogeneity. This effect has been postulated by a number of investigators,[6,16,19,45,46] and could be incorporated with the theories presented here.

(iii) The anomalous transport coefficients are formed phenomenologically in Chapter V, and are in good agreement with experimental evidence. We have also presented a dimensional theory of the spectral structure of plasma turbulence in Chapter V. This lays the foundation for developing an analytic theory of turbulent transport coefficients.

(iv) The theory of striations presented in Chapter IV is a quasi-linear theory, i.e., the nonlinear diffusion equation has been solved by iteration. A completely nonlinear development may show additional features.

REFERENCES

1. J. W. Chamberlain, "Physics of the Aurora and Airglow," Academic Press, New York and London, 1961.

2. G. Haerendel, et al., Aurora and Airglow, Proceedings of the Nato Advanced Study Institute, July 29-Aug. 9, 1968.

3. G. Atkinson, Auroral Arcs, Results of the Interaction of Dynamic Magnetosphere with the Ionosphere, J. Geoph. Res. Sp. Phys, 75, 4745-4755 (1970).

4. High Altitude Chemical Releases, IIT Research Institute, Chicago (1968).

5. G. D. Thorne, Project Secede I, HF Radar Studies of Barium Clouds, RADC-TR-69-214 (1969).

6. H. Föppl, et al., Artificial Strontium and Barium Clouds in the Upper Atmosphere, Planetary and Space Sci. 15, 357-372 (1967).

7. P. M. Banks and T. E. Holzer, Features of Plasma Transport in the Upper Atmosphere, J. Geoph. Res. Sp. Sc. 74, 6304-6316 (1969).

8. G. Haerendel, et al., Highly Irregular Artificial Plasma Clouds in the Auroral Zone, MPI-PAE/Extraterr 21, (1969).

9. N. W. Rosenberg, Chemical Releases at High Altitudes, Science, 152, 1017-1027 (1966).

10. G. T. Rosenberg, et al., AFCRL Barium Release Studies 1967, Air Force Cambridge Research Laboratories, Interim Report.

11. G. T. Best, et al., Photographic Studies of Barium Releases, AFCRL-70-0687 (1970).

12. K. H. Lloyd and D. Golomb, Observations on the Release of a Cloud of Barium Atoms and Ions in the Upper Atmosphere, AFCRL-67-0144 (1967).

13. F. W. Perkins, N. J. Zabusky and J. H. Doles, Deformation and Striation of Plasma Clouds in the Ionosphere, Bell Telephone Company Report (1970).

14. L. H. Holway, Jr., Ambipolar Diffusion in the Geomagnetic Field, J. Geophys. Res. 70, 3635-3645 (1965).

15. G. Haerendel et al., Motion of Artificial Ion Clouds in the Upper Atmosphere, COSPAR International Reference Atmosphere, 77-78, North-Holland Publishing Co., Amsterdam (1965).

16. G. Haerendel et al., Motion of Artificial Ion Clouds in the Upper Atmosphere, Planetary and Space Sci. 15, 1-18 (1967).

17. A. V. Guervich and Y. Y. Tsedilina, Spreading of Moving Inhomogeneity in a Magnetoactive Plasma, Geomagnetizm i Aeronomiya I, 527-532 (1967).

18. A. V. Gurevich and E. E. Tsedilina, Motion and Spreading of Inhomogeneities in a Plasma, Sov. Phys. Uspekhi 10, 214 (1967).

19. T. R. Kaiser et al., Ambipolar Diffusion and Motion of Ion Clouds in the Earth's Magnetic Field, Planetary and Space Sci. 17, 519-559 (1969).

20. A. Simon, Instability of a Partially Ionized Plasma in Crossed Electric and Magnetic Fields, Phys. of Fluids 6, 382-388 (1963).

21. H. Simon and A. M. Sleeper, Polarization, Steepening and Striation in Barium Clouds, RADC-TR-71-292 (1971).

22. L. M. Linson and J. B. Workman, Formation of Striation in Ionospheric Plasma Clouds, J. Geophys. Res. 75, 3211 (1970).

23. H. W. Hendel et al., Collisional Drift Waves, Identification Stabilization and Enhanced Plasma Transport, Phys. of Fluids 11, 2426-2439 (1968).

24. N. S. Buchelnikova, et al., Plasma Turbulence in the Presence of a Drift Instability, Sov. Phys. JETP 25, 548-556 (1967).

25. A. V. Nedospasov, Striations, Sov. Phys. USPEKHI 11, 174-187 (1968).

26. B. B. Kadomtsev, Plasma Turbulence, London and New York, Academic Press (1965).

27. C. M. Tchen, Turbulence by Electrostatic Fluctuations, Lectures in Theoretical Physics, Vol. 9C (Kinetic Theory), Ed. by W. E. Brittin, Gordon and Breach Science Publishers, New York (1967), 265-278.

28. C. M. Tchen, Spectrum of Turbulence in a Plasma with a Strong Magnetic Field, Chapter in book on Nonlinear Phenomena in Plasmas, Edts. Kalman and Feix, Gordon and Breach Publishers, New York (1969), 233-250.

29. C. M. Tchen, Spectrum and Diffusion in a Turbulent Plasma with Collisional and Collisionless Dissipations, Proceedings of the Symposium on Turbulence of Fluids and Plasmas, Polytechnic Press, distributed by Interscience Publishers (1969), p 101-114.

30. C. M. Tchen, Cascade Mechanism of Nonlinear Interactions between Modes in a Turbulent Plasma, IEEE Transactions on Electron Devices, ED-17, 247-251 (1970).

31. C. M. Tchen, Repeated Cascade Theory of Homogeneous Turbulence, Phy. Fluids 16, 13-30 (1973); also Repeated Cascade Theory of Turbulence in a Inhomogeneous Plasma, Phys. Rev. A, June 1973.

32. J. J. Kim and A. Simon, Nonlinear Theory of the ExB Instability, University of Rochester.

33. A. Hasegawa, Dynamics of Aurora Formation, Bell Telephone Laboratories (1970).

34. D. M. Cunnold, An Electron Temperature Gradient Instability and Its Possible Applications to the Ionosphere, J. Geoph. Res. 77, 224-233 (1972).

35. J. R. Apel, Harmonic Generation and Turbulence Like Spectrum in a Beam-Plasma Interaction, Phys. Rev. Letters 19 (1967).

36. T. Farley, Jr., Artificial Heating of the Electrons in the F Region of the Ionosphere, J. Geoph. Res. 68, 401-412 (1963).

37. R. H. Kraichnan, Approximations for Steady-State Isotropic Turbulence, Phys. Fluids 7, 1163 (1964).

38. J. R. Herring, Self-Consistent-Field Approach to Turbulence Theory, Phys. Fluids 8, 2219 (1965).

39. J. R. Herring, Self-Consistent-Field Approach to Nonstationary Turbulence, Phys. Fluids 9, 2106 (1966).

40. L. Onsager, The Distribution of Energy in Turbulence, Phys. Rev. 68, 286 (1945).

41. J. Boussinesq. Mem. pres. par div. Savants a l'acad. sci., Paris 23, 46 (1877).

42. L. F. Richardson, Proc. Roy. Soc. (London) 213A, 349 (1952).

43. H. Lamb, Hydrodynamics, Cambridge University Press, New York (1932), 6th ed., 677.

44. D. Adamson, Analysis of Second Barium Release from Javelin, Langley Research Center.

45. J. N. Shiau and A. Simon, Barium Cloud Growth and Striation in a Conducting Background, RADC-TR-72-320 (1972).

46. T. R. Kaiser et al., Ambipolar Diffusion and Motion of Ion Clouds in the Earth's Magnetic Field, Planet. Space Sci., 17, 519-552 (1969).

V I T A

Ralph D. Hankel received a B. M. E. degree from The City College of New York in 1950 and an M. S. in Mechanical Engineering from Stevens Institute of Technology in 1953 and an M. S. in Industrial Engineering from the same institution in 1957. He began full time study toward a Ph. D. degree in Engineering in Thermal and Fluid Sciences under Professor C. M. Tchen in September 1968. He has been a lecturer in the Mechanical Engineering Department of The City College.

Ralph D. Hankel has held positions as Senior Research Engineer at Curtiss Wright Corporation and as Advisory Engineer at United Nuclear Corporation working in the areas of heat transfer and fluid flow. At the present time he is Manager of the Plant Analysis Section of Gulf United Services in Elmsford, New York.